CHARACTERISATION OF A CHLORORESPIRATORY PATHWAY IN *BETA VULGARIS* AND *TRIFOLIUM REPENS*

A thesis presented in partial fulfilment of the requirements for the degree of

Master of Science in Plant Biology

at

Massey University, New Zealand

Alison Marie Winger

2002

ABSTRACT

The chloroplast respiratory pathway (chlororespiration) is postulated to interact with the photosynthetic pathway through the plastoquinone (PQ) pool. Two enzymes are proposed to operate in the pathway: an NAD(P)H dehydrogenase that is homologous to the mitochondrial NADH dehydrogenase, and a putative terminal oxidase. To study the operation and regulation of the chlororespiratory pathway in two higher plant species, silverbeet (*Beta vulgaris* L.) and white clover (*Trifolium repens* L.), two approaches have been used. The first uses salicylhydroxamic acid (SHAM), an inhibitor of the mitochondrial quinol-oxidising alternative oxidase, to identify the site of inhibition during electron transfer through the photosynthetic electron transfer chain. The second uses antibodies to two subunits of the NAD(P)H dehydrogenase complex, and examines changes in accumulation of these proteins during physiological conditions proposed to regulate the operation of the NAD(P)H dehydrogenase.

For the first part, inhibition by SHAM on the photosynthetic electron transfer chain was shown to be in the vicinity of Q_A using oxygen electrode and fluorescence analysis, and a number of specific photosynthetic electron acceptors, donors and inhibitors in order to isolate specific parts of the photosynthetic electron transfer chain. By the analysis of electron transfer through the whole chain, PS I, PS II and electron transfer from P680 through to Q_A, inhibition by SHAM was shown to be in the vicinity of Q_A. These observations are consistent with the reported effects on chlorophyll fluorescence, but do not exclude the existence of an alternative oxidase in the thylakoid membrane.

To examine the accumulation of the NAD(P)H dehydrogenase complex, antibodies to the NDH-F subunit from barely and the NDH-K subunit from pea were used. Preliminary experiments revealed that the NDH-F antibodies recognised a protein of 79 kDa in isolated silverbeet thylakoid membranes, and the NDH-K antibody recognised a 28 kDa in a preparation of extracted thylakoid membrane proteins from silverbeet. In etiolated silverbeet seedlings, a protein of 31 kDa was recognised by the NDH-K antibody. This recognition was lost in the seedlings following exposure to 12 h and

24 h of light. A protein of 33.1 kDa was recognised by the NDH-K antibody in leaves harvested over a 24 hour period, with no notable difference in level of accumulation throughout the day/night periods. During leaf development in white clover, a protein of 69 kDa, which was more prevalent in senescent leaves, was recognised by the NDH-F antibody, while the NDH-K antibody recognised a protein of 35 kDa that was more prevalent in mature, photosynthetically competent leaves. These results are evaluated in terms of providing evidence for the developmental regulation of chlororespiration in chloroplasts of silverbeet and white clover.

ACKNOWLEDGEMENTS

I would like to say a HUGE thank you to both my supervisors Dr Simon Brown and Dr Michael McManus. Michael, thank you for all your amazing support. I simply can't find words to thank you enough, I know it was tough!!! Simon, thank you also, so much, for believing in me, especially when I had doubts.

I would also like to thank Chris, Trish McLenachan, Liz, Alicia, Richard, Anya and Trish, who gave their time and skill in helping with practical issues. To the people in Michaels lab, who made me smile and helped me keep as sane as possible - Ning (my midnight lab buddy), Balance (thanks for the chocolate!!!!), Trish (thanks for all your wise words!), Vicki, Alicia, Anya, Ranjith, Richard, Simone and Adam. Thank you guys!

Porki, porki, porki. You are the most amazing person I have ever been lucky enough to have in my life. Thanks for all the time you have given to help me in SO many ways. Ahhhh the pool games, the V, and more V, and some more V (and the sing alongs!!) and the welly trips. Te hiki piranga te hoki mo te horo te horo!!!!!! ☺

Thanks to frucor, for the invent of the wonderous liquid, V, and to Tool, u were necessary! I need to give gynaforous hugs and kisses to those of you who, in the last three years, have looked after me. Thanks to Rob, Esther, Neil, Garreth and Lala for the numerous coffees, lunches and chats. To Kerry for your help when I asked! To God who somehow kept me at it! And BIG hugs for Wayne-o, Catherine, Adrian, Duncan, John, and Paul for kind (and stern) words when I needed it, and your love (which I always need). I love you, I love you, I love you!! ♥

Finally, but equally as important, thanks to my family especially my Momma and Dad for their financial assistance!!!!! To Nana and Poppie for your support and love. This is for you. Thank you, thank you, thank you! ☺

I would also like to take this opportunity to thank the Massey University Alumni Association and the J.P. Skipworth Scholarship for financial assistance during the course of this work.

Without everyones support this would not be here now. Actually, I think I may not be here now!!!! God bless you all.

XXX

TABLE OF CONTENTS

LIST OF FIGURES

Page

LIST OF TABLES

CHAPTER 1 INTRODUCTION

1.1 Overview of Photosynthesis

Photosynthesis is the essential, light-driven process, where plants synthesise carbon-rich compounds from atmospheric CO_2. Energy necessary for this process is obtained from sunlight, which is converted into chemical energy by the enzymes of the photosynthetic electron transfer chain. These enzymes are located in and around the thylakoid membrane of chloroplasts in both photosynthetic algae and plants (Figure 1.1). The enzymes that catalyse the assimilation of CO_2 are located in the stroma.

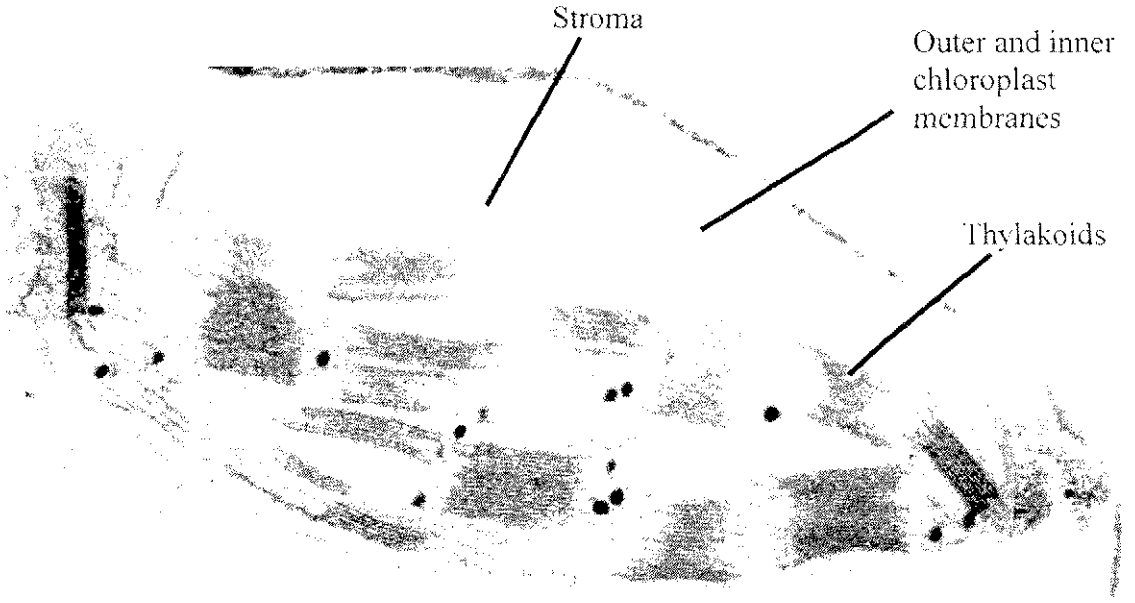

Figure 1.1. A higher plant chloroplast visualised using SEM. Photosynthetic electron transfer reactions occur in and around the thylakoid membrane and CO_2 assimilation occurs in the stroma. The black spots within the chloroplast are starch grains. (Picture courtesy of M. Christiansen, AgResearch, Palmerston North, New Zealand)

1.1.1 Photosynthetic Electron Transfer

Photosynthesis involves the light-initiated transfer of electrons, down a redox potential gradient, from a reduced electron carrier (donor) to an oxidised electron carrier (acceptor). This transfer is driven by the redox potential difference between the acceptor and the donor. Photosynthetic electron transfer involves three protein complexes, photosystem (PS) II, cytochrome b_6f and PS I (Figure 1.2).

Initiation of electron transfer is by the excitation of a special pair of chlorophyll molecules, called P680, which are located in the PS II protein complex that spans the thylakoid membrane. This process depends on the absorption of light energy by chlorophyll molecules, that with specific binding proteins are associated with PS II in the thylakoid membrane, which then transfer the absorbed energy to P680. The excited P680 ($P680^*$) loses an electron to the first in a series of electron carriers, thereby becoming highly oxidised ($P680^+$). $P680^+$ is highly oxidising, so rapidly gains another electron to return to its reduced state. The electron is acquired from the process of water splitting (Equation 1) which is mediated by a lumenal protein complex associated with PS II called the oxygen-evolving complex (OEC).

$$\mathbf{2H_2O + 4\ photons \rightarrow 4H^+ + 4e^- + O_2} \qquad \mathbf{(1)}$$

The electron released by P680 passes down a redox potential gradient, through PS II, and then reduces the mobile electron carrier plastoquinone (PQ). Reduced PQ (plastoquinol or PQH_2) is oxidised by the cytochrome b_6f complex, which reduces plastocyanin (PC), another mobile electron carrier. At this stage, a second special pair of chlorophyll molecules, called P700, located in the second photosystem (PS I), are oxidised by the absorption of a photon. As with $P680^+$, $P700^+$ must be reduced, and PC provides the electron. Electron transfer continues from P700 to the terminal electron acceptor, ferredoxin (Fd), which is a powerful reductant. Ferredoxin can now participate in one of two reactions: the first is as a substrate of ferredoxin: $NADP^+$ reductase (FNR) to reduce $NADP^+$ and complete linear electron transfer, or alternatively, as a substrate

of the enzyme ferredoxin: quinone reductase (FQR) to complete cyclic electron transfer as PQ is reduced (Figure 1.2).

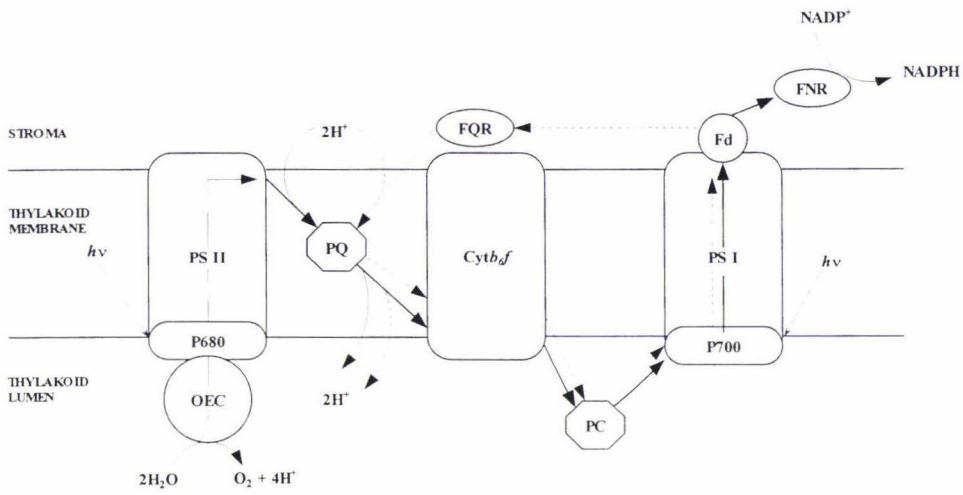

Figure 1.2. Diagrammatic representation of photosynthetic electron transfer chain in higher plants. Electron transfer is initiated by a photon absorbed by P680. There are two pathways of photosynthetic electron transfer, the linear pathway (solid lines) and the cyclic pathway (dashed lines). Abbreviations: OEC, oxygen evolving complex; PS II, photosystem II; PQ, plastoquinone; PC, plastocyanin; PS I, photosystem I; Fd, ferredoxin; FNR, ferredoxin:$NADP^+$ reductase; FQR, ferredoxin: quinone reductase.

In association with electron transfer is the coupled translocation of protons across the thylakoid membrane from the stroma to the thylakoid lumen, generating a proton electrochemical potential ($\Delta\mu_{H+}$). The $\Delta\mu_{H+}$ drives the synthesis of ATP, from ADP + P_i by the ATP synthase complex.

1.2 Overview of Mitochondrial Respiration

Mitochondrial electron transfer is analogous to photosynthetic electron transfer in that it involves the transfer of electrons, through a series of enzymes, from an electron donor (reduced substrates such as NADH and succinate) to an electron acceptor (O_2). The

enzymes involved in the respiratory chain are located in the inner mitochondrial membrane (Figure 1.3).

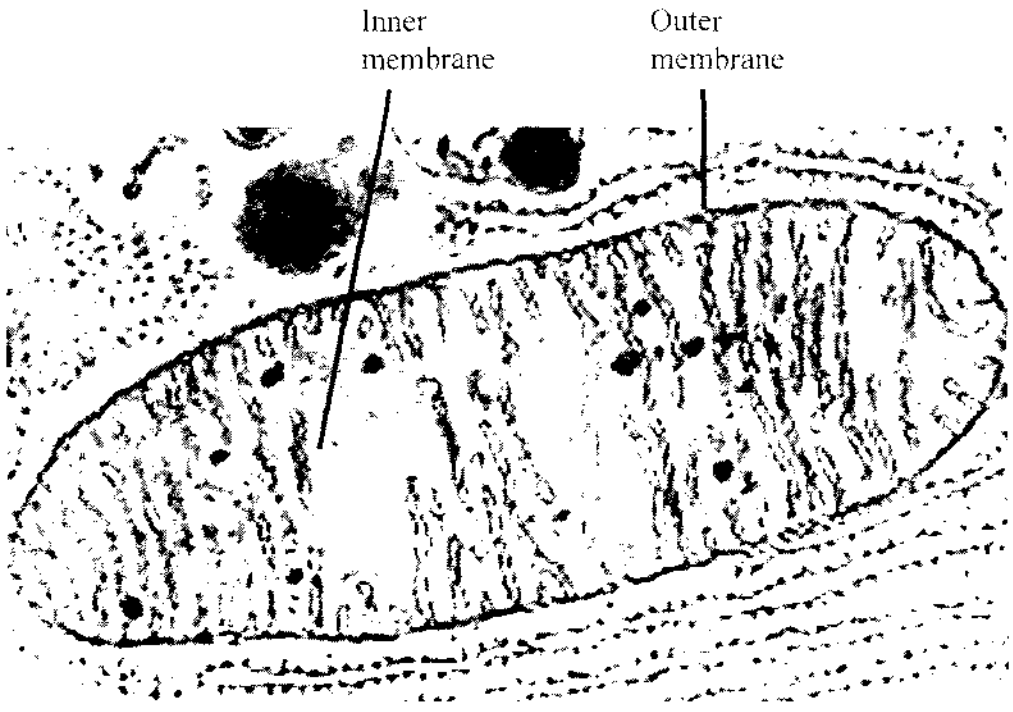

Figure 1.3. A mitochondrion visualised using SEM. The respiratory electron transfer chain enzymes are located in the inner mitochondrial membrane (Microsoft® Encarta® Online Encyclopaedia 2001).

1.2.1 Respiratory Electron Transfer

As in photosynthetic electron transfer, the respiratory reactions involve the transfer of electrons down a redox potential gradient, which is coupled to the generation of $\Delta\mu_{H^+}$ (via proton translocation across the membrane), which drives ATP synthesis (among many other processes). The enzymes coupled to ATP synthesis (by $\Delta\mu_{H^+}$) are: NADH dehydrogenase, the cytochrome bc_1 complex and cytochrome oxidase (Figure 1.4). Although the respiratory chains of plants and other eukaryotes are similar, plant mitochondria, like some fungal mitochondria, have an additional terminal oxidase in their chain, which is known as the alternative oxidase (AOX). Plant mitochondria also

have an NADH dehydrogenase on the external face of the inner membrane and a rotenone-insensitive NADH dehydrogenase.

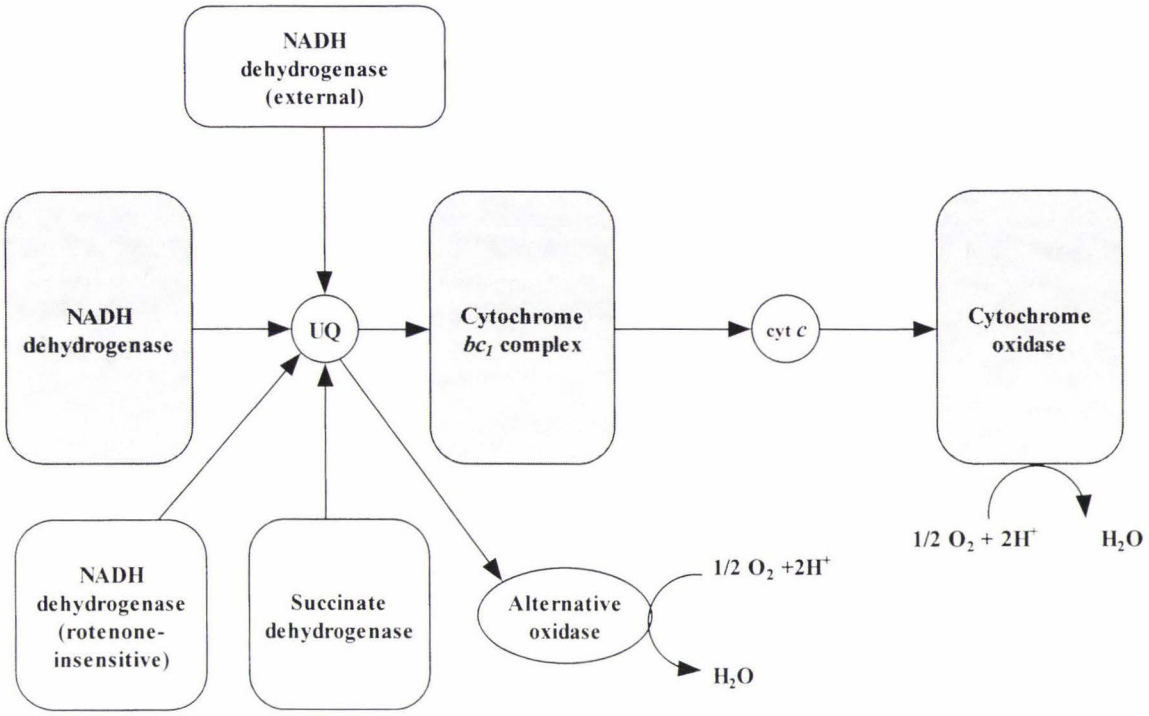

Figure 1.4. Diagrammatic representation of the plant mitochondrial respiratory electron transfer chain. The enzymes that contribute to $\Delta\mu_{H+}$ are shaded. The localisation of each enzyme in the mitochondrial membrane is not shown. Abbreviations: UQ, ubiquinone; cyt c, cytochrome c.

The two main substrates of the respiratory electron transfer chain are succinate, an intermediate of the tricarboxylic acid cycle, and NADH. The oxidation of NADH or succinate is catalysed by NADH dehydrogenase or succinate dehydrogenase (SDH), respectively. Both NADH dehydrogenase and SDH transfer electrons to ubiquinone (UQ), yielding ubiquinol (UQH_2). UQH_2 can be oxidised by either the AOX (which then reduces molecular oxygen), or by the cytochrome bc_1 complex. The cytochrome bc_1 complex reduces cytochrome *c* (cyt *c*), which is oxidised by cytochrome *c* oxidase, which in turn reduces molecular oxygen to water.

1.3 Chlororespiration

The photosynthetic and respiratory electron transfer chains have a number of strong similarities that include the involvement of a membrane-bound electron transfer chain coupled to the generation of ATP by $\Delta\mu_{H+}$, similar components such as quinones, the cytochrome bc_1/b_6f complexes and an ATP synthase, and in each, the reactions occur in distinct closed membrane systems - i.e. the thylakoid membranes and mitochondria.

However, Bennoun (1982) observed further that the photosynthetic PQ pool in the thylakoid membranes of *Chlamydomonas reinhardtii*, was partially reduced in the dark by a stromal reductant and after a short period was re-oxidised. On the basis of these observations, Bennoun (1982) proposed the operation of a respiratory chain in the thylakoid membrane that is involved in a process termed chlororespiration. Inhibitor studies using algae have shown that the chlororespiratory and photosynthetic pathways interact through a common intermediate, namely PQ (Bennoun, 1982; Godde, 1982; Buchel and Garab, 1995; Cournac *et al.*, 2000). Godde and Trebst (1980) first found evidence for an NADH dehydrogenase enzyme in the thylakoid membranes of the photosynthetic algae *C. reinhardtii* and *Chlorella*. This enzyme has homology with the mitochondrial NADH dehydrogenase, and is thought to be responsible for the reduction of PQ in the dark (Cuello *et al.*, 1995a). The competition between chlororespiratory and photosynthetic electron transfer chains in higher plants and algae is proposed to be a similar mechanism to that of respiration and photosynthesis in cyanobacteria (Lajko *et al.*, 1997). This competition is most prevalent in chloroplasts under stress, at which time an increase in chlororespiratory activity and a decline in photosynthesis is observed.

It has been suggested that a terminal oxidase is also involved in the chlororespiratory pathway (Bennoun, 1982; Bennoun, 1994). This oxidase is proposed to be involved in the oxidation of PQH_2, with the concomitant consumption of O_2. Some work has been done to characterise the chlororespiratory oxidase both in algae, cyanobacteria and higher plants, but any definitive characterisation remains elusive. A conceptual model

of the chlororespiratory electron transfer chain and its interaction with the photosynthetic electron transfer chain is shown (Figure 1.5).

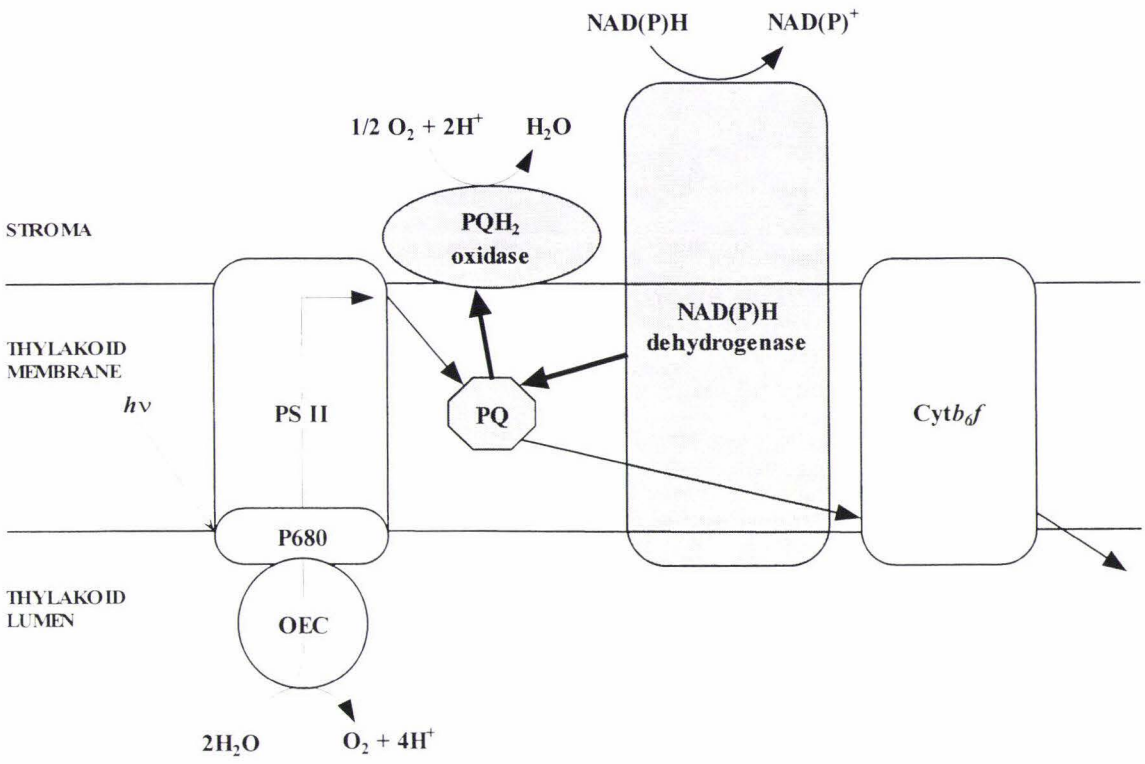

Figure 1.5. Diagrammatic representation of the interaction between the chlororespiratory and photosynthetic electron transfer chains. Interaction between the two pathways occurs at PQ. The shaded enzymes are thought to be involved in the proposed chlororespiratory chain of higher plants.

Interaction between the chains occurs (at least) at PQ, where in chlororespiration, the PQ pool is reduced by electrons from NAD(P)H which was oxidised by the NAD(P)H dehydrogenase. Plastoquinol can be oxidised by the putative terminal oxidase, with the consumption of molecular oxygen. In photosynthesis however, electrons are donated to PQ by PS II or FQR and are transferred to cytb_6f and continue through the rest of the photosynthetic chain (Section 1.1).

Initial studies on chlororespiration focused on the unicellular green alga, *Chlamydomonas reinhardtii* (Bennoun, 1982; Peltier *et al.*, 1987). However, it has also been proposed that the pathway occurs in higher plant chloroplasts (Bennoun, 1982). Increasingly, evidence has accumulated in support of this hypothesis in a variety of plant species including tobacco (Garab *et al.*, 1989; Lajko *et al.*, 1997), pea (Sazanov *et al.*, 1998b), spinach (Asada *et al.*, 1992) and sunflowers (Groom *et al.*, 1993; Field *et al.*, 1998). It has been calculated that chlororespiration accounts for 10-20% of total cell respiration (Bennoun, 1982; Field *et al.*, 1998), reducing approximately 160 nmol O_2 min^{-1} mg^{-1} chl. (Corneille *et al.*, 1998).

1.4 Respiratory Enzymes in the Chloroplast

Studies characterising components involved in the chlororespiratory chain have indicated two enzymes that have the potential to reduce the PQ pool, NAD(P)H dehydrogenase and succinate dehydrogenase. In contrast, little is known about possible PQ oxidases that would oxidise PQH_2 and reduce O_2, although a possible AOX-like enzyme has been postulated to be the terminal oxidase of the chlororespiratory pathway (Carol *et al.*, 1999; Wu *et al.*, 1999).

1.4.1 NAD(P)H Dehydrogenase

Evidence supporting the existence of a NAD(P)H dehydrogenase complex in the chloroplast, and its involvement in chlororespiration, is based on two lines of experimentation: molecular and kinetic studies.

1.4.1.1 Evidence From Molecular Studies

The chloroplast genome in a large number of plants, including *Marchantia polymorpha* and tobacco (Ohyama *et al.*, 1986; Matsubayashi *et al.*, 1987; Ohyama *et al.*, 1988), contains eleven genes (*ndhA-K*) that have a high degree of homology to genes that encode subunits of the mitochondrial NADH dehydrogenase (Berger *et al.*, 1993).

The mitochondrial NADH dehydrogenase catalyses electron transfer from NADH to UQ, generating $\Delta\mu_{H^+}$ due to proton translocation across the inner mitochondrial membrane. Chloroplast encoded *ndh* genes have been shown to be actively transcribed in a number of higher plants (Matsubayashi *et al.*, 1987), and an NAD(P)H dehydrogenase complex has been isolated from chloroplasts isolated from a number of plant species including barley (Cuello *et al.*, 1995a; Catala *et al.*, 1997), potato (Guedeney *et al.*, 1996) and pea (Elortza *et al.*, 1999). Immunolocalisation of some of the subunits have shown the NAD(P)H dehydrogenase complex to be located in the stromal lamellae of the thylakoid membrane, with subunits NDH-A through to NDH-G embedded in the membrane, and NDH-H through to NDH-K attached to the membrane, exposed to the stroma (Figure 1.6; Berger *et al.*, 1993; Catala *et al.*, 1997; Quiles and Cuello, 1998). NAD(P)H dehydrogenase activity has been detected in barley chloroplasts (Vera *et al.*,1990). The complex is present in low levels, with an estimate of 1 NAD(P)H dehydrogenase complex per 50-100 PS II complexes (Burrows *et al.*, 1998).

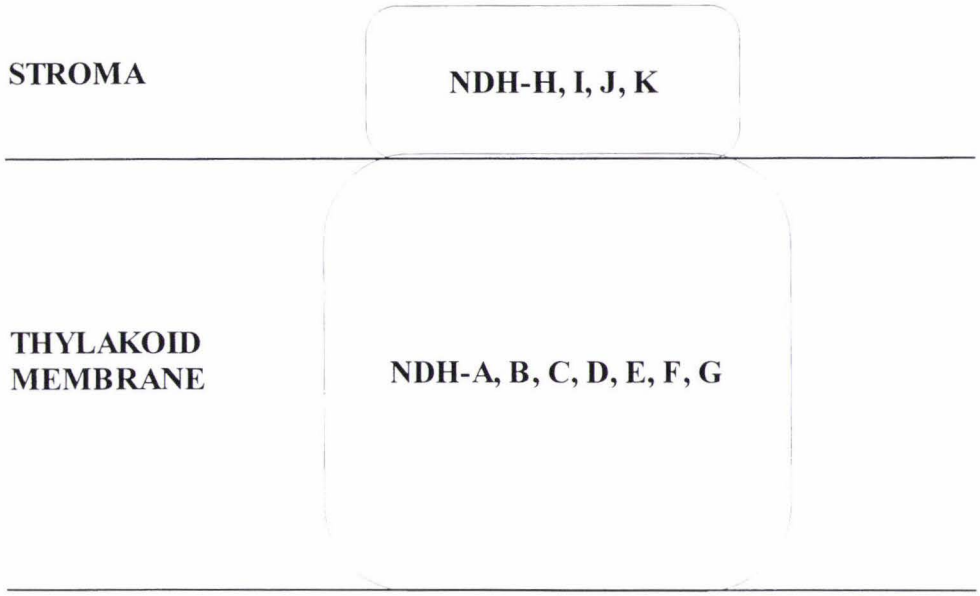

Figure 1.6. Schematic representation of the chloroplastic NAD(P)H dehydrogenase complex of higher plants. To date, 11 proteins have been identified in the complex, with NDH-A to NDH-G located in the thylakoid membrane, and NDH-H to NDH-K located on the stromal lamellae of the membrane.

Recent studies investigating the requirement of a whole, functional NAD(P)H dehydrogenase in the chloroplasts of higher plants have shown that under favourable, unstressed conditions, plants lacking a functional NAD(P)H dehydrogenase still exhibit normal growth (Sazanov *et al.*, 1998a). However, when the mutant plants are placed under physiological stress, or when all *ndh* genes are deleted, plants are rendered non-viable (Kofer *et al.*, 1998; Shinakai *et al.*, 1998; Horvath *et al.*, 2000)

These data strongly support the presence and importance of an active large, multi-subunit complex, which catalyses the oxidation of NAD(P)H, with a location in the stromal lamellae of the thylakoid membrane. Genes of the chloroplast NAD(P)H dehydrogenase have homology to the mitochondrial NADH dehydrogenase genes, lending further support for the function of this chloroplast enzyme as a donor of electrons to PQ.

1.4.1.2 Evidence From Kinetic Studies

Studies on the mechanism of action of the chloroplastic NADH dehydrogenase complex have involved the use of photosynthetic inhibitors such as DCMU (Bennoun, 1994; Corneille *et al.*, 1998), which inhibits electron flow from PS II to PQ, and mitochondrial NADH dehydrogenase inhibitors including amytal (Endo *et al.*, 1998) and rotenone (Corneille *et al.*, 1998).

The mitochondrial NADH dehydrogenase has a NADH-oxidising subunit responsible for the oxidation of NADH. In the chloroplast NAD(P)H dehydrogenase, no NADH oxidising subunit has been identified. The apparent lack of a NADH-oxidising subunit suggests that either NADH is not the substrate for the chloroplastic complex, or that another enzyme operates in co-operation with the NAD(P)H dehydrogenase (Friedrich *et al.*, 1995).

Two proposals for oxidation by the chloroplast NAD(P)H dehydrogenase complex have been put forward based on isolation and purification studies. The first proposes that the NAD(P)H dehydrogenase complex is associated with the FNR enzyme, implying that the preferred substrate for the chlororespiratory pathway is NADPH as this is the substrate for FNR (Quiles and Cuello, 1998). Support for this hypothesis comes from studies that demonstrate PQ reduction upon addition of NADPH and ferredoxin to a suspension of ruptured chloroplasts (Endo *et al.*, 1998), where the addition of NADPH alone didn't induce PQ reduction. Guedeney *et al.* (1996) probed the NDH activity band with antibodies raised against NDH subunits and antibodies raised against FNR and found that both recognised the activity band, thus proposing co-precipitation of the two enzymes. The second proposal suggests that the NAD(P)H dehydrogenase is not associated with the FNR enzyme, and that NADH is the preferred substrate (Seidelguyenot *et al.*, 1996; Corneille *et al.*, 1998; Elortza *et al.*, 1999). NADH required for this proposed mechanism is provided by starch degradation (Bennoun, 1982; Sazanov *et al.*, 1998a). Support for this hypothesis includes studies that show concomitant decreases in starch concentration and chlororespiratory activity, 4 hours after the beginning of the dark period (Buchel and Garab, 1995).

pool in the light (Willeford *et al.*, 1989), contrary to the present chlororespiratory paradigm of PQ reduction in the dark.

1.4.3 Chlororespiratory Oxidase

The specific oxidase of this pathway is as yet unknown, although it has been widely assumed that such an oxidase may be homologous to a mitochondrial respiratory oxidase due to the similarity between the mitochondrial respiratory and the chlororespiratory pathways. Evidence for the presence and activity of a chlororespiratory oxidase are, again, based on two kinds of experimentation; kinetic studies, which involve the use of various substrates and specific inhibitors, and molecular studies which focus on the isolation and characterisation of the oxidase gene(s) and protein(s).

1.4.3.1 Evidence From Kinetic Studies

These studies have generally involved the use of mitochondrial respiratory oxidase inhibitors. As discussed in Section 1.2.1, the plant mitochondrial respiratory electron transfer chain involves two oxidases, a cytochrome *c* oxidase (COX), and an alternative oxidase (AOX). These oxidases are distinguishable from each other on the basis of their different inhibitor sensitivities and substrate specificities. The AOX is cyanide-insensitive and salicylhydroxamic acid (SHAM)-sensitive, whereas COX is cyanide-sensitive and SHAM-insensitive. Cytochrome oxidase is also sensitive to a number of other inhibitors that include azide, CO and NO (Table 1.1).

Table 1.1. Characteristics of the alternative oxidase and the cytochrome oxidase of plant mitochondria. Abbreviations: O_2, oxygen; SHAM, salicylhydroxamic acid; KCN, cyanide; NO, nitric oxide; CO, carbon monoxide; Fe, iron; Cu, copper.

Characteristic	Alternative Oxidase (AOX)	Cytochrome Oxidase (COX)
No. of subunits	2 (both nuclear genes)	15 (3 mitochondrial genes + 12 nuclear genes)
Specific substrate	Ubiquinol, O_2	Cytochrome c, O_2
Inhibitor sensitivity	SHAM, propyl gallate, disulfiram	KCN, NO, CO, azide
Prosthetic groups	2 Fe atoms	Haem *a*, haem a_3, Cu_A (2 Cu atoms), Cu_B (1 Cu atom)

Bennoun (1982) carried out fluorescence measurements on dark-adapted algal cells using the oxidase inhibitors listed in Table 1.1. In all cases an increase in fluorescence was observed, which is characteristic of electron accumulation in PS II and PQ due to the restriction of electron flow. This increase was interpreted in terms of the inhibitors blocking the oxidase, thereby eliminating electron flow from PQH_2 to the chlororespiratory oxidase. From these results it was hypothesised that an oxidase, homologous to a mitochondrial oxidase, was involved in the chlororespiratory electron transfer chain, though this oxidase has a lower affinity for oxygen than the mitochondrial enzyme (Bennoun 1982; Bennoun, 1994). A number of other studies have been carried out which also use the oxidase inhibitors, primarily cyanide (Buchel and Garab, 1995; Buchel *et al.*, 1998), SHAM (Maione and Gibbs, 1986; Peltier *et al.*,

1987; Casper-Lindley and Bjorkman, 1996), and *n*-propyl-gallate (Josse *et al.*, 2000). Results from these studies have shown the putative plastid terminal oxidase to be cyanide-sensitive (Garab *et* al., 1989; Buchel *et* al., 1998; Josse *et al.*, 2000), and *n*-propyl-gallate-sensitive (Josse *et al.*, 2000). Results from studies using the mitochondrial AOX inhibitor, SHAM are inconclusive as some have shown the oxidase to be SHAM-insensitive (Peltier *et al.*, 1987; Buchel *et al.*, 1998), while others have shown it to be SHAM-sensitive (Bennoun, 1982; Garab *et al.*, 1989).

1.4.3.2 Genetic Experiments

A possible identity of the putative chlororespiratory oxidase has come from genetic studies using the *Arabidopsis thaliana* mutant, IMMUTANS (Carol *et al.*, 1999; Wu *et al.*, 1999). This mutant exhibits a variegated phenotype. It was shown that the green sectors were the wild type genotype, while the white sectors contained abnormal, pigment-deficient chloroplasts. The *IMMUTANS* (*IM*) gene encodes a 40.5 kDa protein that has limited similarity to the mitochondrial AOX, although it is functionally similar (Wu *et al.*, 1999; Josse *et al.*, 2000). It has been hypothesized that one of the functions of the IM protein is essential in the prevention of photo-oxidative damage in the early stages of chloroplast development (Carol *et al.*, 1999; Wu *et al.*, 1999; Josse *et al.*, 2000). Immunolocalisation of the terminal oxidase to the stromal lamellae of the thylakoid membrane has been suggested (Carol *et al.*, 1999).

Experiments *in vitro*, and computer analysis of the transit peptide suggest the IM protein is synthesized in the nucleus, imported into the chloroplast and embedded into the thylakoid membrane, alongside the photosynthetic and chlororespiratory proteins (Carol *et al.*, 1999). Josse *et al.* (2000) expressed the *IM* gene in *Escherichia coli* and showed that 2mM cyanide inhibited O_2 consumption by approximately 80%, thus implying an oxidase function for the IM protein. Josse *et al.* (2000) did not report on the effect of SHAM on the O_2 consumption by IM. Further work is required to determine the exact role of this protein in the chloroplast, and the possible lack of chlororespiratory activity needs to be analysed in the white sectors of the mutant.

1.5 The Possible Functions of Chlororespiration

The functional significance of chlororespiration is uncertain, but a number of roles have been postulated. Firstly, it has been suggested that chlororespiration is highly active during periods of extreme environmental stress (Garab *et al.*, 1989), and that during "unstressed" periods, this pathway is not necessary for plant viability (Burrows *et al.*, 1998; Sazanov *et al.*, 1998a). Forms of "stress" that cause an increase in chlororespiratory activity include: high light and nitrogen-limitation (Peltier and Schmidt, 1991), carbon dioxide limitation (Horvath *et al.*, 2000), water deficit stress (Burrows *et al.*, 1998), and heat stress (Lajko *et al.*, 1997; Sazanov *et al.*, 1998a). Secondly, chlororespiration could be involved in the development of the chloroplast, from the immature etioplast through to a senescent chloroplast (Cuello *et al.*, 1995b; Catala *et al.*, 1997). A third proposed function of chlororespiration is that the *ndh* gene products are involved in the photosynthetic metabolism of green plants (dePamphilis and Palmer, 1990).

1.5.1 Environmental Stresses

1.5.1.1 High-Light Damage

High levels of light can cause irreversible damage to PS II due to excess photons entering the photosynthetic electron transfer chain at P680. Chlororespiration has been proposed to eliminate some of this stress by oxidising the PQH_2 pool via the chlororespiratory oxidase. Oxidation of the PQH_2 pool allows more electrons to leave PS II and flow through the photosynthetic electron transfer chain, hence preventing over-reduction of PS II (Damdinsuren *et al.*, 1995). Tobacco plants deficient in the chloroplastic NAD(P)H dehydrogenase were subjected to supra-saturating levels of light, and the levels of photoinhibition and physiological damage compared to wild-type plants. The mutant tobacco plants demonstrated a more severe photoinhibition of PS II, and a lower rate of recovery from the treatment than the wild-type controls (Horvath *et al.*, 2000). These results are consistent with a role of chlororespiration in relieving the

photosynthetic electron transfer chain of excess electrons, thereby protecting PS II from irreversible damage (photoprotection).

1.5.1.2 Nitrogen Limitation

Photosynthetic and chlororespiratory electron transfer pathways are differentially regulated by nitrogen availability (Peltier and Schmidt, 1981). A 1.5- to 2-fold increase in the rate of chlororespiration can be seen in nitrogen-limited *Chlamydomonas* cells, in association with a 7- to 8-fold decrease in the photosynthetic rate (Peltier and Schmidt, 1991). This response may be expected as nitrogen limitation causes an increase in the levels of starch. This increase will induce an increase in starch degradation, causing elevated levels of NADH, a potential substrate of the chlororespiratory NADH dehydrogenase enzyme.

1.5.1.3 Carbon Dioxide Limitation

Tobacco mutants lacking a functional NAD(P)H dehydrogenase complex (Δ*ndhB*) were analysed phenotypically and by fluorescence under conditions of limited carbon dioxide. Mutant plants exhibited retarded growth and impaired reduction of PQ in the dark (Horvath *et al.*, 2000). Interestingly, under favourable conditions, no significant phenotypic effect was observed. It was suggested from these results that the chloroplastic NAD(P)H dehydrogenase is necessary during periods of limited carbon dioxide but is not necessary for growth in favourable environmental conditions.

1.5.1.4 Heat Stress

Incubation of *Chlamydomonas* at higher temperatures (30°C to 50°C) causes an increase in chlororespiratory electron transfer, while suppressing photosynthetic electron transfer (Lajko *et al.*, 1997). A similar heat stress response of chlororespiration, in the dark, has also been observed in tobacco (Sazanov *et al.*, 1998a). As electron flow through the photosynthetic chain is slowed in elevated temperatures regardless of the number of electrons entering the chain, the chlororespiratory oxidase acts as an alternative route for the electrons, thereby assisting in the protection of PS II.

1.5.2 Developmental Regulation

Catala *et al.* (1997) hypothesised that chlororespiration was most active in non-functional chloroplasts, such as etioplasts (non-green, non-functional chloroplasts) and senescent chloroplasts, while being only minimally active in mature, fully-functional chloroplasts. Evidence in support of this hypothesis includes studies that show an increase in expression of some *ndh* genes during senescence (Vera *et al.*, 1990), and a higher level of chloroplast NADH dehydrogenase activity has been observed in older, senescent leaves (Cuello *et al.*, 1995a). A higher accumulation of some of the NDH proteins is also observed in etioplasts and senescent tissues (Berger *et al.*, 1993; Guera *et al.*, 2000). Additional support for a developmental role of chlororespiration can be seen in many gymnosperms, including *Pinus thunbergii*, which lack all or many *ndh* genes (Wakasugi *et al.*, 1994). Gymnosperm chloroplasts do not go through a developmental stage where they are non-photosynthetic (either developing chloroplasts (etioplasts) or senescent chloroplasts), therefore not requiring the chlororespiratory pathway. Other plant species lacking some or all of the chloroplast *ndh* genes include the holoparasitic plant *Cuscuta reflexa* (Haberhausen and Zetsche, 1994), and the non-photosynthetic parasitic plant *Epifagus viginiana* that has lost all of the *ndh* genes as well as all of the photosynthetic genes from its chloroplast genome (dePamphilis and Palmer, 1990; Wolfe *et al.*, 1992).

1.5.3 Evidence for a Photosynthetic Metabolism Role of Chlororespiration

Photosynthetic metabolism will involve the recycling of NADH produced from the degradation of starch, and NADPH which is a product of photosynthesis (dePamphilis and Palmer, 1990). Chlororespiration is proposed to oxidise this NADH/NADPH (Sazanov *et al.*, 1998a). As NADPH:$NADP^+$ ratios are tightly regulated in chloroplasts, due to efficient carbon fixation that relies on specific ratios of these compounds, it is proposed this metabolic function is necessary. An increase in fluorescence is seen in the 4 hours following dark adaption, which corresponds to the time scale of high levels of starch degradation in tobacco. This increase in fluorescence disappears after

approximately 4 hours in the dark, therefore it is proposed that chlororespiration utilises the NADH produced from starch degradation (Sazanov *et al.*, 1998).

1.6 Salicylhydroxamic Acid

Salicylhydroxamic acid (SHAM) is a small, hydrophobic molecule that is capable of chelating Fe (Springer *et al.*, 1987; Figure 1.7). It is a commonly used potent inhibitor of the mitochondrial AOX, although the mechanism of inhibition is relatively unknown. It is due to its inhibitory properties in mitochondria that SHAM has been utilised in studies investigating the chlororespiratory terminal oxidase (Bennoun, 1982). A major discrepancy in these studies is that the photosynthetic and mitochondrial respiratory pathways are analogous, and so it is conceivable that some of the mitochondrial respiratory oxidase inhibitors might have an inhibitory effect on various sites of the photosynthetic chain. As yet, very little is known about the possible photosynthetic inhibitory effects of these mitochondrial inhibitors, despite the finding of a potential inhibitory effect of SHAM on photosynthesis (Diethelm *et al.*, 1990).

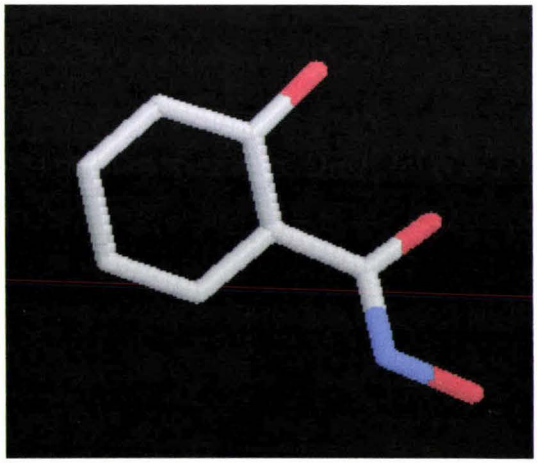

Figure 1.7. Stick model of salicylhydroxamic acid. Carbon – white, oxygen – red, nitrogen – blue. Figure taken from the protein data bank (PDB) and visualised using Rasmol software (Berman *et al.*, 2000).

1.7 Aims

Salicylhydroxamic acid (SHAM) is a potent inhibitor of the mitochondrial AOX. Recently, studies examining the enzymes involved in chlororespiration have utilised this mitochondrial inhibitor on the premise that it should have similar inhibitory effects on the chloroplast respiratory chain, inhibiting a possible AOX (Bennoun, 1982). However, no work has yet been undertaken to determine whether SHAM has any effect on photosynthetic electron transfer. For the first part of this thesis, therefore, the inhibitory properties of the mitochondrial AOX inhibitor, SHAM on the photosynthetic chain are examined.

In parallel research, eleven genes (*ndhA-K*), homologous to genes encoding the mitochondrial NADH dehydrogenase (complex I) of the respiratory chain, have been identified in the chloroplast genome (Matsubayashi *et al.*, 1987; Ohyama *et al.*, 1988). These genes are transcribed and the proteins assembled into a multi-subunit complex, located in the thylakoid membrane (Berger *et al.*, 1993). The exact nature and function of this protein complex is not fully understood. However, it is widely assumed to be involved in the chloroplastic respiratory electron transfer pathway (Berger *et al.*, 1993). Regulation of the chloroplastic NAD(P)H dehydrogenase complex is still largely unknown, although the complex has been shown to be most active in chloroplasts with limited photosynthetic capacity (Vera *et al.*, 1990; Catala *et al.*, 1997), and also in mature chloroplasts in the four hours following sunset (Sazanov *et al.*, 1998a). For the second part of this thesis, the regulation of two subunits of the chloroplast NAD(P)H dehydrogenase, NDH-F and NDH-K at the level of protein expression is investigated. Specifically, the accumulation of these two subunits over a 24-hour time period and at various stages of leaf development is examined.

CHAPTER 2 MATERIALS AND METHODS

2.1 Chemicals

Unless otherwise stated, the chemical reagents used were at least analytical grade, obtained from either BDH Laboratory Supplies (Poole, Dorset, England) or Sigma Chemical Company (St. Louis, Mo, USA). All solutions were made up in MilliQ water unless otherwise specified, and stored at either 4°C or room temperature as required.

2.2 Plant Material

2.2.1 Silverbeet

Silverbeet (*Beta vulgaris* var. Fordhook) was grown in the field for the bioenergetic studies, and in a greenhouse (see Section 2.2.2) for the biochemical and molecular analysis. In addition to the glasshouse conditions described in Section 2.2.2, silverbeet plants were grown under a controlled light period (14 hours) from 6 am through to 8 pm and watered appropriately.

2.2.2 White Clover

White clover (*Trifolium repens* (L.) cv. Grasslands Challenge, genotype 10F (AgResearch Grasslands, Palmerston North, New Zealand; Figure 2.1) was grown in a greenhouse, using a horticultural grade bark/peat/pumice (Dalton Nursery Mix, Tauranga, New Zealand) mixed in a ratio of 50:30:20 with the addition of nutrients (3 gL^{-1} dolmite, 3 gL^{-1} agricultural lime, 0.5 gL^{-1} iron sulphate, 50 gL^{-1} osmocote) at the Plant Growth Unit, Massey University, Palmerston North, New Zealand (Figure 2.1). The greenhouse was temperature-controlled with a minimum of 12°C (night) and 18°C (day), and venting at 25°C. Plants were automatically irrigated for 5 minutes at 10 am

and again at 5 pm using a timer-controlled mist watering system (Automation Services Ltd., Auckland, New Zealand). Aphids and white fly were controlled by spraying with the insecticide Attack® (Crop Care Holdings Ltd., Richmond, Nelson, New Zealand), and blackspot was controlled by Benlate (Du Pont de Nemours and Co., In., USA).

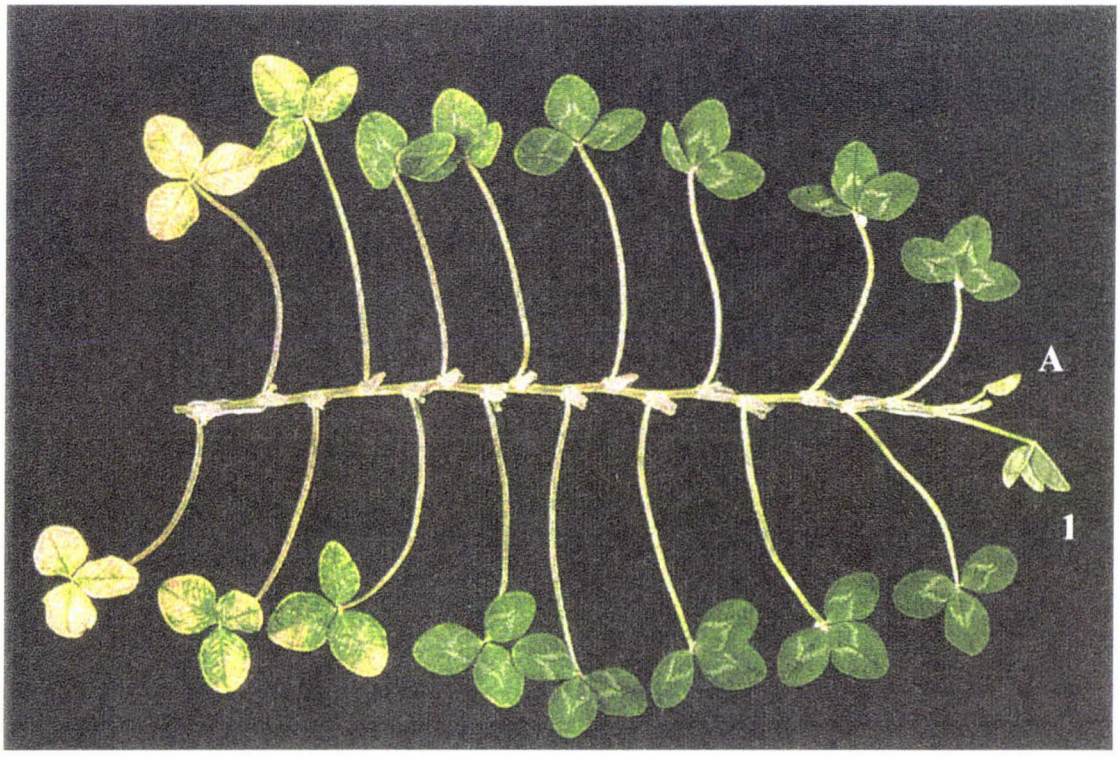

Figure 2.1. An excised white clover stolon displaying various stages of leaf development. The apex (A) and leaf 1 (1) are indicated.

2.3 Preparation of Samples

2.3.1 Preparation of Intact Chloroplasts

Intact chloroplasts were prepared from young, freshly harvested leaves of silverbeet, and from freshly harvested leaves of white clover at varying stages of development using a modification of the protocol described by Bartlett *et al.* (1982).

Approximately 10 to 20 g of silverbeet leaves or 5 g of white clover leaves were blended, in 100 ml or 60 ml respectively, of chloroplast grinding buffer (2 mM Na_2EDTA, neutralised, 1 mM $MgCl_2$, 1 mM $MnCl_2$, 330 mM sorbitol, 5 mM sodium ascorbate, 50 mM HEPES-KOH, pH 7.5). The slurry was filtered through 4 layers of miracloth (CALBIOCHEM, CN Biosciences Inc., La Jolla, CA, USA), the supernatant centrifuged to 3000 x g (Sorvall SS-34 rotor) and stopped immediately (with brake off). The pellet was resuspended in 1 - 2 ml of chloroplast grinding buffer, loaded onto a 10-80% Percoll step gradient (10% or 80% PBF-Percoll (3% w/v polyethylene glycol 8000, 1% w/v BSA, 1% w/v Ficoll 400 in Percoll) made up in chloroplast grinding buffer supplemented with 2 mM glutathione), prepared in 30 ml glass corex tubes, and centrifuged for 10 minutes at 15, 000 x g in a GS-3 rotor. A green band containing the whole chloroplasts formed at the interface of the percoll solutions. This was carefully removed using a wide bore pipette tip, resuspended in 5 to 10 volumes of chloroplast grinding buffer and then centrifuged to 3000 x g (SS-34 rotor) before stopping immediately. Intact chloroplasts were washed again with chloroplast grinding buffer, centrifuged as before and resuspended finally in either 0.2 ml to 1.0 ml of protein extraction buffer (PEB; 0.1% (w/v) SDS, 1 mM Na_2EDTA, 50 M Tris-HCL, pH 6.8), or 0.2 ml to 1.0 ml chloroplast grinding buffer as indicated. All manipulations were done at 4°C or on ice and 100 µl aliquots were stored at -20°C.

Microscopy was used to determine whether this protocol resulted in intact chloroplasts. A drop of chloroplast preparation was placed on a clean microscope slide and examined under the light microscope and the confocal microscope.

2.3.2 Preparation of Thylakoid Membranes

Thylakoid membranes were harvested by one of two methods, either directly from whole leaves, or from isolated whole chloroplasts.

2.3.2.1 Thylakoid Isolation From Whole Leaves

Thylakoid membranes were prepared from young, freshly harvested leaves of silverbeet grown in the field. The method used to isolate thylakoid membranes from whole leaves was modified from a previously described protocol of Robinson and Yocum (1980). Leaves (10 to 20 g) were torn into pieces of approximately 2 cm square and blended for 5 seconds, in 100 ml of grinding buffer (400 mM NaCl, 2 mM $MgCl_2$, 0.2% (w/v) BSA, 20 mM Tricine-AMPD, pH 7.6). The homogenate was filtered through 4 layers of cheesecloth and then centrifuged at 3000 x g for 5 minutes in a Sorvall SS-34 rotor. The chloroplast pellet was then resuspended gently in approximately 40 ml of wash buffer (150 mM NaCl, 5 mM $MgCl_2$, 0.2% (w/v) BSA, 20 mM Tricine-AMPD, pH 7.3) and centrifuged as before. The pellet was resuspended finally in 1 ml of wash buffer to yield a concentration of 1-2 mg chl ml^{-1} for bioenergetic studies. Thylakoids harvested using this method for western analysis were resuspended finally in 0.5 to 1 ml of protein extraction buffer (0.1% (w/v) SDS, 1 mM Na_2EDTA, 50 mM Tris-HCL, pH 6.8). All isolation steps were performed at 4°C or on ice and the final thylakoid suspension was either stored on ice for up to 2 hours, or frozen at -20°C for longer term storage.

2.3.2.2 Thylakoid Isolation From Isolated Chloroplasts

The method for isolation of thylakoid membranes from whole chloroplasts was modified from the previously described method of Elortza *et al.* (1999). Whole, intact chloroplasts (Section 2.3.1) were lysed by freezing and thawing and then washed three times with 20 mM Bistris (pH 6.0), with centrifugation at 3000 x g for 10 minutes (SS-34 rotor) after each wash. The pellet was then resuspended in 20 mM Bistris, 0.3 M NaCl, centrifuged at 4500 x g for 5 minutes and the protein concentration measured using the BioRad DC protein assay method (Section 2.4.2). Thylakoid membrane

proteins were then extracted from the isolated thylakoids using the method of Elortza *et al.* (1999). For this, proteins (including NDH-K) were extracted in a volume of 1:1 protein to 1% (v/v) Triton X-100 in solubilisation buffer (1 mM EDTA, 1 mM PMSF, 8% (v/v) glycerol, 50 mM sucrose, 20 mM Bistris, pH 6.0) for 30 minutes on ice. The sample was then centrifuged briefly at 3000 x g and the supernatant used for analysis.

2.3.3 Preparation of Tris-Washed Thylakoid Membranes

Tris-washing results in the dissociation of the oxygen evolving complex (OEC) from the thylakoid membrane (Yamashita and Butler, 1968). The method used to obtain OEC-free thylakoids was as described by Yamashita and Butler (1968). Isolation was as for whole leaf thylakoids (Section 2.3.2.1.) except following the first centrifugation step, the chloroplast pellet was resuspended in 10 ml of 0.8 M Tris (neutralised), to give an approximate thylakoid concentration of 0.1 mg chl ml^{-1}, and left to stand on ice for 10 minutes. The suspension was then centrifuged at 3000 x g for 5 minutes, and the pellet was resuspended in 1 ml of wash buffer to a concentration of 1 - 2 mg chl ml^{-1}. The entire isolation procedure was performed at 4°C or on ice.

2.3.4 Preparation of Etioplasts

Etioplasts were obtained by dark germinating silverbeet seeds in a growth cabinet (CONTHERM, model 190 FPC, Day-Night Precision Incubator, Contherm Scientific Company, Petone, New Zealand) at a constant temperature of 25°C. Seeds were scattered in trays containing vermiculite and watered once with tap water prior to being placed in the growth cabinet.

Seedlings were harvested after the specified number of hours under continuous light (approximately 12 $\mu mols^{-1}m^{-2}s^{-1}$) and etioplasts prepared using a modified protocol previously described by El Amrani *et al.* (1994). The initial zero hour harvest was done 9 days after planting and the subsequent harvests were at appropriate times following exposure to the light.

Cotyledons (0.3 g to 1 g) germinated in the dark (0 hour harvest) were excised under dim green light (non-photosynthetic) provided by a 60 Watt lamp covered with green cellophane, and placed in approximately 60 ml of ice-cold etioplast grinding buffer (330 mM sorbitol, 2 mM EDTA, 2 mM $MgCl_2$, 1% (w/v) soluble PVP, 10 mM ascorbic acid, 5 mM cysteine, 50 mM Tris-HCl, pH 7.6). Subsequent harvests of cotyledons from seedlings exposed to 12 and 24 hours of continuous light were undertaken in the light. Cotyledons were then homogenised in a blender for 5 seconds, filtered through 3 layers of miracloth and centrifuged at 500 x g for 10 minutes in a SS-34 rotor. The pellet was resuspended in 1 ml of etioplast washing medium (etioplast grinding buffer with out PVP, ascorbic acid and cysteine), loaded onto a 35%-70% Percoll step gradient (35% or 70% PBF-Percoll made up in etioplast wash buffer supplemented with 2 mM glutathione) prepared in 30 ml glass corex tubes, and centrifuged for 10 minutes at 15, 000 x g in a GS-3 rotor. As with the intact chloroplast isolation, intact etioplasts were found at the interface of the two percoll solutions. Etioplasts were removed using a wide bore pipette, diluted with 10 volumes of washing medium and centrifuged again at 3000 x g for 10 minutes (SS-34 rotor). The etioplast pellet was resuspended finally in 0.3 to 0.6 ml of either protein extraction buffer (0.1% (w/v) SDS, 1 mM Na_2EDTA, 50 mM Tris-HCL, pH 6.8) or etioplast wash buffer as indicated. All steps were performed on ice or at 4°C and samples stored at -20°C.

2.3.5 Whole Leaf Protein Extraction

The method used to extract whole leaf proteins was a modified protocol described by Catala *et al.* (1997). One freshly harvested, young silverbeet leaf (10 to 20 g) was homogenised to a fine powder in liquid nitrogen using a mortor and pestle. The powder was resuspended in approximately 40 ml of protein extraction buffer (0.1% (w/v) SDS, 1 mM Na_2EDTA, 50 mM Tris-HCL, pH 6.8), mixed well, filtered through 6 layers of miracloth and centrifuged for 10 minutes at 20, 000 x g (SS-34 rotor). The supernatant, containing the whole leaf protein extract was then decanted, and 100 µl aliquots were stored at -20°C.

2.3.6 DNA Extraction

The method employed for the isolation of DNA from all samples was a modified CTAB protocol (Doyle and Doyle, 1990). A sample of chloroplasts was centrifuged briefly at 13, 000 x g (Eppendorf Centrifuge, model 5417R) to pellet the chloroplasts, and the supernatant was removed. Six hundred µl of CTAB extraction buffer (2% (w/v) CTAB, 1% (w/v) PVP, 1.4 M NaCl and 20 mM EDTA, 0.1 M Tris-HCl, pH 8.0) was added, the pellet was resuspended by inversion and the mixture was incubated at 60°C, for 20-30 minutes with occasional inversions. An equal volume of chloroform was then added, the mixture shaken vigorously, and left to stand for 2 minutes. After centrifugation at 13, 000 x g (Eppendorf Centrifuge) for 1 minute, the upper aqueous phase was transferred to a clean eppendorf using a wide bore pipette and 600 µl isopropanol was added. The two solutions were mixed by gentle inversion, and left to stand at room temperature for 10 to 15 minutes. After centrifugation at 13, 000 x g for 1 minute, the DNA pellet was washed with 600 µl of 80% (v/v) ethanol and centrifuged again at 13, 000 x g for 1 minute. After another 4 washes, the DNA pellet was air-dried and then resuspended in 5 to 10 µl of sterile MilliQ water.

2.4 Analytical Methods

2.4.1 Chlorophyll Concentration of Isolated Thylakoid Membranes

The chlorophyll concentration of isolated thylakoid membrane samples was determined using the method of Arnon (1949). Thylakoid preparations (25 µl) were added to 5 ml of 80% (v/v) acetone, filtered, and the absorbance measured at 710 nm, 663 nm, and 645 nm in a glass cuvette. Total chlorophyll concentration (mg chl ml^{-1}) was calculated as described in Equation 2.

$$[\text{Chl } a] + [\text{Chl } b] = \{8.02(A_{663} - A_{710}) + 20.2(A_{645} - A_{710})\}DF \quad (2)$$

Note: DF is the dilution factor.

2.4.2 Measurement of Photosynthetic Electron Transfer

The activity of the electron transfer chain was determined using an oxygen electrode (Rank Brothers Ltd., Bottisham, UK) connected to a digital data acquisition system (Brown and Dykstra, 1999). Actinic light was provided using a Leitz slide projector fitted with a RG645 filter giving a photon flux density of 1000 μmoles photons m^{-2} s^{-1} at the cuvette. The electrode was calibrated daily using sodium dithionite and assuming a saturating O_2 concentration at 25°C of 253 μM. All assays were performed at 25°C in assay buffer (25 mM MES-AMPD, pH 6.5).

Thylakoid quality (rate of electron transfer) was determined by an initial assay using the electron acceptor FeCN (Table 2.1a) to determine the maximum rate of electron transfer. A steady rate of oxygen evolution was obtained over approximately 30 seconds, 5 mM of the photosynthetic electron transfer uncoupler ammonium chloride (NH_4Cl) was then added to the preparation, and the rate measured over the next 30-40 seconds. The rate of maximal electron transfer was then calculated using Equation 3. Optimal rates are at least 150 nmol O_2 mg^{-1} chl h^{-1}. Only thylakoid preparations with rates equal to or above this value were used in these studies.

$$\frac{\underline{\text{Slope } (NH_4Cl) \times 3600} \times (253 \times 10^{-6}) \times V_{Total}}{\text{Calibration}} \quad (3)$$
$$\text{Total chl (mg ml}^{-1}\text{)}$$

Note: Calibration is (saturated O_2 value – deficient O_2 value).

Appropriate electron acceptors/donors and inhibitors (Tables 2.1a-c) were added to 2 ml of assay buffer in the oxygen electrode cuvette, 20 μg chl ml^{-1} of thylakoid preparation

was added and the cuvette then illuminated. Once a steady rate of O_2 evolution/consumption was established. NH_4Cl (5 mM) was added and the resultant rate measured over approximately 40 seconds. An appropriate volume of SHAM (in DMSO) or DMSO was then added, typically at 80 to 100 seconds. Controls in which neither SHAM nor DMSO were added were also carried out.

Table 2.1a. Specific electron acceptors of the photosynthetic electron transfer chain.

Acceptor	Solvent	Accepts from	Conc. Used
FeCN	Water	Q_B site in PS II	1.5 mM
***p*BQ**	Ethanol	PQ	0.26 mM
SiMo	50% (v/v) DMSO	Q_A in PS II	0.1 mM
MV	Water	PS I	50 µM

Note: FeCN, potassium ferricyanide; *p*BQ, *p*-benzoquinone; SiMo, silicomolybdate; MV, methyl viologen; DMSO, dimethyl sulphoxide; Q_B, quinone B; PQ, plastoquinone; PS II, photosystem two; PS I, photosystem one.

Table 2.1b. Specific electron donors of the photosynthetic electron transfer chain.

Donor	Solvent	Donates to	Conc. Used
Ascorbate	Water	DCIP	2.5 mM
DCIP	Ethanol	Cytochrome b_6f complex	0.1 mM
DPC	Methanol	P680	0.5 mM

Note: DCIP, 2, 6-dichlorophenolindophenol; DPC, 1, 5-diphenylcarbazide; P680, special pair of chlorophyll molecules that absorb light of wavelength 680 nm.

Table 2.1c. Specific electron inhibitors of the photosynthetic electron transfer chain.

Inhibitor	Solvent	Inhibits	Conc. Used
DCMU	Water	Q_B site in PS II	20 µM
Azide	Water	Catalases	1 mM

Note: DCMU, 3- (3, 4-dichlorophenyl)-1, 1-dimethylurea.

Assays using SiMo as an acceptor were modified from the standard assay due to the relative instability of the SiMo (stable for approximately 30 seconds). To do this, a thylakoid membrane preparation (20 μg chl ml^{-1}) was added to 2 ml assay buffer, and illuminated with continuous red light. Once a steady rate of oxygen evolution was established, NH_4Cl (5 mM) was added and the resultant rate measured over 30 seconds, after which SiMo (0.1 mM in 50% (v/v) DMSO) was added and the rate was measured over 10 seconds. Finally, SHAM (20 mM) was added and the rate was measured over the next 15 to 20 seconds.

2.4.3 Chlorophyll Fluorescence Measurements

A schematic representation of the system used in the measurement of fluorescence is shown in Figure 2.2. Pulses (50 ms, 10 seconds apart) of actinic light were provided by 12 blue light emitting diodes (of wavelength 430nm). Timing of light pulses was controlled by a 10 MHz clock on a card in the PC. Assays, containing 2 ml wash buffer, 20 μg chl ml^{-1} of the thylakoid preparation and appropriate electron acceptors/donors and inhibitors, were performed in a 1 cm cuvette. Illumination at 470 nm resulted in chlorophyll fluorescence that was detected by a photodiode detector (Silicon photodiode - IPL 10530 DAL) protected by a 645 nm filter (Schott filter RG645). This filter allows only light of wavelength longer than 645 nm through, thus specifically measuring chlorophyll fluorescence. The amount of fluorescence emitted by the sample was recorded on a digital storage oscilloscope (Tektronix - TDS 544A) operating in high resolution mode (15 bit resolution). Analysis of the fluorescence data was performed using specific fluorescence software (Simon Brown, Massey University, Palmerston North, New Zealand, *per comm.*).

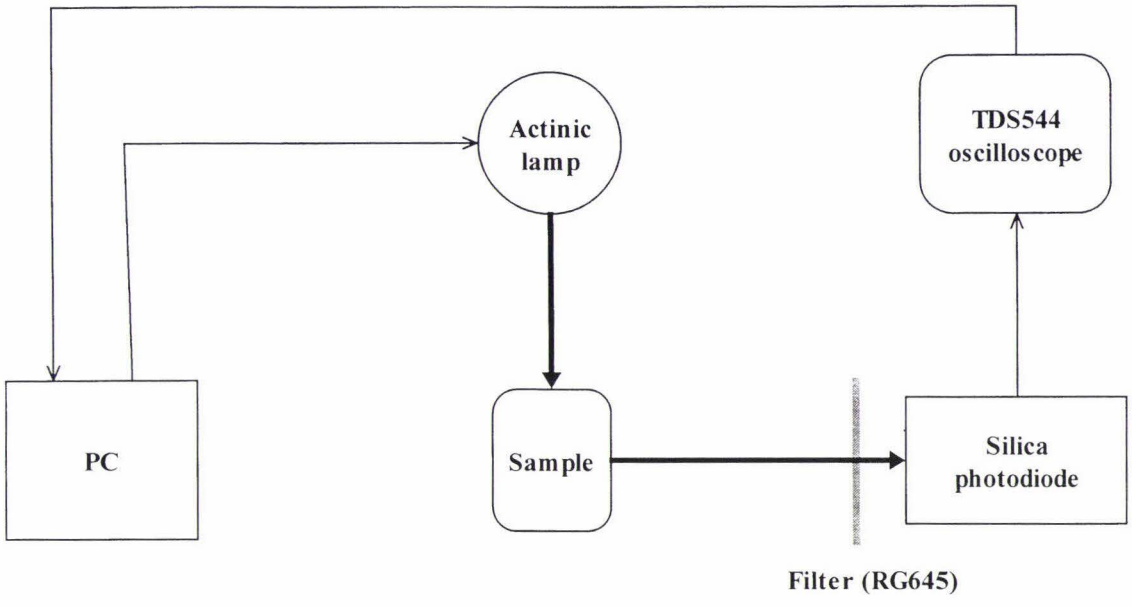

Figure 2.2. Schematic representation of the fluorescence set up. Pulses of light (50 ms), provided by 12 blue LEDs (wavelength 470 nm), 10 seconds apart excited the sample. Light of wavelength greater than 645 nm was detected by the photodiode and visualised on the oscilloscope.

2.4.4 PCR Amplification of DNA

The sequences of the primers used are shown in Figure 2.3. Five µl of the 'top' reaction (2.5 µl of 2 mM dNTPs, 1.25 µl primer 1, 1.25 µl primer 2), 19 µl of the 'bottom' reaction (16 µl ddH_2O, 2.5 µl 10X PCR reaction buffer (Roche Diagonstics Corporation, IN, USA), and 0.5 µl Taq polymerase (Roche Diagonstics) and 1 µl of DNA was added to a PCR tube. PCR was performed using a PTC-200 Peltier Thermal Cycler. The following protocol was used to amplify the silverbeet *ndhF* gene: thirty-six cycles of 94°C for 40 seconds, 57°C for 30 seconds and 72°C for 1 minute.

ND2110 RM: *ndh F* reverse primer (primer no. A7348 D11)

5' CCC YAB ATA TTT GAT ACC TTC KCC 3'

ND972 F: *ndh F* forward primer (primer no. A7348 D12)

5' GTC TCA ATT GGG TTA TAT GAT G 3'

Figure 2.3. Sequences of the *ndhF* primers used in PCR to amplify a partial sequence of the silverbeet *ndhF* gene. Note Y = C or T; B = C or G or T; K = G or T.

The PCR products were then separated using agarose gel electrophoresis (Section 2.4.6.1), and a specific DNA fragment purified using the DNA Wizard Column Clean-up method. For this, 1 ml of Wizard™ Minipreps DNA purification resin (Promega Corporation, Madison, WI, USA; preheated to 37°C for 10-15 minutes, shaken vigorously and cooled to 30°C) was added to the DNA, and the resin/DNA mix pipetted into a syringe barrel attached to a Wizard™ filter. The syringe plunger was slowly depressed and the eluate discarded. Two ml of column wash solution (Promega Corp.) was then added to the syringe, flushed through the column, and the eluate discarded. The column was washed again, detached from the syringe, placed in a capless eppendorf and centrifuged for 2 minutes at 13, 000 x g (Eppendorf Centrifuge). Fifty µl of MilliQ water (preheated to 70°C) was added to the column in a fresh eppendorf, the mixture left to stand for 5 minutes and the column was centrifuged at 13, 000 x g for 2 minutes to elute the DNA. A quantifying agarose gel (Section 2.4.6.1) was then run to determine the amount of DNA present in the samples, and hence how much sample is required for the sequencing reaction (Equation 4).

$$\textbf{Sample required} = \frac{\textbf{Number of base pairs of DNA / 20}}{\textbf{Sample DNA concentration}} \qquad \textbf{(4)}$$

2.4.5 DNA Sequencing

The isolated DNA fragment, obtained using the DNA Wizard Column method (Section 2.3.4), was then sequenced. For this, 3.2 µl of primer (1 primer per reaction), 4 µl 'big dye' (as supplied by L. Berry, Institute of Molecular Biosciences, Massey University), 4 µl of 5X sequencing buffer (10 mM $MgCl_2$, 400 mM Tris, pH 9.0) and the determined amount of DNA was made up to 20 µl with MilliQ water. The DNA fragment to be sequenced was then amplified using the same PCR program as the initial amplification (Section 2.4.4). To precipitate the DNA, 50 µl of absolute ethanol and 2 µl of sodium acetate (3 M, pH 4.6) was added to the reaction, the mixture placed on ice for 30 minutes and the precipitated DNA collected by centrifugation at 13, 000 x g for 30 minutes (Eppendorf Centrifuge). The supernatant was removed, and 400 µl of 70% (v/v) ethanol was added, and the sample centrifuged for 10 minutes at 13, 000 rpm. The supernatant was then removed and the DNA pellet left to air dry.

Samples were then sequenced using an automated DNA sequencer (ABI Prism model 377, Perkin Elmer Ltd, Vic, Australia) by Ms Lorraine Berry (Institute of Molecular Biosciences, Massey University).

2.4.6 Electrophoresis

2.4.6.1 Agarose Gel Electrophoresis

Thirty ml of molten 1.2% (w/v) agarose in 1X TAE buffer (40 mM Tris, 20 mM glacial acetic acid, 1 mM EDTA, pH 8.0) was poured into a horizontal gel apparatus and the well-forming comb inserted at one end. Once the agarose had polymerised, the gel was covered with 1X TAE buffer. Three µl of DNA mixed with 3 µl of 6X dye (0.25% bromophenol blue, 0.25% xylene cyanol, 40% (w/v) sucrose) was loaded in each well, and the gel run for approximately 1 hour at 100mV. Routinely, 2 µl of a 1Kb Mass DNA ladder (GIBCO BRL, Life Technologies, USA) was also run in a separate lane as the standard. On the conclusion of electrophoresis, gels were placed in a solution of 0.1 µg mL^{-1} ethidium bromide for approximately 15 minutes, destained with water for

approximately 15 minutes and then visualised using a UV transilluminator. The quantity of DNA could be obtained by comparisons of the intensity of staining with the mass ladder.

2.4.6.2 Linear Slab Gel SDS-PAGE

SDS-PAGE was undertaken using the BioRad Mini-Protean apparatus.

Table 2.2. Composition of resolving and stacking gels used to construct SDS-PAGE gels. Reagents are listed in the order of addition.

Reagent	Resolving gel (ml)	Stacking gel (ml)
4X resolving gel buffer (0.4% (w/v) SDS, 1.5 M Tris-HCl, pH 8.8)	2.5	-
4X stacking gel buffer (0,4% (w/v) SDS, 0.5 M Tris-HCl, pH 6.8)	-	2.5
Water	4.5	6.5
40% (w/v) acrylamide stock solution	3	1
APS (10% w/v)	0.1	0.1
TEMED	0.01	0.01

The resolving gel solution was made up as outlined in Table 2.2, and poured into the middle of glass plates of a gel sandwich, up to approximately 1 cm from the base of the well-forming comb. Isobutanol-saturated water was then carefully layered on top, and the gel left for 45 minutes to polymerise. The isobutanol-saturated water was then discarded, the gel rinsed 3 times with MilliQ water, dried with filter paper and the stacking gel solution (Table 2.2) layered onto the resolving gel and a well-forming comb inserted. After polymerisation for 30 minutes the comb was carefully removed,

the glass sandwich placed in the electrophoresis chamber, and running buffer (25 mM Tris, 190 mM glycine, 1% (w/v) SDS) was added to completely cover the gel.

Samples were prepared for electrophoresis by mixing with an equal volume of 2X SDS-PAGE loading buffer (20% (v/v) glycerol, 5% (w/v) SDS, 10% (v/v) 2-mercaptoethanol, 0.01% (w/v) bromophenol blue, 60 mM Tris-HCl, pH 6.8), and boiled for 3 minutes. Equal amounts of protein from all samples was then added to the wells. In separate lanes a blank (boiled loading buffer), and 5 µl of pre-stained molecular weight standards (Low Range Molecular Markers, Bio-Rad) were also loaded. Electrophoresis was undertaken at 200 V for 45 to 60 minutes.

Following SDS-PAGE separation, gels were either stained for protein, or subjected to western analysis (Section 2.4.7). For protein staining, gels were immersed in Coomassie Brilliant Blue stain (0.1% (w/v) Coomassie Brilliant Blue R-250, 40% (v/v) methanol, 10% (v/v) acetic acid) for 1 hour, and then rinsed with multiple changes of destain (30% (v/v) ethanol) until the protein bands were clearly visible and the background was clear of stain.

2.4.7 Western Analysis of SDS-PAGE Gels

2.4.7.1 Protein Concentration of Samples for Western Analysis

Protein determination of samples used in western analysis was performed using the Bio-Rad DC (detergent compatible) protein assay, which is based on the method described by Lowry (1951).

A total volume of 5 µl of sample was added to a microtitre plate well followed by 25 µl of reagent A and then 200 µl reagent B. After 15 minutes incubation at room temperature, the absorbance was measured at 595 nm with a microtitre plate reader (Anthos Labtec HT2, Version 1.21E), and the protein concentrations read from a standard curve generated by the same assay using 5 µl of BSA (0 to 1.5 mg ml^{-1}) as the protein sample. All assays were done in triplicate.

As the measurement of protein concentrations with the Bio-Rad DC kit were not reliable with the samples in the presence of Triton X-100, a small aliquot of the thylakoid membrane pellet prior to protein extraction was resuspended in PEB, with the intention of extracting relative levels of protein from each sample. Protein concentrations were measured as described above.

2.4.7.2 Transfer of Proteins From SDS-PAGE Gel to Membrane

Proteins separated by SDS-PAGE gel were transferred to a polyvinylidene fluoride transfer membrane (Polyscreen PVDF transfer membrane, NEN™ Life Science Products, Boston, MA, USA) using a Trans-Blot Electrophoretic Transfer Cell (Bio-Rad). The apparatus was set up as shown in Figure 2.4.

To eliminate air bubbles between the membrane and the gel, the cassette was assembled immersed in transfer buffer (190 mM glycine, 10% (v/v) methanol, 25 mM Tris-HCl, pH 8.3). The PVDF membrane was soaked for 10 seconds in 100% (v/v) methanol prior to placing it onto the gel. The cassette was then placed in the electrophoresis tank and covered with transfer buffer. Transfer was carried out for at least 1 hour at 30 V or overnight at 4°C.

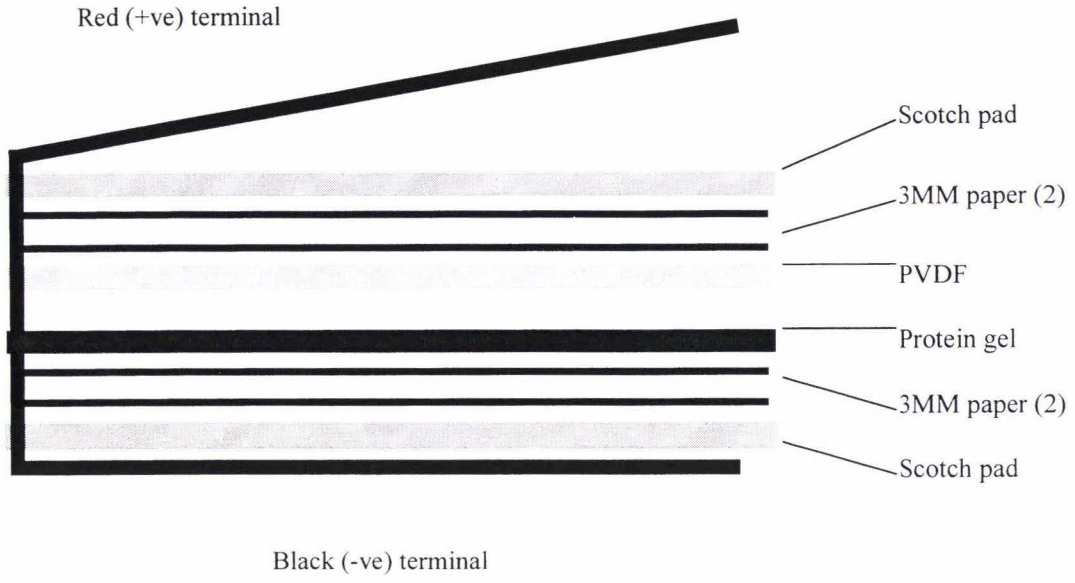

Figure 2.4. Set-up of the cassette used to transfer proteins from SDS-PAGE gel to PVDF membrane. (adapted from Hunter (1998))

2.4.7.3 Immunodetection of Target Proteins

Following protein transfer to a PVDF membrane, the membrane was peeled from the gel, placed protein-side up into an appropriate sized container and blocked in 0.5% (w/v) I-Block (Tropix, Bedford, MA, USA) at room temperature for 1 hour or at 4°C overnight. The blocking solution was then discarded and the membrane rinsed briefly with PBSalt-Tween 20 (0.05% (v/v) Tween 20 in PBSalt (250 mM NaCl, 50 mM sodium phosphate, pH 7.4)). The membrane was then incubated with a 1:1000 dilution (in PBSalt-Tween 20) of either the NDH-F or the NDH-K antibody for at least 1 hour at room temperature, with gentle shaking. Following incubation with the primary antibody, the membrane was washed three times for 5 minutes with PBSalt-Tween 20 and then incubated with the secondary antibody (anti-rabbit IgG antibody, Sigma) at the recommended concentration of 1:10, 000 (diluted in PBSalt-Tween 20), at room temperature, with gentle shaking. After a 1 hour incubation, the membrane was washed three times for 5 minutes with PBSalt-Tween 20 and twice for 5 minutes with 150 mM Tris, pH 9.7. The membrane was then immersed in substrate (0.01% (w/v) 5-bromo-4-chloro-3-indoyl phosphate (BCIP; Boehringer Mannheim, Germany), 0.02% (w/v) *p*-

nitro blue tetrazolium chloride (NBT; Aldrich Chemical Company, WI, USA), 1% (v/v) dimethyl sulphoxide (DMSO), 8 mM $MgCl_2$, 150 mM Tris-HCl, pH 9.7) and the reaction allowed to continue in the dark for approximately 15 minutes. The reaction was stopped when bands were clearly visible by discarding the substrate solution and rinsing the membrane several times in RO water.

2.4.8 Estimation of Protein Molecular Weights

The molecular mass of proteins recognised by western analysis were estimated by comparison to the mobility of the standard molecular marker proteins. The distance between the origin and the centre of each marker protein was plotted against the log of the marker protein size, and a regression equation was fitted to the curve. The size of the protein of interest was determined using the regression equation (Harnes and Rickwood, 1981).

CHAPTER 3 THE EFFECT OF SALICYLHYDROXAMIC ACID ON PHOTOSYNTHETIC ELECTRON TRANSFER

In this part of research, the site of inhibition of the photosynthetic electron transfer chain of silverbeet by SHAM, the mitochondrial AOX inhibitor, was identified and characterised.

3.1 Measurement of Electron Transfer Rates

An optimal rate of maximal electron transfer in isolated thylakoids in the presence of FeCN is at least 150 nmol O_2 mg^{-1} chl h^{-1}. Thylakoid preparations with rates less than this were not used in this study. The Q_B electron acceptor FeCN was used to facilitate maximal electron flow through thylakoids uncoupled with 5 mM NH_4Cl (Figure 3.1). Addition of ammonium chloride reduces the electrochemical potential that exists over the thylakoid membrane thus allowing easier entry of H^+ into the thylakoid lumen. As the transport of H^+ across the membrane is no longer limited, electron transfer through the photosynthetic chain, which pulls H^+ into the lumen, occurs at a higher rate. Another limiting factor of electron transfer in isolated thylakoid membranes is the absence of a final electron acceptor as Fd is loosely bound to the stromal lamellae of the membrane and is washed away during the isolation procedure. Therefore, an artificial electron acceptor was used in all assays.

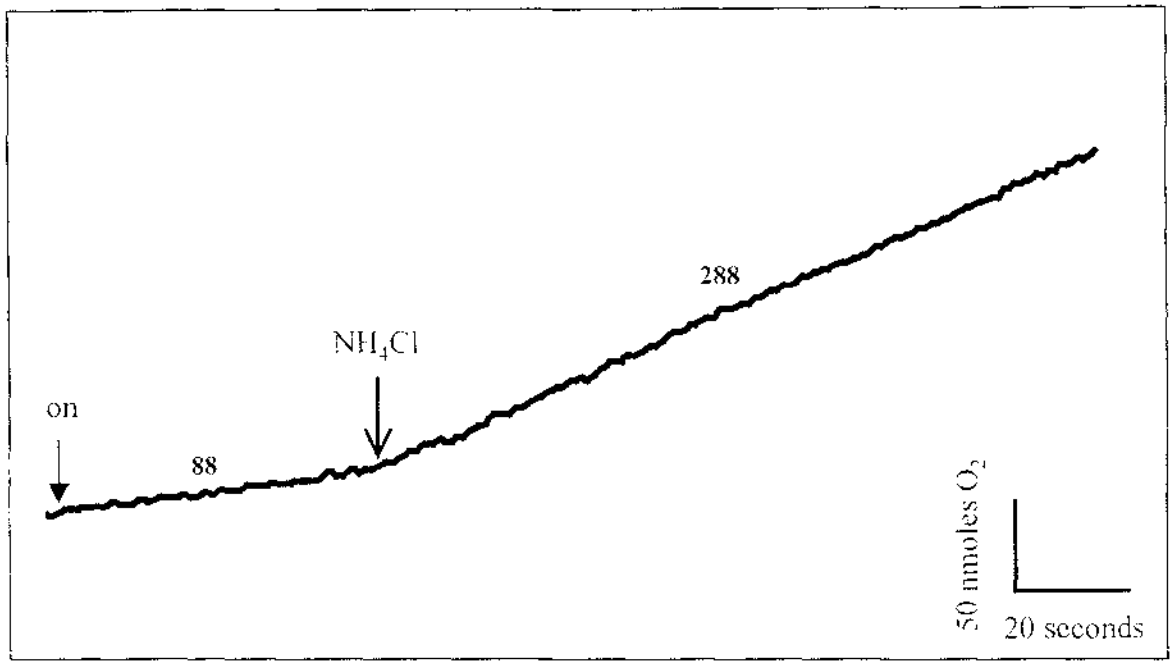

Figure 3.1. Typical oxygen electrode trace of H_2O to FeCN assay used to determine electron transfer rate of each thylakoid preparation. Once a steady rate of oxygen evolution was established in the presence of FeCN and light, NH_4Cl (5 mM) was added to the assay to allow maximal electron transfer through the chain. The point at which the light was turned on is depicted by the solid arrow. Numbers on the trace represent the rate of oxygen evolution in nmoles O_2 mg^{-1} chl h^{-1}.

3.2 Effect of SHAM on Whole Chain Electron Transfer

Initially, an inhibitory effect of SHAM on photosynthetic electron transfer was examined using methyl viologen (MV) as the terminal acceptor. Methyl viologen is reduced by PS I and subsequently reduces O_2, therefore electron transfer from water to MV was measured as O_2 consumption. Characterisation of inhibition by SHAM was analysed by two methods, using an oxygen electrode and fluorescence.

In the dark, essentially no electron transfer was seen in a sample of isolated thylakoids in assay buffer (Figure 3.2). Saturated light (1000 μmoles photons m^{-2} s^{-1}) of wavelength 645 nm resulted in a slight increase in oxygen consumption to give a rate of 41 nmoles O_2 mg^{-1} chl h^{-1}. Ammonium chloride (5 mM) was then added to the assay, which allowed maximal electron transfer to occur (200 nmoles O_2 mg^{-1} chl). Once a steady rate of oxygen consumption was observed, SHAM (20 mM) was added, resulting in a large decrease in oxygen consumption by MV, to 50 nmoles O_2 mg^{-1} chl h^{-1}. A control was carried out that comprised the addition of DMSO without added SHAM (data not shown). The rate of normal oxygen consumption over time decreased by approximately 10%.

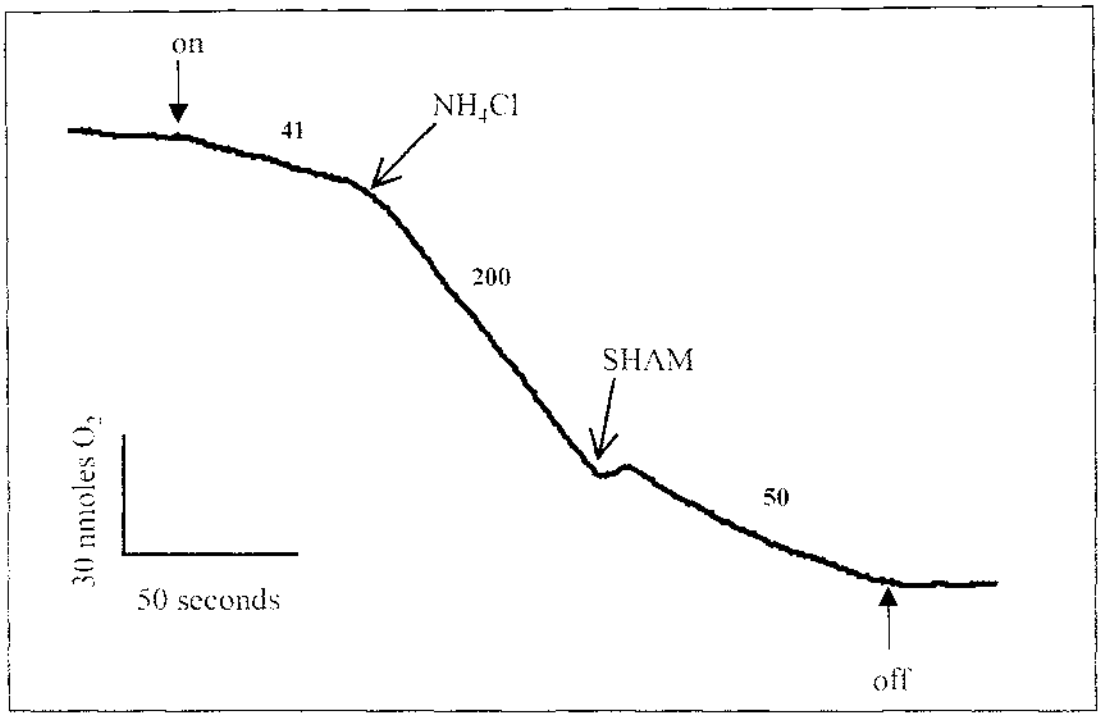

Figure 3.2. A typical oxygen electrode trace of whole chain electron transfer inhibition by 20 mM SHAM. Whole chain electron transfer was established by the addition of MV (50 μM) to a preparation of isolated thylakoids in assay buffer. Once a steady rate of oxygen consumption was established in the presence of light, NH_4Cl (5 mM) was added to allow maximal electron transfer. SHAM (20 mM) was added to the assay once a steady rate of maximal oxygen consumption was established. The points at which the light was turned on and off are depicted by the solid arrows. Numbers on the trace represent the rate of oxygen consumption in nmoles O_2 mg^{-1} chl h^{-1}.

Fluorescence data also showed an effect on electron transfer by SHAM. When MV was added to a sample of isolated thylakoids in assay buffer, a decrease in F_m (maximal fluorescence) was observed (Figure 3.3). This decrease in F_m is due to MV acting as an electron acceptor from PS I, thus alleviating the build up of electrons in PS II due to less restricted flow of electrons through the photosynthetic chain. Following addition of SHAM (20 mM) to the assay, an increase in F_m was observed, although the F_m remained significantly lower than that of the control.

Determination of the relative redox states of the PQ pool in this assay was done to further characterise the inhibitory properties of SHAM. This was achieved by normalising the fluorescence traces against the control. Addition of MV to isolated thylakoids resulted in an increase in the area over the curve compared to the control (Figure 3.4). Following addition of SHAM (20 mM) to the sample, a decrease in the area over the curve from the control was observed (Figure 3.4). The F_v/F_m of each fluorescence assay which is indicative of the size of each fluorescence trace is shown in Table 3.1.

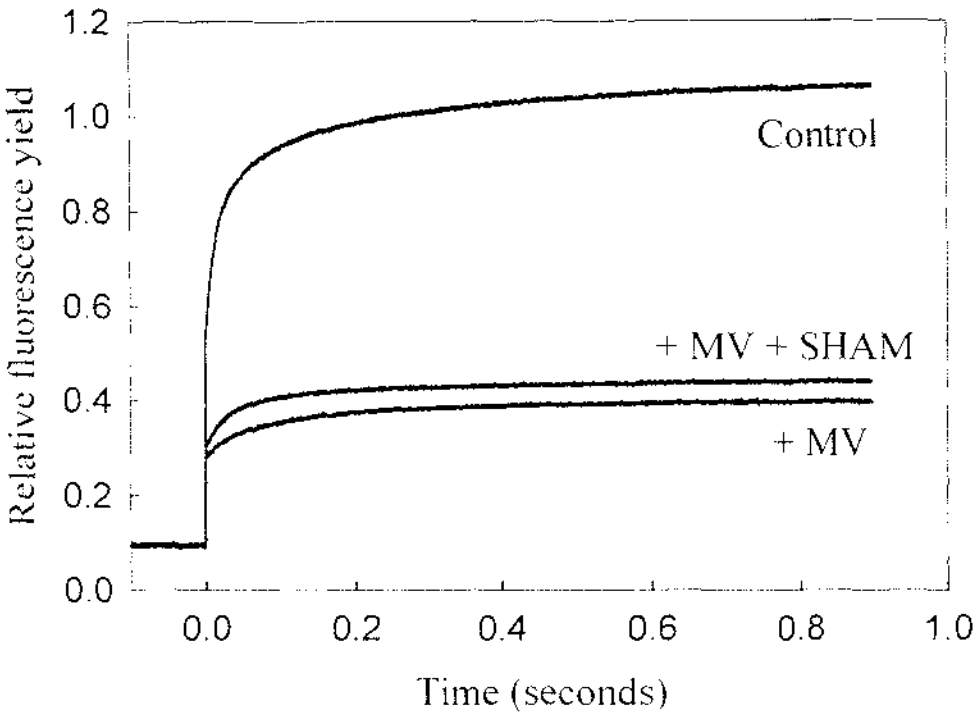

Figure 3.3. A typical fluorescence transient of whole chain electron transfer in the presence of 20 mM SHAM. Control is the fluorescence of a preparation of silverbeet thylakoids in wash buffer (Control). Whole chain electron transfer was established by the addition of MV (50 μM) to the assay (+ MV). SHAM (20 mM) was added to the whole chain assay and fluorescence yield measured (+ MV + SHAM).

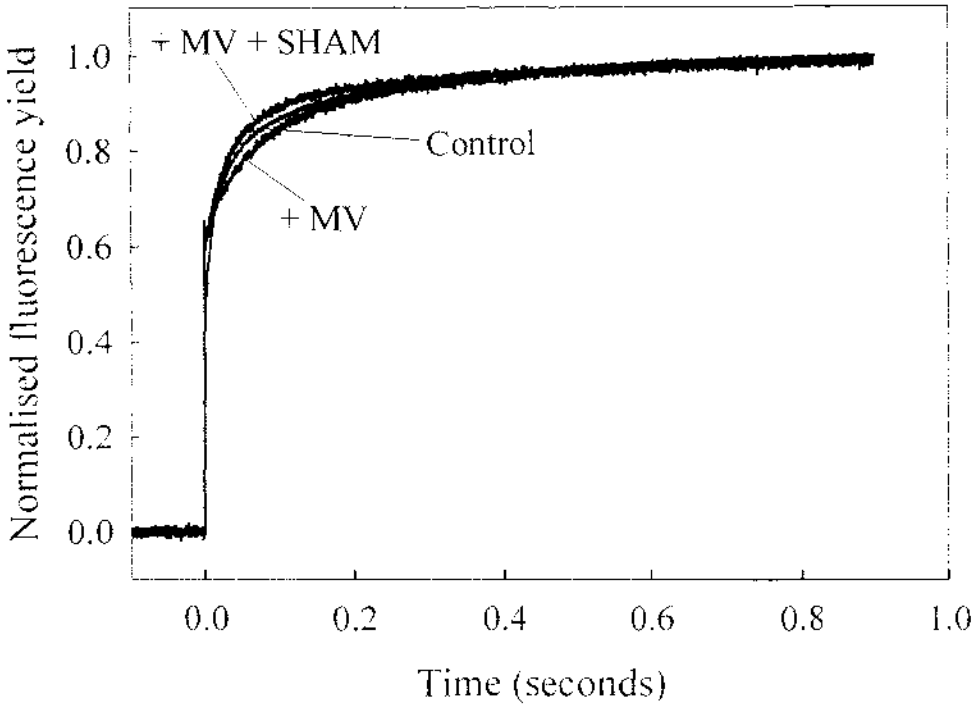

Figure 3.4. Normalised fluorescence of whole chain electron transfer in the presence of 20 mM SHAM. The fluorescence yield was normalised, against the control, to determine the relative size of available electron acceptors available before and after addition of SHAM (20 mM). Control is a preparation of thylakoids in wash buffer. Addition of MV (50 μM) to the assay was done to establish whole chain electron transfer (+ MV). SHAM (20 mM) was added to the whole chain assay (+ MV + SHAM).

Table 3.1. F_v/F_m values for whole chain, FeCN and DCMU fluorescence assays. The value represents the height of the fluorescence curve, with higher curves having more inhibition of electron transfer.

Treatment	F_v/F_m
Control	0.464
+ 50 μM MV	0.377
+ 50 μM MV, + 20 mM SHAM	0.384
Control	0.486
+1.5 mM FeCN	0.286
+ 1.5 mM FeCN, + 20 mM SHAM	0.345
Control	0.612
+ 10 μM DCMU	0.614
+ 10 μM DCMU, + 20 mM SHAM	0.478

The quenching effect of SHAM compared to the control fluorescence trace was unexpected as inhibitors of photosynthetic electron transfer always cause an increase in F_m due to the restriction of electron transfer through the chain. This restriction of electron transfer results in excited electrons from P680 releasing their energy as light (fluorescence). Therefore, it was necessary to determine whether SHAM altered the fluorescence emission spectrum.

A fluorescence spectrum of 10 µg chl ml^{-1} thylakoid preparation in assay buffer compared to 10 µg chl ml^{-1} thylakoid preparation in assay buffer plus SHAM showed that SHAM did quench fluorescence, by almost 3 fold, but it did not cause a shift in the wavelength of the peak (Figure 3.5). To determine whether this quenching was due to the solvent SHAM was dissolved in, DMSO, a control of thylakoids, assay buffer and 60 µl of DMSO was also performed (Figure 3.5). No quenching of fluorescence was seen in this assay therefore eliminating a possible quenching artefact of DMSO.

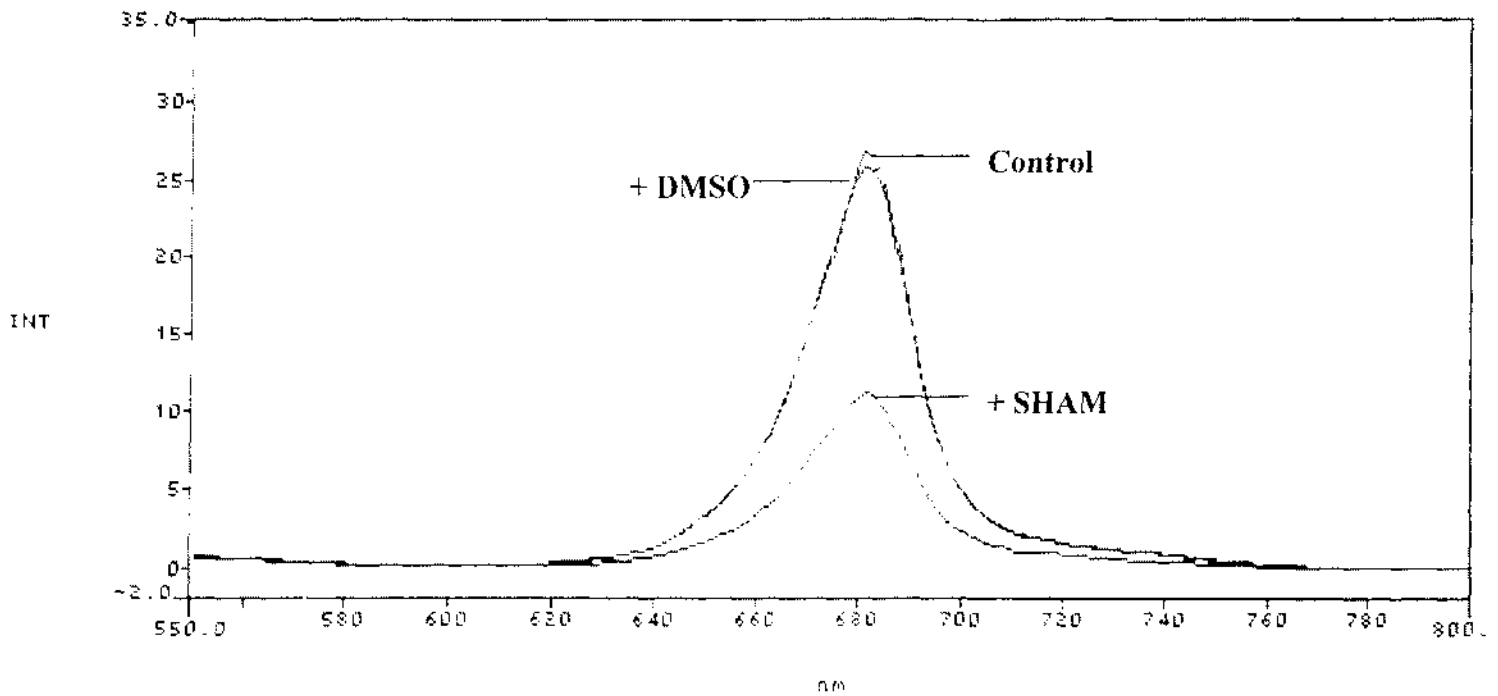

Figure 3.5. Fluorescence spectrum of thylakoid preparation in assay buffer plus SHAM and thylakoid preparation in the presence of DMSO. 10 µg of thylakoid preparation was examined by fluorescence in the presence of SHAM (20 mM) (SHAM) and DMSO (60 µl) (DMSO).

3.3 SHAM Titration

Chlororespiratory studies that have utilised SHAM as a terminal oxidase inhibitor used concentrations of SHAM around 2 to 5 mM. To determine what concentration of SHAM was best for the inhibition analysis, a SHAM titration was performed. Varying concentrations of SHAM, from 2 mM up to 30 mM, were added to a sample of 20 μg chl ml^{-1} of thylakoid preparation, 1.5 mM FeCN and 5 mM NH_4Cl in assay buffer. Oxygen evolution rates were measured 10 to 15 seconds prior to SHAM addition, and in the 20 seconds following SHAM addition (Figure 3.6). Concentrations as low as 2 mM did result in an inhibition however this level of inhibition was not reliable enough for this study. A concentration of 20 mM was chosen as this gave at least 50% inhibition consistently. Therefore any inhibitory effect would be seen. A control was also performed to ensure that the inhibition observed was not due to the solvent DMSO. While some inhibition (5-10%) was observed, this was most likely due to the drift of the electrode, which was calculated at approximately 10%.

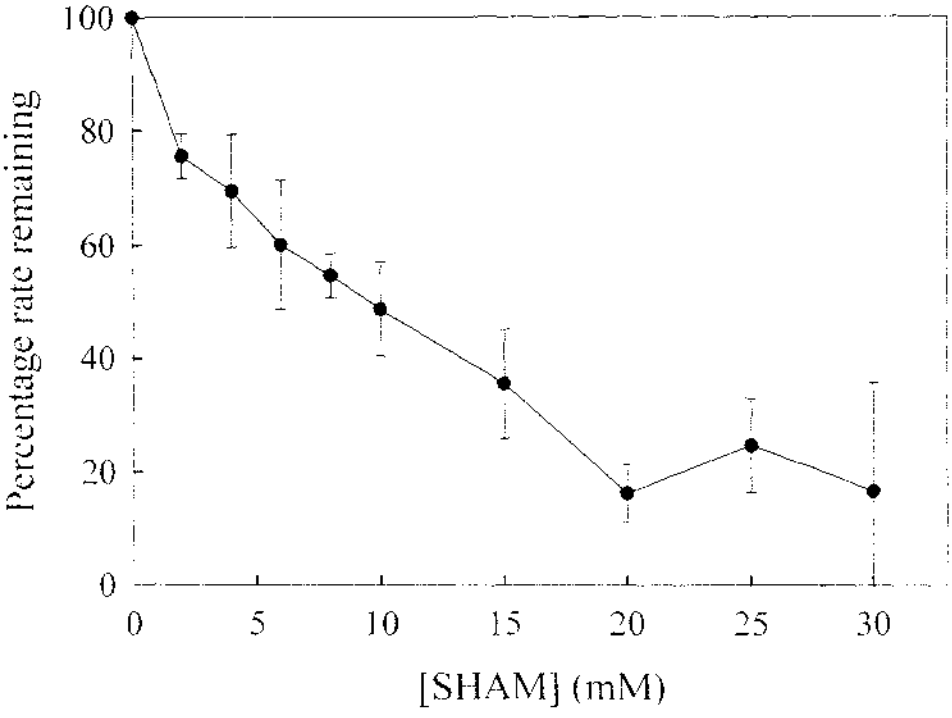

Figure 3.6. Effect of increasing concentrations of SHAM on electron flow from H_2O through to FeCN. Maximal electron transfer from H_2O to FeCN was established by the addition of FeCN (1.5 mM) and NH_4Cl (5 mM) to a preparation of isolated silverbeet thylakoids in assay buffer. SHAM (2 mM to 30 mM) was added to the assay and percentage rate of oxygen evolution remaining measured. Standard error bars are shown.

3.4 Effect of SHAM on Partial Chain Electron Transfer

Further characterisation of the site of SHAM inhibition on photosynthetic electron transfer utilised a series of specific electron acceptors/donors and inhibitors (Izawa, 1980) that permits the isolation of regions of the electron transfer chain. The sites of action of these acceptors/donors and inhibitors on the photosynthetic chain are shown in Figure 3.7.

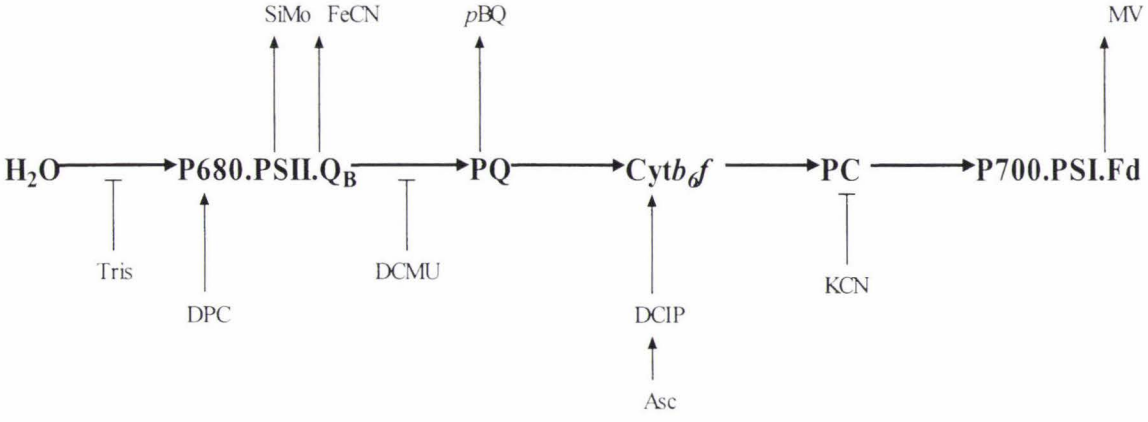

Figure 3.7. Sites of action of various electron acceptors, donors and inhibitors. Arrow heads represents electron donors and acceptors, while the terminal arrows show electron inhibitors. Abbreviations: FeCN, potassium ferricyanide; SiMo, silicomolybdate; DPC, 1,5-diphenylcarbazide; DCMU, 3-(3,4-dichlorophenyl)-1,1-dimethylurea; pBQ, *p*-benzoquinone; Asc, ascorbate; DCIP, 2,6-dichlorophenolindophenol; Asc, ascorbate; KCN, potassium cyanide; MV, methylviologen; Q_B, quinone binding site; Q_A, quinone A, Fd, ferrodoxin.

The two main regions of the photosynthetic chain, PS I activity (Asc/DCIP → MV) and PS II activity (H_2O → SiMo, H_2O → FeCN, H_2O → *p*BQ, DPC → MV) were examined separately. For clarity, the results of each of these experiments are shown separately.

3.4.1 PS I

This experiment involved measuring electron transfer through the latter half of the photosynthetic electron transfer chain (cytochrome b_6f through to PS I). The final electron acceptor MV, the PS II inhibitor DCMU, the cyt b_6f complex electron donor DCIP, the DCIP electron donor ascorbate (Asc), the catalase inhibitor azide, and NH_4Cl were all added to a preparation of isolated thylakoids. Maximal electron flow from DCIP/Asc to MV was first established (296 nmoles O_2 mg^{-1} chl h^{-1}) , followed by the addition of SHAM (20 mM) (Fig. 3.8). No significant change in O_2 consumption was observed following addition of SHAM (285 nmoles O_2 mg^{-1} chl h^{-1}).

3.4.2 PS II

Analysis of SHAM inhibition on the first part of the chain from PS II to PQ was examined using the PQ electron acceptor *p*BQ (Figure 3.9A) and the PS II electron acceptor FeCN (Figure 3.9B). To a preparation of thylakoids in assay buffer the appropriate acceptor (*p*BQ or FeCN) was added and NH_4Cl. Once a steady rate of oxygen evolution was obtained (106 and 170 nmoles O_2 mg^{-1} chl h^{-1}, respectively), SHAM was added to the assay, and in both assays resulted in a decrease in oxygen evolution by the OEC (34 and 30 nmoles O_2 mg^{-1} chl h^{-1}, respectively).

Fluorescence analysis was also performed on these two assays. However due to circumstances beyond my control, results can only be presented for the FeCN assay. Firstly, a fluorescence measurement was taken of a preparation of thylakoids in assay buffer (control). This was followed by a fluorescence measurement after the addition of the specified acceptor (*p*BQ or FeCN). A subsequent fluorescence transient was taken following the addition of SHAM to the preparation. To examine the relative size of the PQ pool in the assay, the FeCN transient was normalised against the control (Figure 3.10). Addition of SHAM (20 mM) to the assay resulted in a decrease in the area over the curve from that of curve in the presence of the acceptor and from the curve of the control (Figure 3.10; Table 3.1).

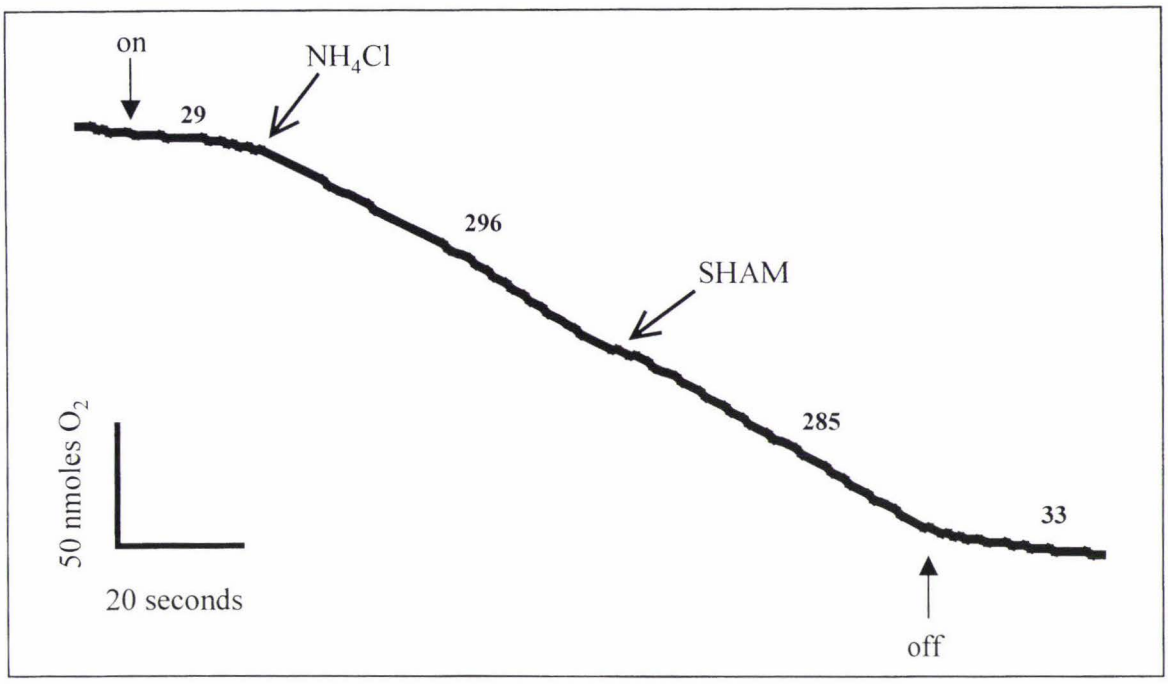

Figure 3.8. Typical oxygen electrode trace of inhibition by 20 mM SHAM on the assay DCIP/Asc through to MV. Electron transfer from Asc/DCIP through to MV was established by the addition of ascorbate (2.5 mM), DCIP (0.1 mM) and MV (50 μM) to a preparation of isolated thylakoids in assay buffer. Once a steady rate of oxygen consumption was established in the presence of light, NH_4Cl (5 mM) was added to allow maximal electron transfer. SHAM (20 mM) was added to the assay once a steady rate of maximal oxygen consumption was established. The points at which the light was turned on and off are depicted by the solid arrows. Numbers on the trace represent the rate of oxygen consumption in nmoles O_2 mg^{-1} chl h^{-1}.

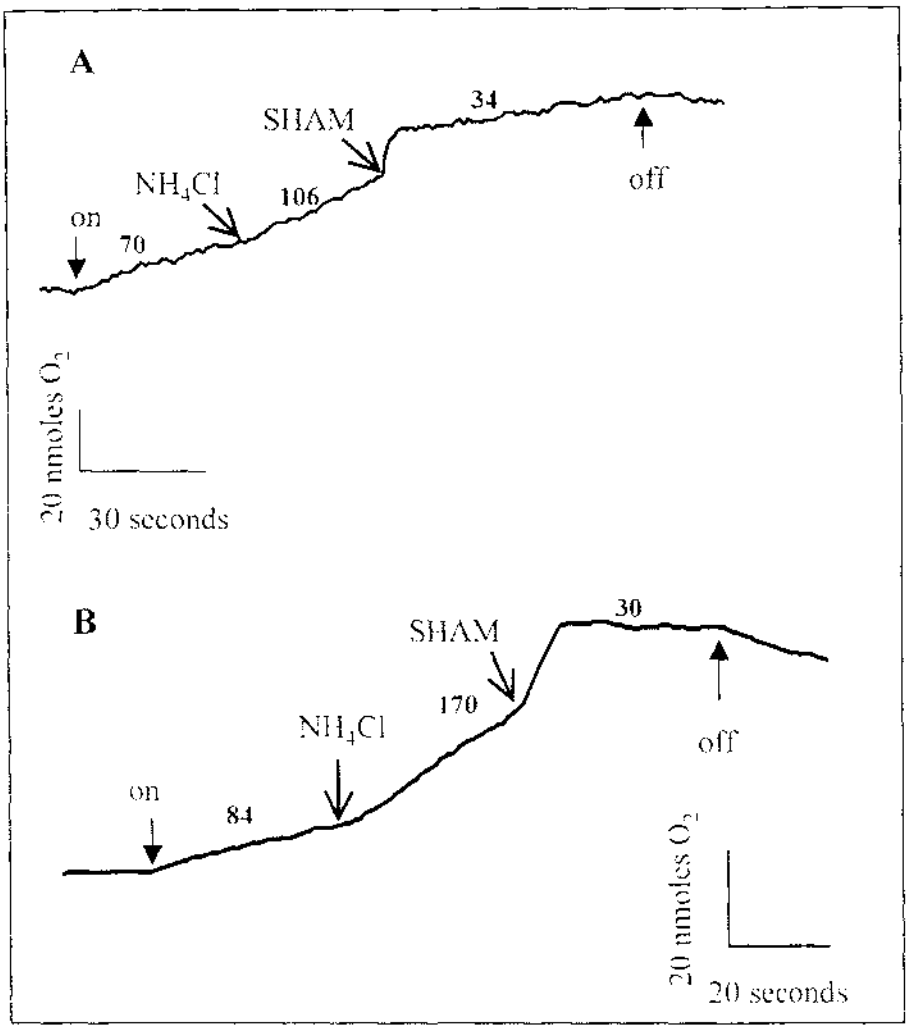

Figure 3.9. Typical oxygen electrode traces of inhibition by SHAM on the PS II assays H_2O through to *p*BQ, and H_2O to FeCN. Electron transfer through the partial chain assays H_2O to *p*BQ (A) and H_2O to FeCN (B) was carried out as defined in Section 3.4.2. Once a steady rate of oxygen evolution was established in the presence of light, NH_4Cl (5 mM) was added to allow maximal electron transfer. SHAM (20 mM) was added to each assay once a steady rate of maximal oxygen evolution was established. The points at which the light was turned on and off are depicted by the solid arrows. Numbers on the trace represent the rate of oxygen evolution in nmoles O_2 mg^{-1} chl h^{-1}.

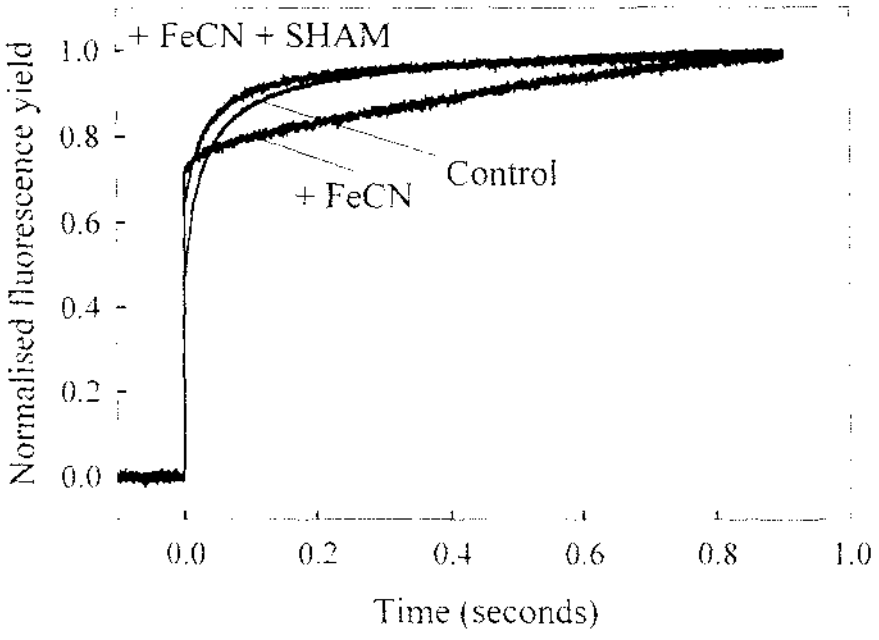

Figure 3.10. Normalised fluorescence yield showing the effect of 20 mM SHAM on pool size of isolated silverbeet thylakoids in the presence of FeCN. The control is a preparation of thylakoids in wash buffer (Control), the addition of FeCN (1.5 mM) is shown as +FeCN. SHAM (20 mM) was then added to the assay (+FeCN +SHAM).

Analysis of the effect of SHAM on the PQ pool compared to the effect by DCMU was undertaken to further characterise the site of inhibition by SHAM. The addition of DCMU to a preparation of thylakoids in assay buffer resulted in an increase in F_m compared to the control (Figure 3.11). Addition of SHAM (20 mM) to a preparation of thylakoids in assay buffer had a quenching effect on fluorescence compared to the control (Figure 3.11). When DCMU was added to this SHAM assay, F_m increased but not to the level observed when DCMU was added alone, or even to that of the control. Examination of the relative size of the PQ pool revealed, however, that SHAM resulted in a smaller PQ pool (smaller relative area over the curve) compared to DCMU (Figure 3.12). This result suggests that SHAM acts either at, or prior to, the DCMU inhibition site of Q_B.

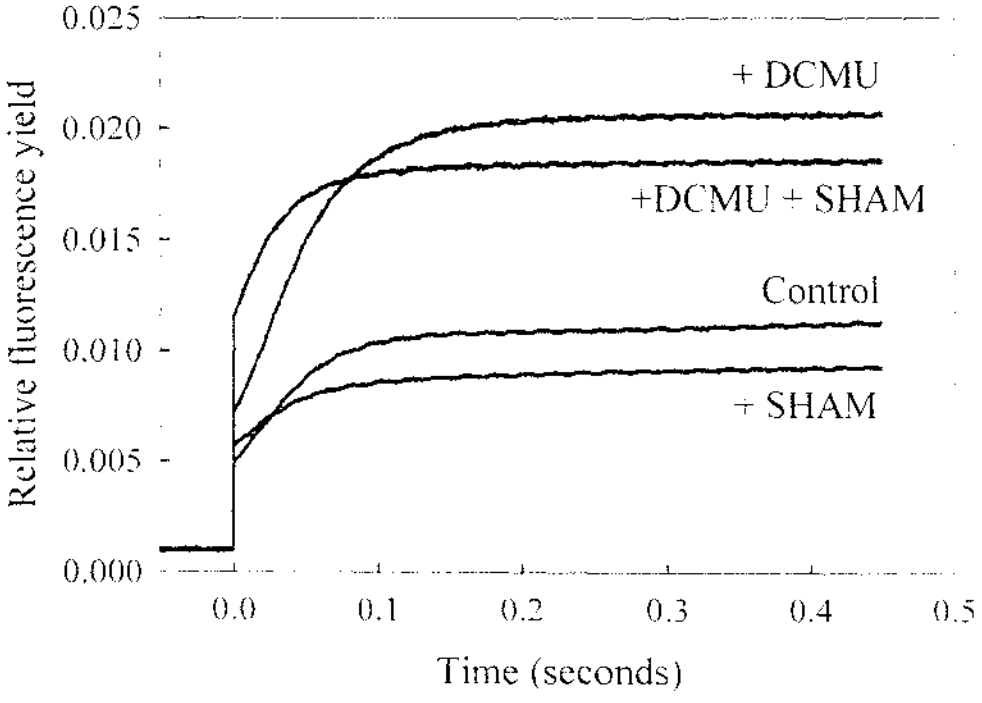

Figure 3.11. The effects of SHAM on F_M of isolated silverbeet thylakoids. The control is a preparation of thylakoids in wash buffer (Control). + SHAM = addition of SHAM (20 mM); − DCMU = addition of the Q_B inhibitor DCMU (10 μM); + DCMU + SHAM = addition of both DCMU and SHAM to the control.

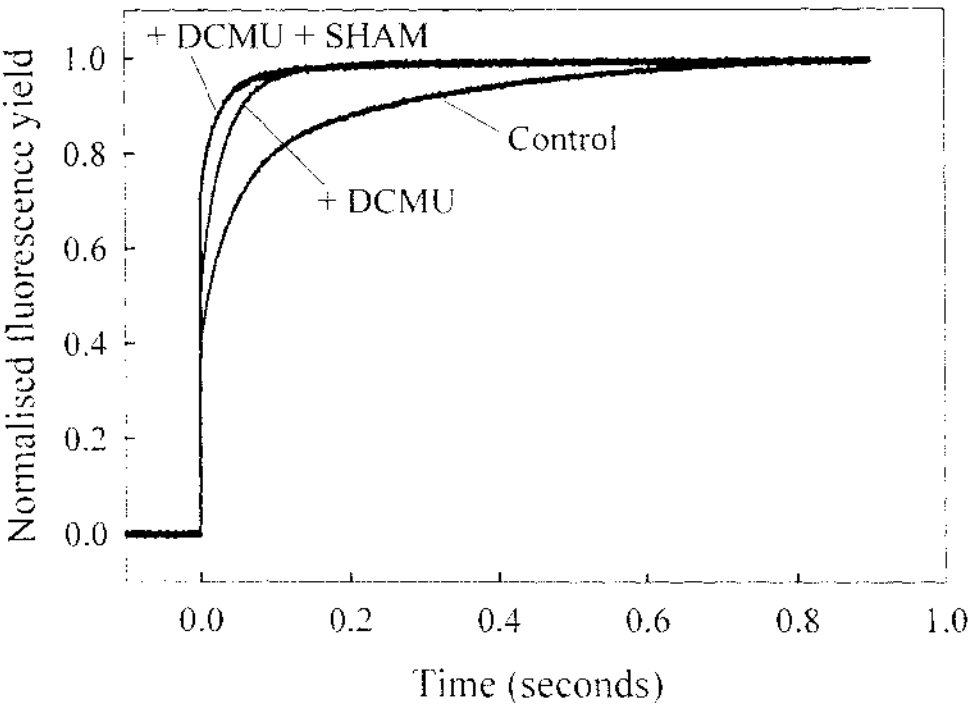

Figure 3.12. Normalised fluorescence yield showing the effect of DCMU and SHAM on pool size of isolated silverbeet thylakoids. The control is a preparation of thylakoids in wash buffer (Control). + DCMU = addition of DCMU (10 μM); + DCMU + SHAM = addition of SHAM (20 mM) to the DCMU assay.

3.5 Effect of SHAM Within the PS II Complex

To further characterise the site of SHAM inhibition on photosynthetic electron transfer, SHAM inhibition within the PS II complex was examined. Photosystem II contains a number of molecules involved in electron transfer (Figure 3.13).

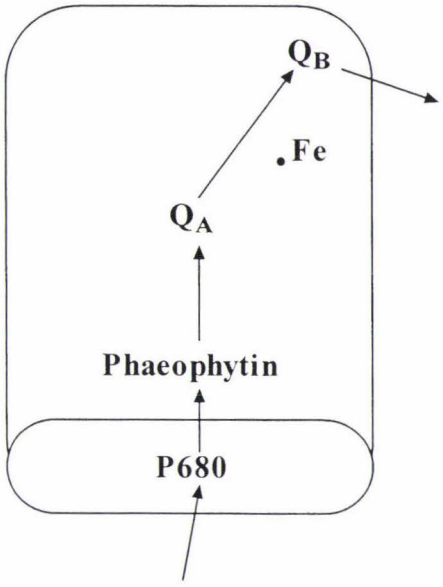

Figure 3.13. Schematic representation of the redox components present in PS II.

Two assays were performed in this section of work. The determination of the inhibition by SHAM of electron transfer in the absence of the OEC complex, and the determination of inhibition by SHAM of electron transfer from H_2O through to the Q_A electron acceptor SiMo.

3.5.1 Determination of SHAM Inhibition in the Absence of the OEC

Removal of the oxygen evolving complex (OEC) was achieved by Tris-washing of thylakoid membrane preparations (Section 2.3.2.1). As the OEC donates electrons into the photosynthetic chain, removal of the OEC results in loss of photosynthetic electron flow. In this system, electron transfer was re-established by the addition of the artificial P680 donor, DPC. The final electron acceptor MV was again used, and electron flow from DPC through to MV was measured (Figure 3.14A). Once electron transfer in the light was established, NH_4Cl was added to give a maximal electron transfer rate of 105 nmoles O_2 mg^{-1} chl h^{-1}. Following the addition of SHAM to the assay, a decrease of oxygen consumption by MV to give a rate of 48 nmoles O_2 mg^{-1} chl h^{-1} was observed. This indicates that the inhibitory action of SHAM is not on the OEC.

3.5.2 SHAM Inhibition of Electron Transfer From Water to Silicomolybdate

To examine whether SHAM inhibits prior to Q_B, the specific Q_A electron acceptor SiMo was used. The protocol for this assay is different from that of all other oxygen electrode assays performed in this study, as SiMo is quite unstable. To a preparation of thylakoids in assay buffer and NH_4Cl in saturating light, SiMo (50 μg) was added. As soon as a rate of oxygen evolution was obtained, SHAM was added to the assay (Figure 3.14B). The rate of oxygen evolution following addition of SHAM was taken in the time closest the point of addition, directly after the electrode stabilised from the addition. An inhibition of oxygen evolution by the OEC was observed following the addition of SHAM (from 236 nmoles O_2 mg^{-1} chl h^{-1} to 65 nmoles O_2 mg^{-1} chl h^{-1}). A summary of oxygen electrode analysis performed in this thesis is given in Table 3.2.

These results suggest that the site of SHAM inhibition is inside PS II, somewhere between P680 and Q_B.

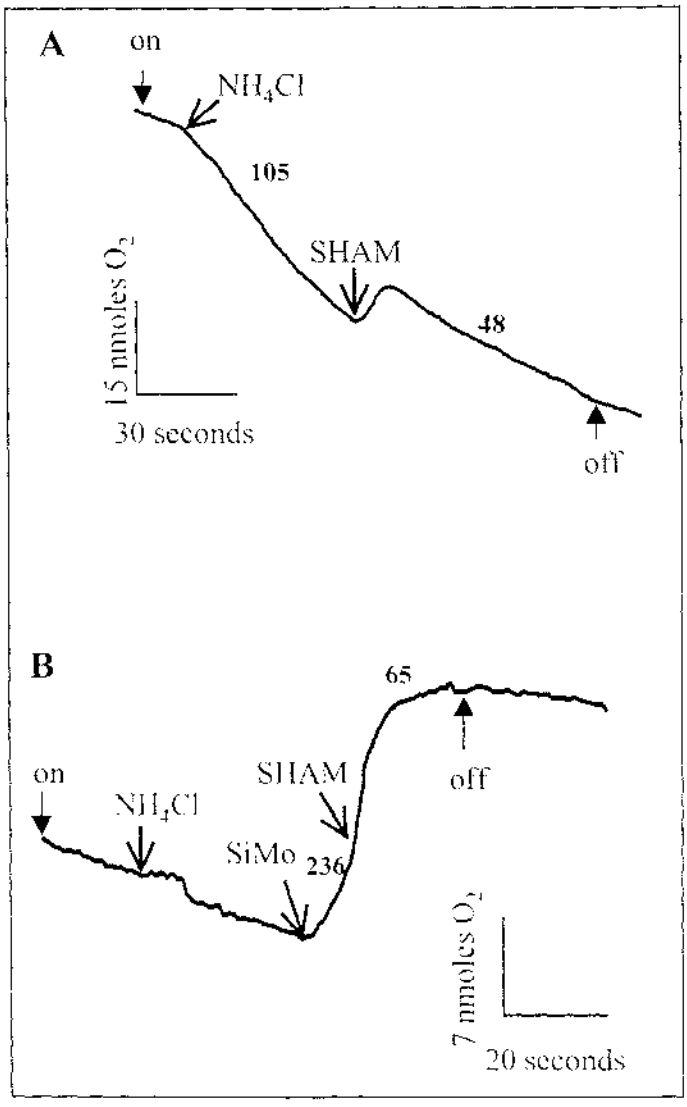

Figure 3.14. Typical oxygen electrode traces of inhibition by SHAM on the PS II assays DPC through to MV, and H_2O to SiMo. Electron transfer through the partial chain assays DPC to MV (A) and H_2O to SiMo (B) was carried out as defined in Section 3.5. Once a steady rate of oxygen consumption was established in the presence of light. NH_4Cl (5 mM) was added to allow maximal electron transfer. Addition of SiMo is as indicated on the trace. SHAM (20 mM) was added to each assay once a steady rate of maximal oxygen evolution was established. The points at which the light was turned on and off are depicted by the solid arrows. Numbers on the trace represent the rate of oxygen consumption in nmoles O_2 mg^{-1} chl h^{-1}.

Table 3.2. Effect of 20 mM SHAM on electron transfer through the defined assays. n represents the number of replicates in each assay. Assays are defined in text.

Reaction	Rate of Electron Transfer Remaining (% ± SE) (n)
Whole Chain	
$H_2O \rightarrow MV$	58 ± 5 (9)
PS I	
Asc/DCIP → MV	93 ± 2 (5)
PS II	
$H_2O \rightarrow pBQ$	31 ± 4 (11)
$H_2O \rightarrow FeCN$	20 ± 2 (17)
$H_2O \rightarrow SiMo$	16 ± 5 (4)
DPC → MV	50 ± 3 (4)

CHAPTER 4 DETERMINATION OF CHLOROPLASTIC NAD(P)H DEHYDROGENASE PROTEIN ACCUMULATION

The aim of this part of the thesis was to investigate the regulation of two subunits of the chloroplast NAD(P)H dehydrogenase, NDH-F and NDH-K at the level of protein accumulation. Specifically, the accumulation of these two subunits over a 24-hour time period and at various stages of leaf development was examined.

4.1 Isolation of Intact Chloroplasts

In these studies whole, intact chloroplasts were isolated from leaves/cotyledons of white clover and silverbeet leaf material. To ensure that the chloroplasts isolated were intact, fresh chloroplast preparations were examined by light microscopy, and by confocal microscopy.

4.1.1 Light Microscopy of Chloroplasts

Light microscopy is a simple, and effective way of determining the intactness of chloroplasts. Light microscope examination of a preparation of isolated whole chloroplasts from silverbeet at a magnification of 1500X, show mostly rounded, intact chloroplasts (Figure 4.1A). Determination of mitochondrial contamination in these samples was not carried out but at the magnification used, mitochondria would be visualised by staining the sample with one of a number of stains, including janus green B or crystal violet (A. Rowland, Institute of Molecular Biosciences, Massey University, Palmerston North, New Zealand, *per comm.*).

4.1.2 Confocal Microscopy of Chloroplasts

Confocal microscopy of chloroplasts utilises the fluorescence nature of chlorophyll to visualise chloroplasts. Chloroplasts prepared from silverbeet leaves were examined at a magnification of 7200X. The chloroplasts were visualised as rounded, red coloured spots (Figure 4.1B), by confocal microscopy suggesting that the preparation contained predominantly intact chloroplasts, as broken chloroplasts tend to loose their shape and are not seen as rounded spots (Liz Nickless, Institute of Molecular Biosciences, Massey University, Palmerston North, New Zealand, *per comm.*).

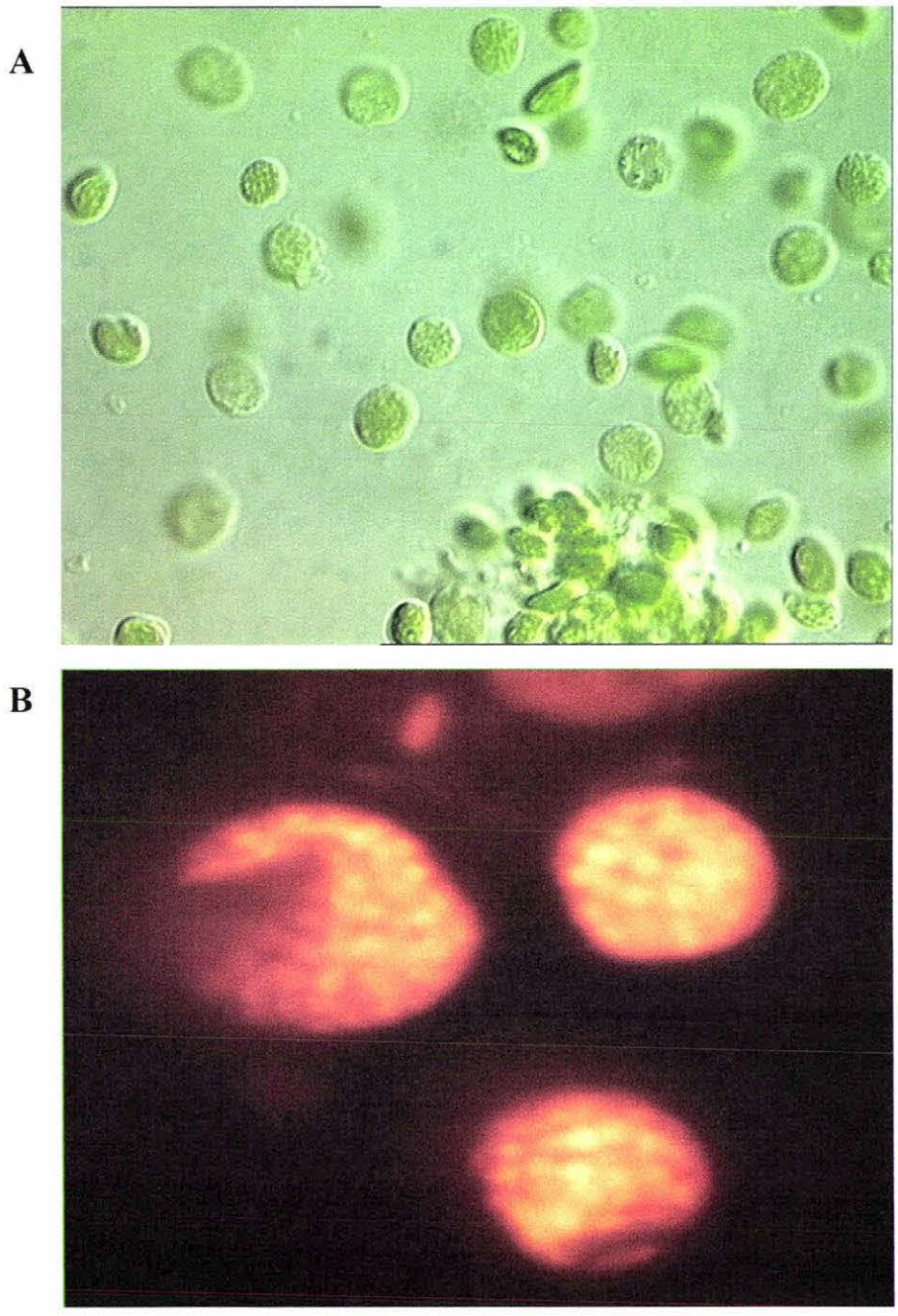

Figure 4.1. Light and confocal microscope images of whole chloroplast preparations. Whole chloroplast samples were examined under the light microscope (A) and the confocal microscope (B) to determine intactness of the chloroplasts. Magnifications are 1500X and 7200X for the light and confocal images, respectively.

4.2 Isolation of the Chloroplast *ndhF* Gene Using RT-PCR

The PCR primers ND2110RM and ND972F (Figure 2.3) were used to PCR amplify the chloroplast *ndhF* gene from DNA isolated from chloroplasts of silverbeet. The conditions used for the PCR reaction were as described in Section 2.4.4. A discrete product of approximately 1200 bp was visualised with ethidium bromide staining, (Figure 4.2, Lane 3) corresponding putatively to the expected 1138 bp *ndhF* gene. A negative control (containing PCR mixture and primers, but no DNA) was also performed, and ethidium bromide staining determined that no amplified product appeared in this lane (Figure 4.2, Lane 2). To confirm the PCR product was the *ndhF* gene, the product was purified and sequenced (Section 2.4.5) using an automated DNA sequencer. The sequence of the PCR product is shown in Figure 4.3, with the electrophoretogram shown in Appendix I. The peaks on the electrophoretogram are clean and distinct thereby showing the presence of only 1 DNA sequence in the PCR fragment isolated as the putative *ndhF* gene.

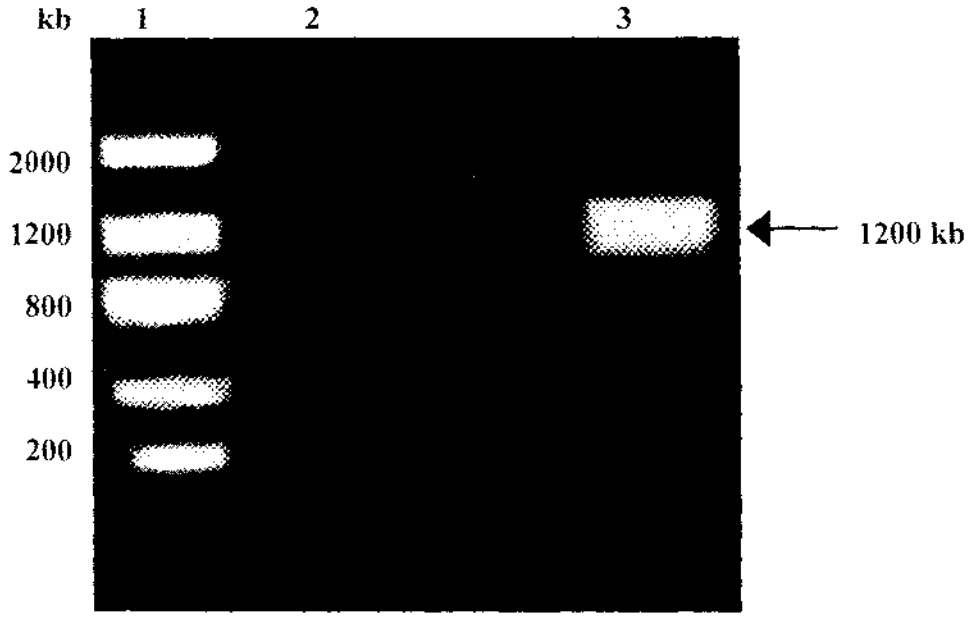

Figure 4.2. Separation of PCR products from silverbeet chloroplast DNA amplified with ND1656F and ND1762R primers. PCR mix (3 µl) was analysed by electrophoresis in a 1.2% (w/v) agarose gel in TAE buffer. DNA was stained with ethidium bromide and visualised with a UV transilluminator.

Lane 1 - Low molecular weight DNA mass ladder (Gibco BRL Life Technologies Ltd)

Lane 2 - Negative control (containing PCR mixture minus DNA)

Lane 3 - PCR product amplified from silverbeet chloroplast DNA using ND1656F and ND1762R primers

Primer – ND1656F

1 TGGGTCCCTT ATCGAGCTGC TTTATTTCAT TTGATTACTC
41 ATGCTTATTC AAAAGCATTA TTGTTTTTAG GATCTGGATC
81 CCTTATTCAT TCAATGGAAA CTATTGTNGG ATATTCTCCG
121 GATAAAAGTC AAAATATGGT TCTTATGGGG GGG

Primer – ND1762R

1 CCCCAAACCA TTCGGAATTC CATCAATTAT TCNTCTATCA
41 AAAAACGAAA CTATTTCGGC CAAATCTCGT NCACCCTTAA
81 TTATAGATGT TGCGTAAAAA GCANNTATA TAACCGCGGT
121 TAGCAGACCA ATTATATATG ATACTTATTA TTTTGTCCCA
161 AAAAATTCTC TTTTGACCTC TTTTATTAAA TGAATTAATT
201 AAGTCAAAAT TTTTTAACGA TGAATAAACG GGTTTATAAA
241 AAAAGAAAGC TATAAATATT CCCCAATAAG CTATACTAAC
281 TGAAAAAGTG GCATTTATCC CAAATTCATA CCAGTCCATA
321 GAAGTATTCG AATTAGAATG TAAAAGGTTT ATAGATGGAG
361 TTAACCATNT AGTTAATATA TCCAAATCCA TTCCTTCTTGA

Figure 4.3. Sequences of the PCR products using the forward and reverse *ndhF* primers in a preparation of silverbeet chloroplastic DNA. ND1656F is the forward primer and ND1762R is the reverse primer. N represents a nucleotide on the electrophoretogram that could not be identified as A, C, G or T.

To confirm that the amplified product was the chloroplast *ndhF* gene, the fragment amplified using the reverse primer ND 2110 RM, was used in a BLAST search using the blastn function (Altschul *et al.*, 1997). Results from the search showed only hits with chloroplast *ndhF* genes from a number of higher plant species (Table 4.1). The nucleotide sequence was translated and a further BLAST search undertaken using the blastp function. As with the nucleotide search, the protein showed homology with chloroplast NDH-F proteins from a number of other plant species. Other comparisons of the literature have shown that there exists a higher degree of sequence identity between the mitochondrial NADH dehydrogenase of animals and plants than between the mitochondrial NADH dehydrogenase and chloroplastic NAD(P)H dehydrogenase of the same plant, thus suggesting that cross-reactivity of the chloroplast NDH antibodies with the mitochondrial homologue is unlikely (Friedrich and Scheide, 2000).

Sequences producing significant alignments:	Score (bits)	E Value
gi|6424764|gb|AF130229.1|AF130229 Phytolacca americana NADH...	412	e-113
gi|6625941|gb|AF206713.1|AF206713 Talinum triangulare NADH ...	396	e-108
gi|6449186|gb|AF194843.1|AF194843 Cistanthe mucronulata NAD...	394	e-107
gi|6449172|gb|AF194829.1|AF194829 Tetragonia tetragonioides...	389	e-105
gi|6449167|gb|AF194824.1|AF194824 Aptenia cordifolia NADH d...	389	e-105
gi|6625943|gb|AF206714.1|AF206714 Maihuenia poeppigii NADH ...	365	2e-98
gi|6449201|gb|AF194858.1|AF194858 Quiabentia verticillata N...	365	2e-98
gi|6449195|gb|AF194852.1|AF194852 Pereskia aculeata NADH de...	365	2e-98
gi|6449166|gb|AF194823.1|AF194823 Allionia violacea NADH de...	359	1e-96
gi|7636084|emb|AJ400848.1|SOL400848 Spinacia oleracea compl...	357	5e-96
gi|6449208|gb|AF194865.1|AF194865 Ullucus tuberosus NADH de...	357	5e-96
gi|6449177|gb|AF194834.1|AF194834 Basella alba NADH dehydro...	355	2e-95
gi|6449165|gb|AF194822.1|AF194822 Amaranthus quitensis NADH...	343	7e-92
gi|6449196|gb|AF194853.1|AF194853 Portulaca grandiflora NAD...	337	4e-90
gi|6449206|gb|AF194863.1|AF194863 Talinopsis frutescens NAD...	331	3e-88
gi|6449183|gb|AF194840.1|AF194840 Calyptridium umbellatum N...	331	3e-88
gi|6449164|gb|AF194821.1|AF194821 Amaranthus palmeri NADH d...	323	7e-86
gi|6449198|gb|AF194855.1|AF194855 Portulaca mundula NADH de...	319	1e-84
gi|6449169|gb|AF194826.1|AF194826 Mirabilis jalapa NADH deh...	319	1e-84
gi|6449168|gb|AF194825.1|AF194825 Bougainvillea alba NADH d...	319	1e-84
gi|6449179|gb|AF194836.1|AF194836 Calandrinia compressa NAD...	315	2e-83
gi|6449197|gb|AF194854.1|AF194854 Portulaca molokiniensis N...	311	3e-82
gi|12004094|gb|AF213756.1|AF213756 Primula palinuri NADH de...	168	2e-39

Table 4.1. BLAST result of silverbeet *ndhF* PCR fragment. The PCR product amplified using the reverse primer ND 2110 RM was BLAST searched using the blastn function of the NCBI databank. All hits with this search string were with *ndhF* genes from a number of plant species. The table of hits shown is not exhaustive. Score (bits) = as the sum of substitution and gap scores; Expect (E) value = the number of different alignments with scores equivalent to or better than the score that are expected to occur in a database search by chance. (Altschul *et al.*, 1997)

4.3 Determination of Antibody Specificity

The proteins that form the chloroplast NAD(P)H dehydrogenase complex are highly conserved among species, and antibodies raised against a NDH protein in one plant species will likely cross-react with the relevant protein in another plant species.

Antibodies to the NDH-F and NDH-K subunits of the NAD(P)H dehydrogenase, raised against barley and pea, respectively were gifted to this study by Dr. B. Sabater (Universidad de Alcala de Henares, Spain; NDH-F) and Dr. J. Arizmendi (Euskal Herriko Unibertsitatea, Spain; NDH-K). Initial western analysis was performed to ensure these antibodies would cross-react with *ndh* gene products from silverbeet.

4.3.1 Specificity of Anti-NDH-F Antibodies

To determine the specificity of the antibody raised against the NDH-F protein (designated the NDH-F antibody), the accumulation of the NDH-F protein was examined in isolated thylakoids, intact chloroplasts, and in a whole leaf protein extract. The subunit is embedded in the thylakoid membrane and so a protein extraction buffer containing SDS was used as the extractant. Equal protein concentrations (20μg) of whole leaf, intact chloroplast and isolated thylakoid membrane (Section 2.3.2.1) proteins were separated through a 12% (w/v) SDS polyacrylamide gel and the separated proteins either stained with coomassie brilliant blue stain (Figure 4.4A), or transferred onto PVDF membrane and challenged with the NDH-F antibody (Figure 4.4B). In the whole leaf sample of the coomassie blue stained gel, a protein of ca. 60 kDa is easily visualised. This protein is most likely to be the large subunit of RUBISCO. At this staining intensity it is not possible to visualise many other proteins. In the separation of both the whole chloroplast and isolated thylakoid samples, a full range of molecular weight proteins stained with coomassie blue can be visualised. Using western analysis, the antibody recognised bands of ca. 79 kDa and 28.8 kDa in the isolated thylakoid sample (Figure 4.4B). A faint band of ca. 25 kDa was detected in the whole chloroplast sample (Figure 4.4B). The NDH-F protein is proposed to be ca. 70 kDa in mass, and so

the ca. 79 kDa band in the thylakoid preparation may be the NDH-F protein. The other bands recognised by the NDH-F antibody may be due either to non-specific binding of the antibody, or, as they are all smaller than the expected mass, may represent degradation products of the NDH-F protein.

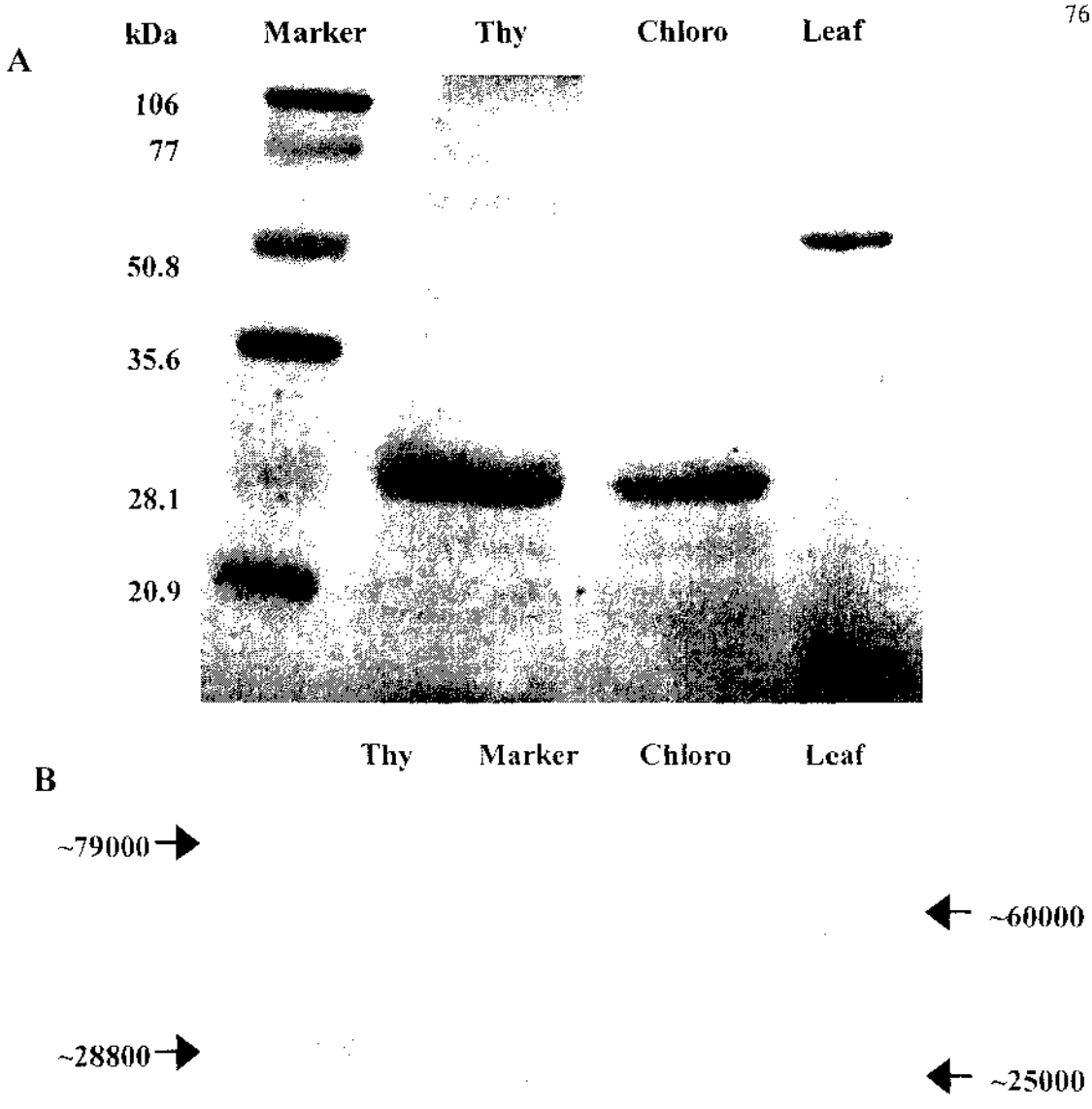

Figure 4.4. Coomassie blue staining (A) and western analysis using the NDH-F antibody (B) of isolated thylakoids, whole chloroplasts and whole leaf proteins. Equal concentrations (20 μg) of protein from isolated thylakoid membranes (thy), whole chloroplasts (chloro) and whole leaf extract (leaf) were separated by a 12% (w/v) SDS-PAGE and stained with coomassie blue (A) or challenged with the NDH-F antibody (B). Numbers on the western blot represent mass of proteins recognised by the NDH-F antibody (in Daltons). Masses of pre-stained molecular weight markers are given in (A), and the pre-stained markers can be visualised on the western blot (B).

4.3.2 Specificity of Anti-NDH-K Antibodies

The NDH-K protein is located on the stromal exposed side of the membrane and is therefore easily extracted with Triton X-100. In addition to determining antibody specificity, the most effective concentration of Triton X to use in extractions was also addressed. To do this, isolated thylakoids were exposed to increasing concentrations of Triton X in the solubilisation buffer, and the amount of NDH-K compared by western analysis.

Equal concentration of protein (15 μg) from samples taken during thylakoid membrane isolation (Section 2.3.2.2), and following protein extraction in the specified percentage of Triton X in solubilisation buffer was analysed. The S1 preparation is the supernatant after freeze/thawing of whole chloroplasts, and S2 is the supernatant following the first wash with 20 mM Bis-tris. Each sample was separated using 12% (w/v) SDS-PAGE and the separated proteins either stained with coomassie blue (Figure 4.5) or challenged with the NDH-K antibody (Figure 4.6). Coomassie staining revealed that the S1 and S2 samples predominantly contained a protein of ca. 50 kDa with a range of other more minor proteins. Treatment of the isolated thylakoids with a range of Triton X concentrations (from 0.1% (v/v) to 1% (v/v)) in the solubilisation buffer resulted in an increasing amount of protein being extracted as determined by an increase in intensity of coomassie blue staining. A range of proteins are present in these samples as shown by a number of coomassie blue stained protein bands. Western blot analysis of these samples show that no protein was recognised by the NDH-K antibody in the S1 and S2 samples. However, an increase in the level of a ca. 28 kDa protein can be seen with the increasing concentration of the Triton X extractant (Figure 4.6). The pellet obtained after the brief centrifugation of the samples following incubation in 1% (v/v) Triton X in solubilisation buffer was also assessed for the presence of NDH-K (Figure 4.6, Lane 1). In this fraction, the greatest level of the ca. 28 kDa protein was observed.

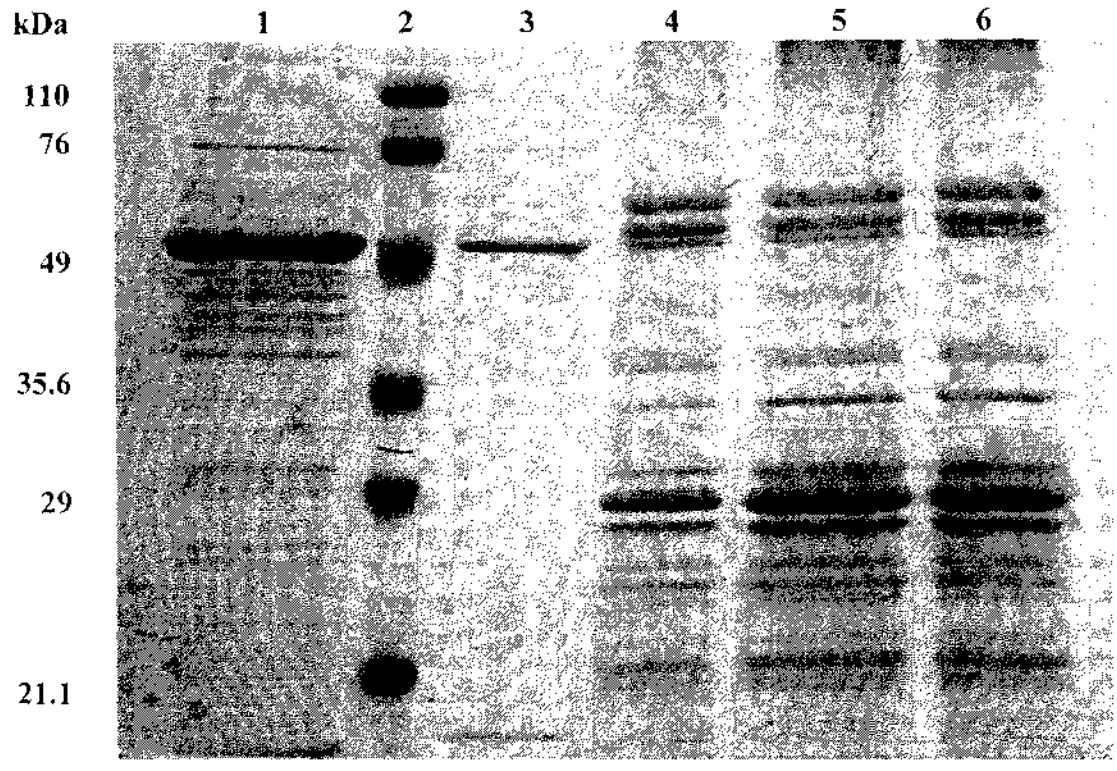

Figure 4.5. Coomassie blue stain of proteins at different stages of thylakoid isolation and following extraction with increasing concentrations of Triton X-100. Proteins were separated by a 12% (w/v) SDS-PAGE and stained with coomassie blue. The numbers listed on the left correspond to the mass of the molecular weight standards, in kDa.

Lane 1 - Supernatant following centrifugation after freeze/thawing of whole chloroplasts (S1)

Lane 2 - Low molecular weight marker (BioRad), with masses indicated

Lane 3 - Supernatant after first wash with 20 mM Bis-tris (S2)

Lane 4 - Extraction of thylakoid membrane proteins in 0.1% (v/v) Triton X-100 in the solubilisation buffer

Lane 5 - Extraction of thylakoid membrane proteins in 0.5% (v/v) Triton X-100 in the solubilisation buffer

Lane 6 - Extraction of thylakoid membrane proteins in 1% (v/v) Triton X-100 in the solubilisation buffer

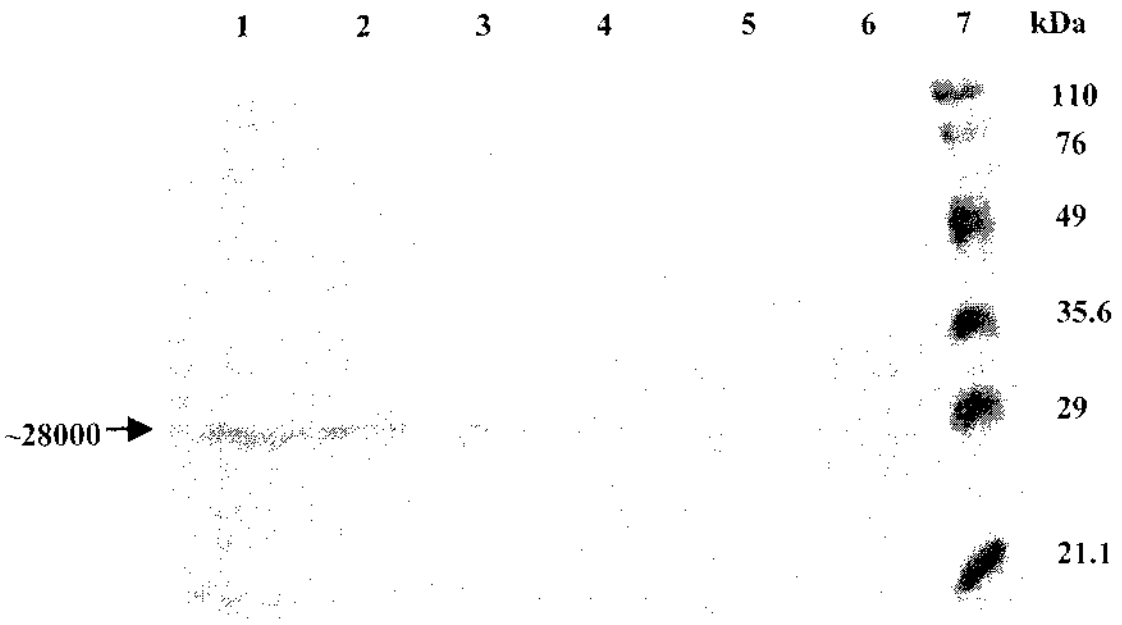

Figure 4.6. Western blot showing levels of NDH-K protein present in samples at different stages of thylakoid isolation, and following extraction with increasing concentrations of Triton X-100. Following separation by a 12% (w/v) SDS-PAGE, proteins were transferred to a PVDF membrane and challenged with the NDH-K antibody. The arrow corresponds to the 28.8 kDa protein recognised by the NDH-K antibody.

Lane 1 - Pellet following centrifugation after incubation in 1% (v/v) Triton X-100 in the solubilisation buffer

Lane 2 - Extraction of thylakoid membrane proteins in 1% (v/v) Triton X-100 in the solubilisation buffer

Lane 3 - Extraction of thylakoid membrane proteins in 0.5% (v/v) Triton X-100 in the solubilisation buffer

Lane 4 - Extraction of thylakoid membrane proteins in 0.1% (v/v) Triton X-100 in the solubilisation buffer

Lane 5 - Supernatant after first wash with 20 mM Bis-tris (S2)

Lane 6 - Supernatant following centrifugation after freeze/thawing of whole chloroplasts (S1)

Lane 7 - Low molecular weight marker (BioRad), with masses indicated

The reported molecular weights of the NDH-F and NDH-K bands are 70kD and 25kD respectively (Catala *et al.*, 1997; Elortza *et al.*, 1999). The mass of the protein band recognised by the NDH-F antibody in silverbeet is ca. 79 kDa. The mass of the protein band recognised by the NDH-K antibody in silverbeet is 28 kDa. These higher molecular weights may be due to a difference in the mass of the protein in silverbeet compared to barely and pea. On further questioning of Dr. Arizmendi, the supplier of the NDH-K antibody, it became apparent that this group has not determined the molecular mass of the protein in pea in any detail (J. Arizmendi, *per comm.*), and so the 25 kDa mass is reported as the approximate molecular weight. In this thesis, the molecular weight of proteins was calculated by plotting relative mobility versus log of molecular weight, an internationally accepted method to calculate the mass of proteins using SDS-PAGE (Section 2.4.8). Therefore, the approximate match in molecular mass between the pea and barely proteins and the silverbeet proteins was deemed sufficient to continue to use the antibody preparation in this research.

4.3.3 Accumulation of the NDH-K Protein During Greening of Silverbeet Seedlings

The accumulation of NDH-K protein in etioplasts and developing chloroplasts was examined. Previous studies have shown some of the subunits of the chloroplastic NAD(P)H dehydrogenase complex to have highest levels of expression in cotyledons grown and harvested in the dark, with diminishing levels of protein following exposure to light (Berger *et al.*, 1993). Therefore, as potential further support for the specificity of the NDH-K antibody, the level of NDH-K protein accumulation in dark-grown cotyledons exposed to increasing lengths of light (0 hour through to 24 hours) was measured using western analysis.

Cotyledons were harvested from 9-day old seedlings germinated and grown in the dark (0 hour) and then following exposure to 12 and 24 hours of light. Following exposure to 12 and 24 hours of light, the visual degree of greening increased from no apparent green cotyledons to rich green cotyledons. Thylakoid membrane proteins were extracted from whole chloroplasts at 0, 12 and 24 hours of light, by the Bis-tris method (Section

2.3.2.2). Equal protein concentrations (10 μg) of each sample were separated on a 12% (w/v) SDS-PAGE, and the separated proteins either stained with coomassie blue (Figure 4.7A) or incubated with the NDH-K antibody (Figure 4.7B). A range of proteins are visible in each sample (Figure 4.7A) on the coomassie blue stained gel, and the protein banding patterns differ, as the proteins present in each sample will vary due to different exposures to light. Western analysis using the NDH-K antibody revealed a single protein band of ca. 31 kDa at 0 hours, with no visible bands at 12 hours or 24 hours (Figure 4.7B).

The result from western analysis is in agreement with the reported results of highest level of protein at 0 hours, and diminishing levels following exposure to light, therefore providing further evidence that the NDH-K antibody does recognise the chloroplast NDH-K protein from silverbeet.

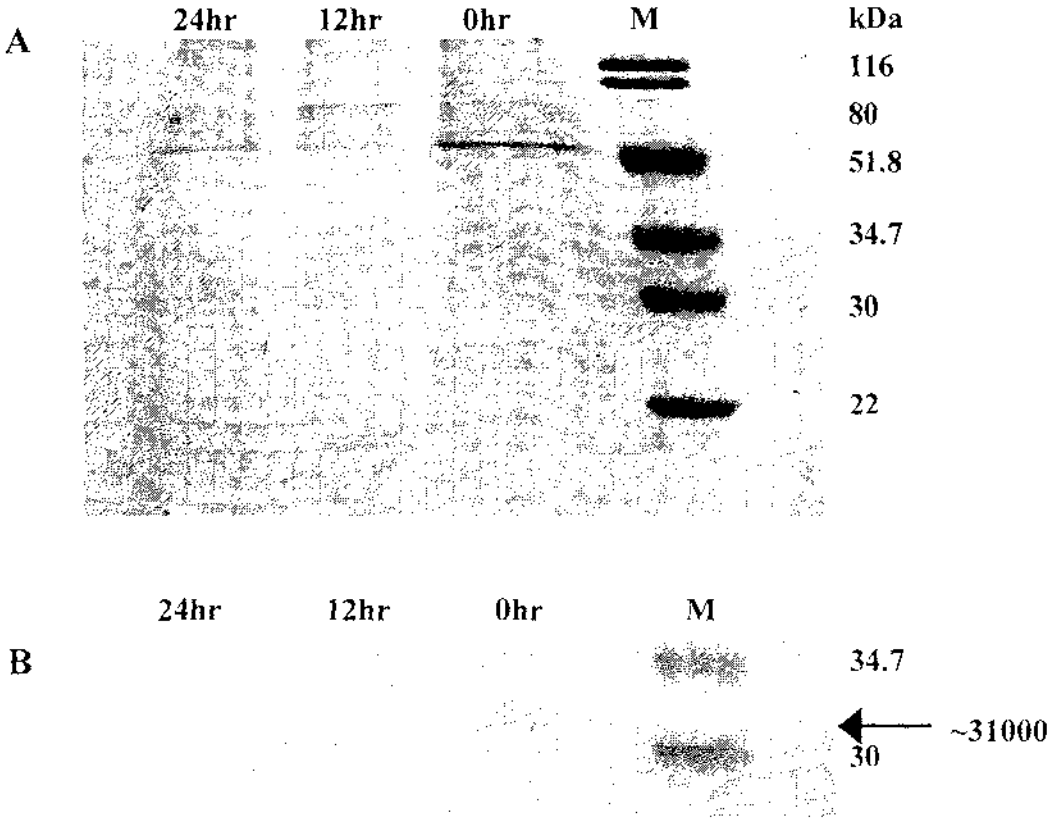

Figure 4.7. Coomassie blue staining (A) and western analysis using the NDH-K antibody (B), of thylakoid proteins extracted from silverbeet cotyledons exposed to 0, 12 and 24 hours of light. Thylakoid proteins were extracted from leaves subjected to 0 hours (0 h), 12 hours (12 h) and 24 hours (24 h) of light, separated by a 12% (w/v) SDS-PAGE and either stained with coomassie blue (A) or probed with the NDH-K antibody (B). A protein of approximately 31 kDa was recognised by the NDH-K antibody in all samples. Low molecular markers are represented as M, with the masses indicated.

4.4 Accumulation of NDH-F and NDH-K During Leaf Development

In some systems, levels of protein expressed during different stages of development or at different times of the day can be used as an indicator of the activity of the enzyme they are associated with. Therefore, relative levels of NDH-F and/or NDH-K proteins at varying stages of leaf development, following different lengths of exposure to light, and at different times of the day were examined.

4.4.1 Diurnal Expression Studies

In this study, diurnal regulation of the NDH-K protein of the multi-subunit NAD(P)H dehydrogenase complex was examined. Whole chloroplasts were isolated from mature green leaves of silverbeet over a 21 hour time period at midday, 6 pm, 10 pm, 5 am, and 9 am. These plants had previously been grown under a controlled light period (14 hours) from 6 am through to 8 pm. Thylakoid membrane proteins were extracted using the Bis-tris method of protein extraction with Triton X-100, and equal volumes (10 μg) of protein separated on a 12 % (w/v) SDS-PAGE gel. Separated proteins were either stained with coomassie blue (Figure 4.8A), or transferred to a PVDF membrane and incubated with the NDH-K antibody (Figure 4.8B). Western analysis of the proteins revealed differential expression of a protein of ca. 33.1 kDa, recognised by the NDH-K antibody over a 24 hour period (Figure 4.8B). The most intense bands of recognition correspond to midday and 5 am, with the 9 am band being slightly lighter, and the 6 pm and 10 pm bands being the least intense. The intensity of each band may not, however, represent different levels of the 33.1 kDa protein as the coomassie blue stained samples suggests a varying amount of protein was loaded (Figure 4.8A). The coomassie stained proteins show a higher intensity of staining in the midday and 5 am samples, and less in the 6 pm, 10 pm and 9 am samples, which correspond to the varying intensities in the western analysis.

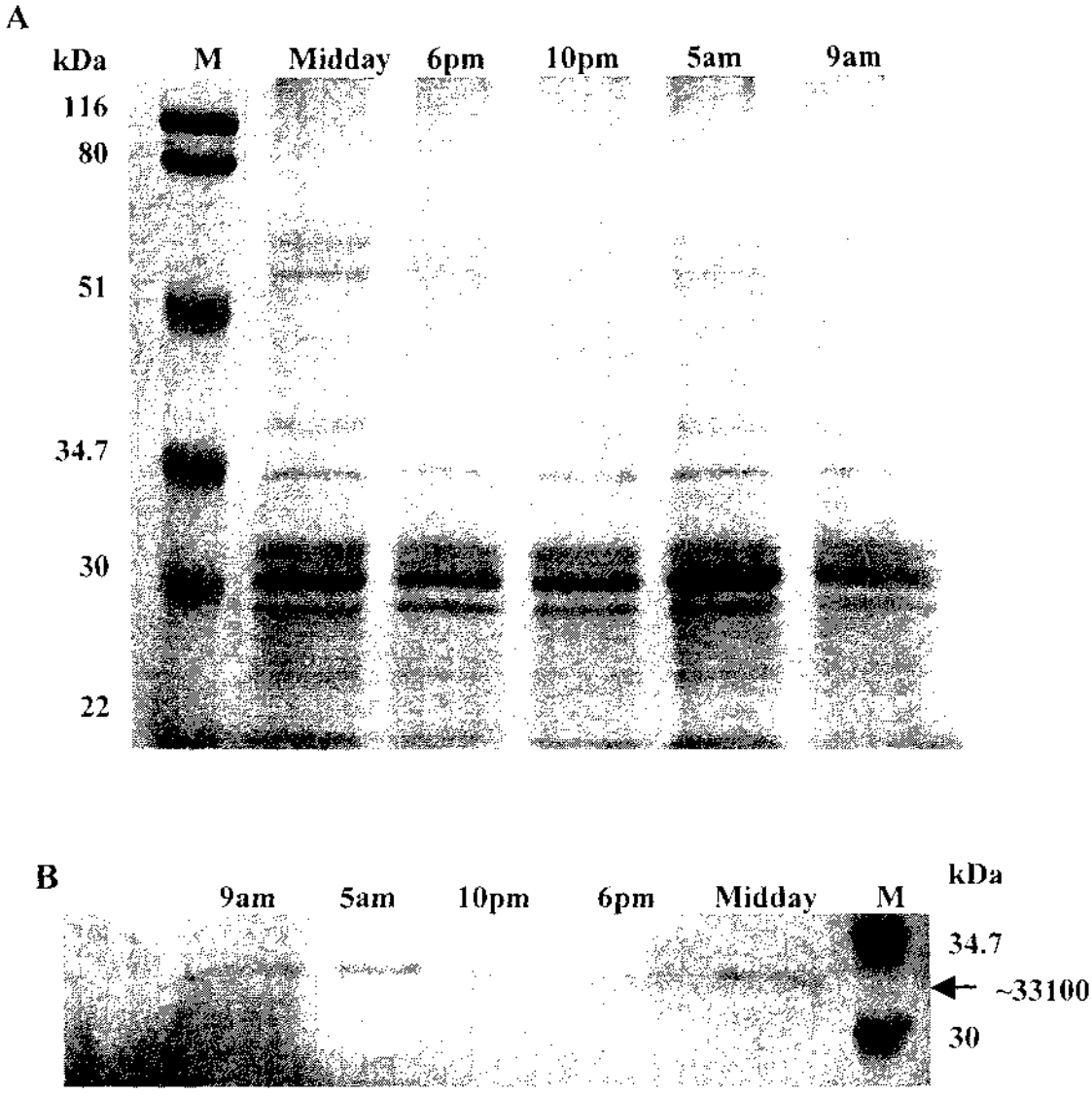

Figure 4.8. Coomassie blue staining (A) and western analysis using the NDH-K antibody (B) of thylakoid proteins extracted over a 24 hour period. Thylakoid proteins were extracted from leaves harvested at midday, 6 pm, 10 pm, 5 am, and 9 am. Proteins were separated by a 12% (w/v) SDS-PAGE and stained with coomassie blue (A), or challenged with the NDH-K antibody (B). A protein of 33.1 kDa was recognised in all samples by the NDH-K antibody. Low molecular markers are represented as M, with masses indicated.

4.4.2 Expression in Newly Initiated and Developing Leaves of White Clover

White clover leaves were harvested from the apex to node 4 (Figure 2.1) and whole chloroplasts isolated and resuspended in PEB. Equal concentrations (20 μg) of protein from each leaf stage were separated by a 12% (w/v) SDS-PAGE and the separated proteins either stained with coomassie blue (Figure 4.9A) or incubated with the NDH-F antibody (Figure 4.9B). Complete separation of proteins in the samples did not occur as seen by the presence of only a higher molecular weight protein band of ca. 68 kDa (Figure 4.9A). The differing intensities of proteins stained with coomassie blue suggest unequal amounts of protein being loaded, with a higher protein concentration in node 3 and 4 samples, and lower concentrations of protein in the node 2 sample. Western analysis of the proteins resulted in patchy blots, possibly due to the NDH-F antibody. In all samples, a protein of ca. 72.4 kDa was recognised by the NDH-F antibody, although all bands appear to be of very similar density (Figure 4.9B). The proteins recognised by the NDH-F antibody are all ca. 72.4 kDa in mass, suggesting that this protein is the NDH-F protein. However, the different concentrations of protein in each sample limits any definitive conclusion from this experiment.

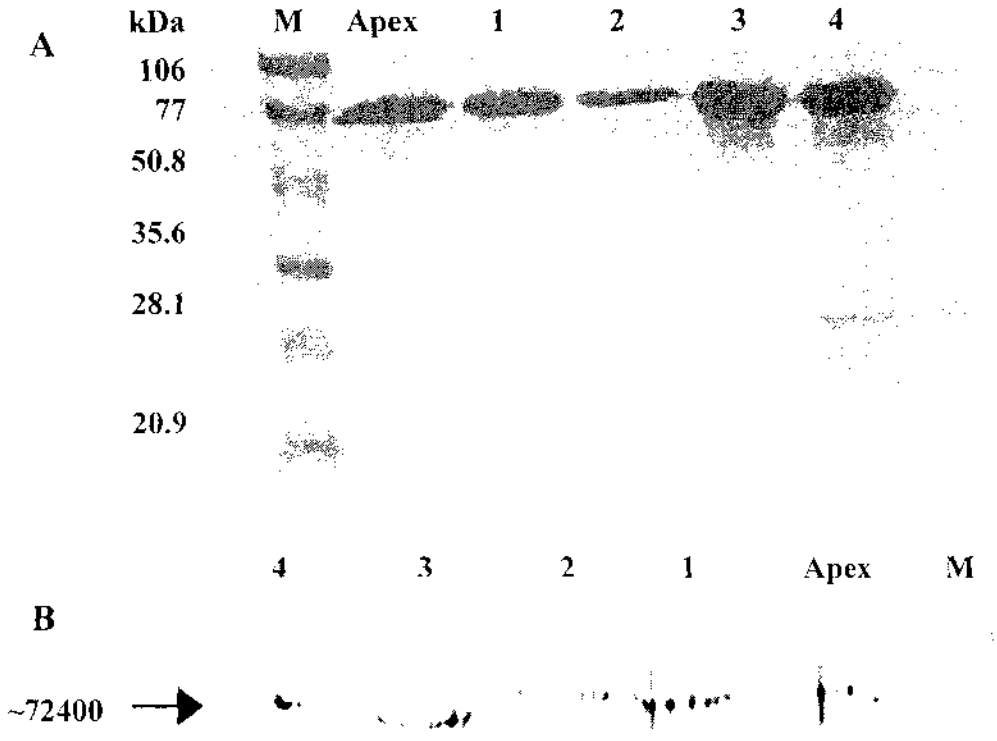

Figure 4.9. Coomassie blue staining (A) and western analysis using the NDH-F antibody (B), of chloroplast proteins at varying stages of early leaf development. Equal concentrations (20 μg) of protein from leaves of the apex (apex), node 1 (1), node 2 (2), node 3 (3) and node 4 (4) were separated by a 12% (w/v) SDS-PAGE and stained with coomassie blue (A). Separated proteins were challenged with the NDH-F antibody (B). Low molecular markers are represented as M, with the masses indicated.

4.4.3 Expression During Leaf Senescence

Early studies looking at the developmental regulation of the NAD(P)H dehydrogenase enzyme, suggested highest activity, and highest protein levels in chloroplasts with limited photosynthetic capacity such as etioplasts and senescent chloroplasts (Vera *et al.*, 1990). In this study, expression of NDH-F and NDH-K proteins at different stages of leaf development in white clover was examined. White clover provides a facile system for studying changes in levels of protein during leaf ontogeny because along the length of a stolon, all stages of leaf development, from initiation at the apex to senescent, are represented (Figure 2.1). Whole chloroplasts from young (leaves from apex to node 2), mature (nodes 3 to 8), pre-senescent (nodes 9 to 11), and senescent (nodes 12 to 14) stages of leaf development were isolated (Section 2.3.1). Samples used for the analysis of accumulation of the NDH-F protein were resuspended finally in PEB, while samples used for the analysis of NDH-K protein accumulation were subjected to Bis-tris extraction with Triton X (Section 2.3.2.2).

To confirm the developmental progression from mature green to senescent leaves, the chlorophyll concentration of each sample was measured (Section 2.4.1). In these measurements, the mature samples had higher chlorophyll concentrations when compared with young, pre-senescent and senescent samples (Figures 4.11A, 4.12A). Equal concentrations of proteins were separated by 12% (w/v) SDS-PAGE and separated proteins either stained with coomassie blue or incubated with NDH-F or NDH-K antibodies. Greater separation of proteins, as determined by a wider range of protein band sizes is evident in coomassie blue stained samples prepared for NDH-K protein analysis (Figure 4.10B). This method involves the isolation of thylakoid membranes prior to protein extraction and so greater access of extraction buffer to thylakoid membrane proteins may occur. In comparison, only proteins of molecular weights ca. 55.3 kDa and 30 kDa are clearly visible in coomassie blue stained gels of samples prepared for NDH-F analysis (Figure 4.10A). The protein of 55.3 kDa may be the large subunit of RUBISCO and the 30 kDa protein the small subunit. It is noteworthy that these proteins are highest in the mature leaves, and lowest in the senescent tissue, a pattern that reflects the photosynthetic activity of these tissues.

In the western analysis, levels of a protein of ca. 69 kDa, recognised by the NDH-F antibody (Figure 4.11B), was highest in pre-senescent leaf tissue (3885 units) followed by senescent leaf tissue (2281 units). Young and mature leaf samples exhibited lower intensity bands recognised by the NDH-F antibody (1749 units and 1306 units, respectively) (Figure 4.11A). These varying protein band intensities do not correspond to the unequal protein loading of the samples.

In contrast, a 35 kDa protein recognised by the NDH-K antibody (Figure 4.12B) had highest band intensities in young and mature leaf samples (2508 units and 2937 units, respectively). Protein accumulation is lowest in pre-senescent tissue (1928 units) but then increases again slightly in senescent tissue (2253 units) (Figure 4.12A).

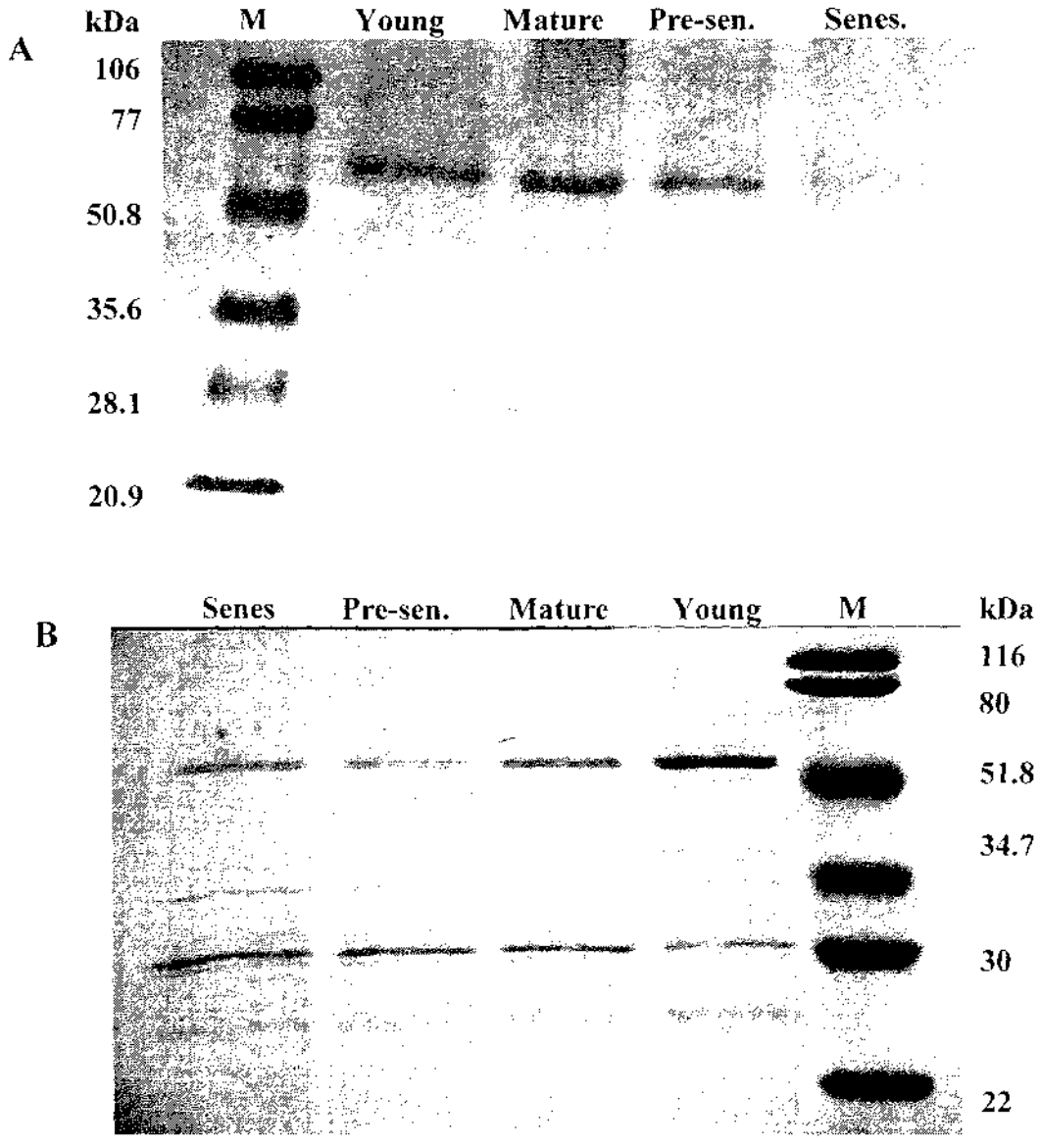

Figure 4.10. Coomassie blue staining of chloroplast proteins (A) and thylakoid proteins (B) extracted at different stages of leaf development in white clover. Proteins from leaves at varying stages of development, were extracted from chloroplasts using SDS (A) or from thylakoids using Triton X-100 (B). Proteins were separated by a 12% (w/v) SDS-PAGE and stained with coomassie blue. Low molecular markers are represented as M, with the masses indicated.

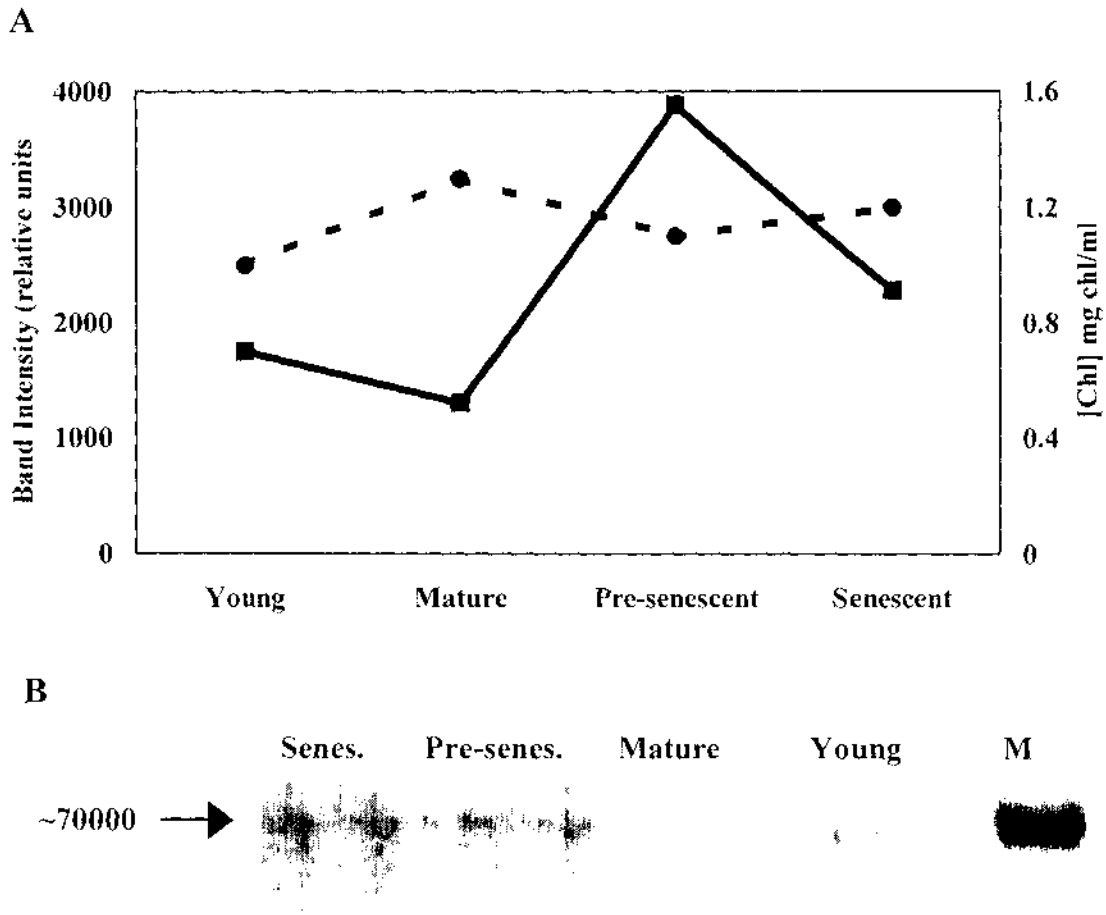

Figure 4.11. Chlorophyll analysis (A) and western analysis using the NDH-F antibody (B), of chloroplast proteins extracted at different stages of leaf development in white clover. Chloroplast proteins were extracted at varying stages of leaf development (young, mature, pre-senescent and senescent), separated by a 12% (w/v) SDS-PAGE and challenged with the NDH-F antibody (B). Densitometry measurements were performed on the western blot to determine relative levels of expression (A). The dashed line represents chlorophyll concentration; solid line represents densitometry measurements of band intensities. The low molecular marker is represented as M.

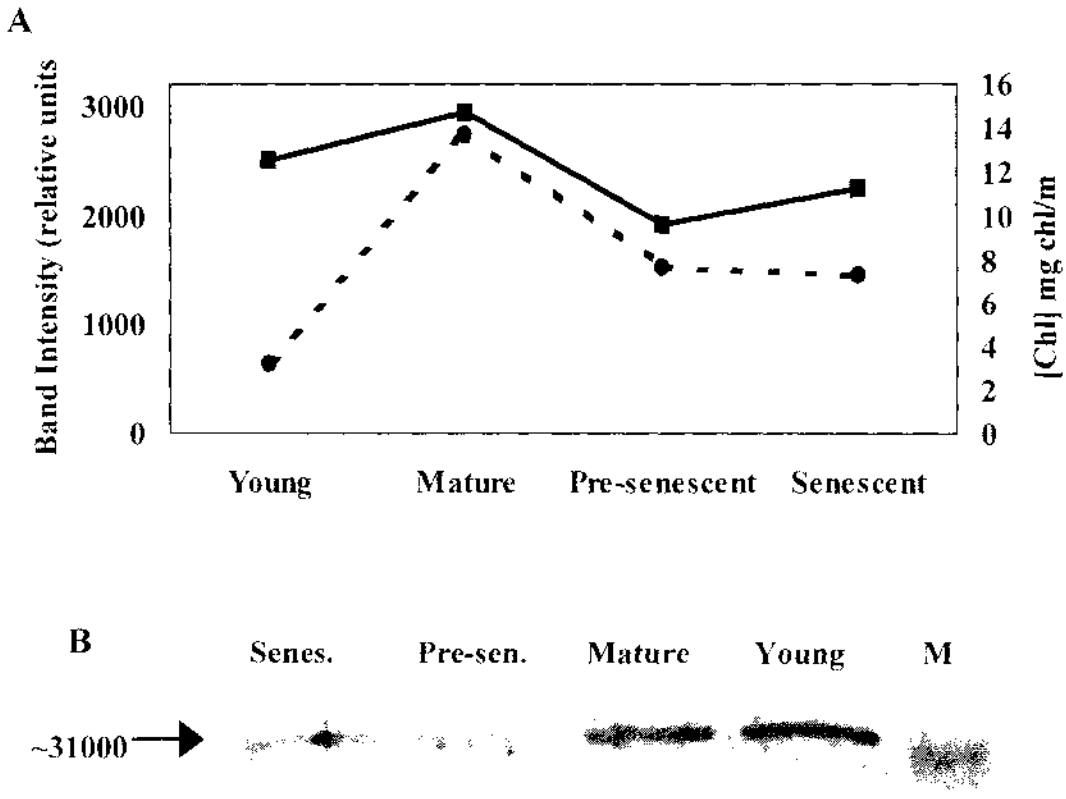

Figure 4.12. Chlorophyll analysis (A) and western analysis using the NDH-K antibody (B), of thylakoid proteins extracted at different stages of leaf development in white clover. Thylakoid proteins were extracted at varying stages of leaf development (young, mature, pre-senescent and senescent), separated by a 12% (w/v) SDS-PAGE and challenged with the NDH-K antibody (B). Densitometry measurements were performed on the western blot to determine relative levels of expression (A). The dashed line represents chlorophyll concentration; solid line represents densitometry measurements of band intensities. The low molecular marker is represented as M.

CHAPTER 5 DISCUSSION

Chlororespiration, the chloroplastic respiratory pathway homologous to the mitochondrial respiratory chain, interacts with the photosynthetic electron transfer chain (Bennoun, 1982) at, at least PQ. First observed in green algae, chlororespiration has also been shown to be present in the chloroplasts of higher plants (Garab *et al*, 1989). To date, however, the mechanism and regulatory control of this pathway remains uncertain. It is widely accepted that a chloroplastic NAD(P)H dehydrogenase, located in the stromal lamellae of the thylakoid membrane, is the donator of electrons to the photosynthetic PQ pool, though the donor of electrons to the NA(P)H DH complex itself is still under debate. The other primary enzyme thought to be involved in chlororespiratory electron transfer is a terminal oxidase. Recent reports suggest the nuclear encoded protein, IMMUTANS to be the terminal oxidase of the chlororespiratory pathway (Carol *et al.*, 1999; Cournac *et al.*, 2000, Josse *et al.*, 2000), though further analysis is required to determine the function of this protein.

5.1 SHAM Inhibition of Photosynthesis

Research on the terminal oxidase of the chlororespiratory pathway has involved the use of mitochondrial electron transfer inhibitors (Bennoun, 1982; Buchel and Garab, 1995). Although this seems reasonable, alternative effects of these inhibitors in the chloroplast must also be taken into account. As SHAM is traditionally used as a mitochondrial alternative oxidase inhibitor, it was assumed that it would also inhibit a putative AOX present in the chloroplast. Pierre Bennoun first implied the presence of an alternative-type oxidase involved in chlororespiration (Bennoun, 1982). Bennoun used whole *Chlorella* cells and measured chlorophyll fluorescence before and after addition of 4-10 mM SHAM. Bennoun reported a decrease in the area over the fluorescence curve following SHAM addition, implying inhibition by SHAM of a alternative-like terminal oxidase. Bennoun proposed this inhibition blocked oxidation of the reduced PQ pool. However, it has since been suggested that SHAM inhibits photosynthetic CO_2 uptake

(Diethelm *et al.* 1990). The aspect of photosynthesis that is sensitive to SHAM is still unknown, be it the electron transfer chain or the carbon fixation pathway. This part of my research therefore, has focused on determination and characterisation of SHAM inhibition on photosynthetic electron transfer, and the major results are summarised in Table 3.2.

Whole chain electron transfer was measured to determine whether SHAM has an inhibitory effect on the photosynthetic chain. Addition of 20 mM SHAM to a preparation of intact thylakoids and MV resulted in a decrease in oxygen consumption by MV (Table 3.2). This decrease of oxygen consumption is indicative of a reduction in electrons reaching MV due to a block in the chain, presumably imposed by SHAM. Inhibition by SHAM of whole chain photosynthetic electron transfer was supported by fluorescence measurements of isolated thylakoids with additions of MV and SHAM. The F_m of thylakoids in the presence of the artificial electron acceptor MV, was much lower than the F_m of the control. The F_m is reflective of the 'freedom' of the electrons in the chain, with a higher F_m representing restriction of electron flow. In a preparation of isolated thylakoid membranes, the natural final electron acceptor, Fd is not present as it is easily dissociated from the membranes in the isolation process. Addition of an artificial electron acceptor (i.e. MV) provides the photosynthetic chain with a final electron acceptor, therefore allowing electrons to pass more freely through the chain, therefore reducing the F_m. Addition of 20 mM SHAM to the preparation of thylakoids and MV resulted in an increase in F_m (Table 3.1). However, the F_m was not as high as that of the control. The increase in F_m from the MV transient suggests an inhibitory effect of SHAM on electron transfer through the photosynthetic chain. However, the F_m was expected to be higher than that of simply isolated thylakoids as electron flow should be more limited in the presence of SHAM. Normalisation of these fluorescence transients revealed that addition of SHAM to the whole chain assay resulted in a decrease in the area over the curve, even from that of the control. This is expected as inhibition of the photosynthetic chain by SHAM will reduced the pool size of electron acceptors available for electron transfer. The conclusion drawn from these experiments is that SHAM does inhibit photosynthetic electron transfer.

The next question is then, where in the photosynthetic chain does SHAM inhibit? A wide range of photosynthetic electron acceptors, donors and inhibitors exist that allow the isolation of specific parts of the chain. Electron transfer through the latter part of the chain, from cytochrome b_6f through to MV was examined. Addition of 20 mM SHAM to the preparation had very little effect on the rate of oxygen consumption by MV (Table 3.2). The slight decrease in oxygen consumption by MV that is seen is likely due to the drift on the oxygen electrode, which is approximately 10%. It was concluded therefore, that SHAM does not inhibit anywhere in this part of the chain.

The first part of the chain, from the OEC to PQ, was then examined. A decrease in the rate of oxygen evolution was seen following the addition of SHAM to thylakoids in the presence of the PQ electron acceptor *p*BQ, and to thylakoids in the presence of the Q_B electron acceptor FeCN (Table 3.2). The OEC is involved in splitting H_2O into O_2, H^+ and electrons. The driving force of this reaction is the redox state of P680. When P680 is excited by a photon, electrons are pulled from the OEC via the splitting of water. Addition of SHAM resulted in a decrease in oxygen evolution by the OEC which is indicative of a build-up of electrons in PS II, therefore restricting further entry of electrons from P680 which in turn results in a decrease in demand for electrons from the OEC. Fluorescence analysis of these assays showed an increase in F_m following the addition of SHAM to both *p*BQ and FeCN assays (Table 3.1). As with the whole chain assay, the F_m following SHAM addition was significantly smaller than that of the controls. Normalisation of both the *p*BQ and FeCN assays revealed a decrease in the area over the curve following the addition of SHAM again, even compared to the control. These results suggest that SHAM inhibits somewhere in the PS II complex. Further evidence for SHAM inhibition in PS II was seen with the use of the Q_B inhibitor, DCMU. If SHAM does inhibit somewhere within PS II, we would expect to see a similar pool size of available electron acceptors as the DCMU inhibited assay. And indeed this is what we observed, with addition of SHAM resulting in a slightly smaller pool of available electron acceptors than that of the DCMU assay. This result is indicative either of inhibition further within PS II than Q_B, or inhibition of additional Q_B sites not already inhibited by DCMU.

therefore that SHAM does not consume O_2 at any great rate, though it is difficult to explain the difference in levels of SHAM inhibition of the various assays.

The final conclusion for this section of work is that SHAM inhibits photosynthetic electron transfer somewhere in PS II, at P680, Phaeophytin, Q_A or the non-haem iron (Figure 5.1). The mode of SHAM inhibition, even in mitochondria where it is often used, is not well understood. However, two models of SHAM inhibition on PS II are proposed. Firstly, that the small hydrophobic SHAM molecule embeds itself in PS II, perturbing molecules involved in electron transfer. As the distances and angles of the molecules involved in electron transfer are critical, this would likely abolish the transfer. Secondly, it is proposed that SHAM chelates the non-haem Fe situated between Q_A and Q_B. This could lead to inhibition of electron transfer from Q_A to Q_B. This second hypothesis seems most likely as SHAM is known to be capable of chelating Fe(III) (Springer *et al.*, 1987). While Debus *et al.* (1986) showed that the removal of the non-haem iron from *Rhodobacter sphaeroides* reaction centres did not affect electron transfer, it is conceivable that the presence of SHAM in the vicinity of the quinones causes much more disruption than the simple removal of the iron. For example, Koulougliotis *et al.* (1993) showed that cyanide binds to the non-haem iron and affects Q_A-Q_B transfer. This is consistent with the effects of other chelators (such as *o*-phenanthroline) which also inhibit PS II electron transfer (Trebst, 1980).

Fluorescence transients shown in this study suggest that previous investigations of the inhibitory effect of SHAM of a terminal oxidase of chlororespiration may not reflect a SHAM effect on an AOX but an effect on PS II. It has been demonstrated here that SHAM inhibits in the PS II complex. This site of inhibition results in the same fluorescence transient seen by Bennoun's initial studies on AOX.

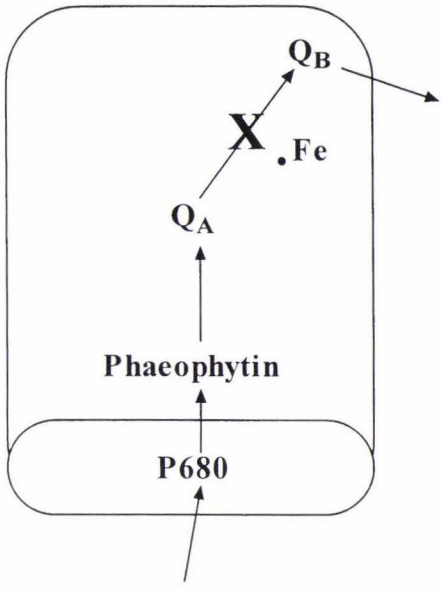

Figure 5.1. Schematic diagram of the PS II complex of higher plants. SHAM inhibits somewhere between phaeophytin and Q_B. We propose inhibition is at the non-haem Fe, where SHAM will chelate the Fe thus hindering electron transfer from Q_A to Q_B.

5.1.1 Future Work

Further characterisation of the exact site of SHAM inhibition in PS II is required. This could be done by the use of electroparamagnetic resonance (EPR), which would examine more closely the effect of SHAM on the non-haem Fe between Q_A and Q_B. The concentration of SHAM required to have an inhibitory effect also requires further analysis. Analysis of SHAM inhibition at concentrations as low as 1-2 mM need to be examined by fluorescence, as this is more sensitive to lower concentrations of inhibitors than the oxygen electrode.

The effect of other mitochondrial respiratory inhibitors used in studies on the putative chloroplast oxidase, such as propyl gallate, on the photosynthetic electron transfer chain should also be undertaken as it is absolutely necessary to know exactly what effects are being observed.

5.2 Expression of NAD(P)H Dehydrogenase Proteins

The first part of this masters thesis determined that the mitochondrial AOX inhibitor, SHAM has an inhibitory effect on the photosynthetic chain, somewhere in PS II. This inhibitory action of SHAM is important to note in studies looking at the properties of the putative chloroplast terminal oxidase, thought to be involved in the chlororespiratory pathway, as inhibition in PS II will confound oxidase results. To investigate the process of chlororespiration more directly, antibodies directed against subunits of the chloroplastic NAD(P)H dehydrogenase complex were used to determine changes in expression of the complex during specific developmental processes in leaves of silverbeet and white clover. Changes in abundance of these subunits would give clues as to whether the NAD(P)H dehydrogenase complex is up-regulated during processes that lend support to a chlororespiratory pathway. However, before the accumulation of the complex could be studied, it was necessary to ensure that the chloroplastic, and not the mitochondrial NDH proteins were being recognised by the antibodies. Therefore, it was important to (i) prepare whole chloroplasts and (ii) to ensure that the antibodies used did recognise the chloroplast components.

The eleven chloroplast *ndh* genes encode proteins which form the chloroplast NAD(P)H dehydrogenase complex. This complex is located in the thylakoid membrane, with subunits NDH-A to NDH-G embedded in the membrane, and subunits NDH-H to NDH-K located on the stromal lamellae of the membrane (Guedney *et al.*, 1996; Figure 5.2).

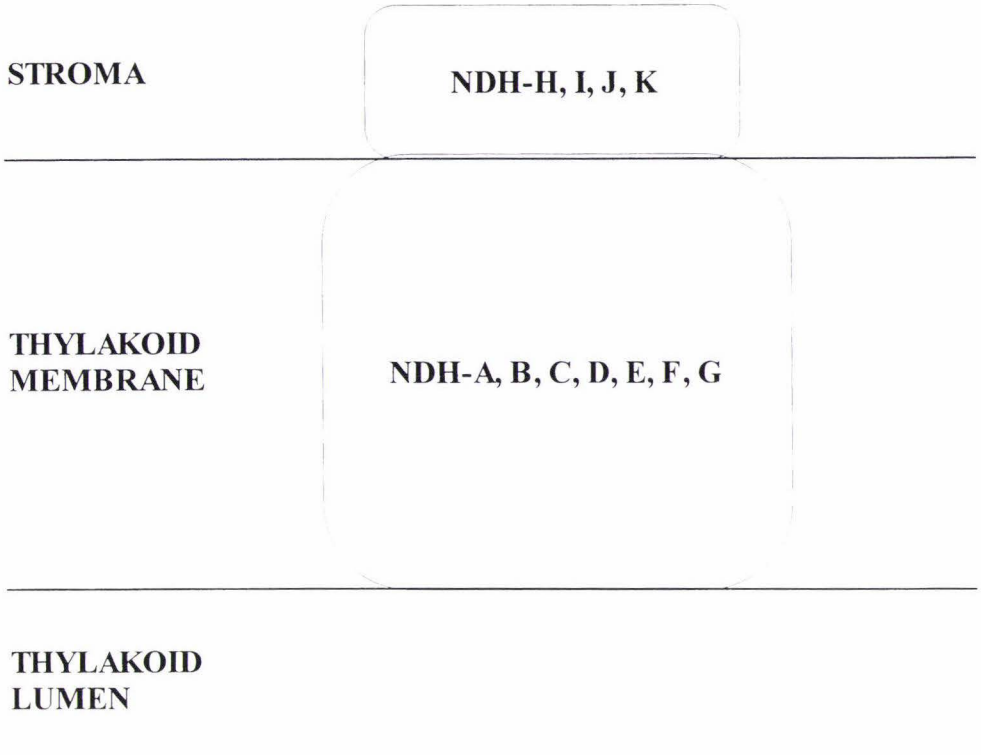

Figure 5.2. Schematic diagram of the chloroplastic NAD(P)H dehydrogenase. To date, 11 proteins have been identified to be involved in the formation of the complex, with NDH-A to NDH-G proteins located in the thylakoid membrane, and NDH-H to NDH-K located on the stromal lamellae of the membrane.

To isolate whole chloroplasts from a crude chloroplast extract, a 10%/80% percoll gradient was used. Whole, intact chloroplasts were located in a green band that formed from centrifugation at high speeds (15, 000 x g) for 10 minutes. The presence of whole, intact chloroplasts was examined using two different microscopy approaches, light and confocal microscopy. The presence of rounded, turgid chloroplasts was observed with both microscopy techniques (Figure 4.1). A lack of misshapen organelles and chloroplast contents in this analysis suggests that this chloroplast extraction protocol did yield intact chloroplasts. This is necessary as it eliminates any possible loss of the proteins under examination in this research. However, detection of mitochondrial contamination was not included in the analysis using microscopy.

Herriko Unibertsitatea, Spain). As an extrinsic thylakoid protein located on the stromal side, detergent extraction in Triton X-100 was sufficient.

A 79 kDa band recognised by the NDH-F antibody was observed in thylakoid membranes isolated directly from leaf tissue, as well as a smaller 28.8 kDa band. Smaller molecular mass bands were seen in the whole chloroplast fraction (ca. 25 kDa) (in 0.1% (w/v) SDS) and whole leaf protein extract (ca. 60 kDa). The reported size of the NDH-F protein is a tentative 70 kDa (Catala *et al.*, 1997), and so the ca. 79 kDa band recognised by the NDH-F antibody may be the NDH-F protein. A number of other bands of varying sizes were also observed in some blots. These bands are likely due to non-specific binding of the antibody to other proteins in the samples, as initial western analysis with both the NDH-F and NDH-K antibodies resulted in non-specific binding, which did not often occur in subsequent blots. Alternatively, as lower molecular mass proteins, they may represent degradation products of the NDH-F protein. However, the identity of these proteins was not pursued further in this thesis.

The NDH-K antibody recognised a band of ca. 28.8 kDa in protein samples extracted from isolated thylakoid membranes treated with Triton X. Increasing concentrations of Triton X resulted in greater amounts of NDH-K being extracted (Figure 4.6). A large amount of protein is also present in the pellet following extraction with 1% (v/v) Triton X, suggesting even this high concentration of Triton does not fully extract all thylakoid proteins. It had been suggested that the optimum amount of Triton X to extract thylakoid proteins was of a ratio of 1:1 protein to Triton X (J. Arizmendi, Euskal Herriko University, *per comm.*). Therefore, all subsequent protein extractions in this research, analysed with the NDH-K antibody, were performed using 1% (v/v) Triton X in a 1:1 ratio with protein.

It was also suggested that the NDH-K antibody gifted by Dr. Arizmendi might cross react with a light dependent protein (J. Arizmendi, *per comm.*). To investigate the specificity of the antibody, western blot analysis using cotyledons germinated and grown up in darkness and harvested after 0, 12 and 24 hours of exposure to light was performed (Figure 4.7). It has been previously shown that the accumulation of NDH

proteins is highest in young, non-photosynthetic chloroplasts (Berger *et al.*, 1993; Catala *et al.*, 1997). If the antibody also recognised a light stimulated protein, recognition in the samples exposed to the increasing levels of light would be expected. However, no such recognition was observed (Figure 4.7B). Instead, the antibody recognised a protein of 31 kDa in the 0 hour sample, with no visible bands in the 12 hour and 24 hour samples. While no band is visible in these latter samples, the protein may still be present, although in lower abundance when compared with the 0 hour sample, and as shown previously (Berger *et al.*, 1993). The reported predicted size of the NDH-K protein in pea is 25 kDa (Elorzta *et al.*, 1999), but the band recognised by the NDH-K antibody in silverbeet is ca. 28.8 kDa.

These preliminary experiments show that the NDH-F and NDH-K antibodies gifted to this research do recognise proteins of the expected size in silverbeet. Further, both Sabater and colleagues, and Arizmendi and colleagues have shown that these antibodies do not cross-react with the mitochondrial homologues (Catala *et al.*, 1997; Elortza *et al.*, 1999). This, coupled with the amino acid sequence comparison (including that undertaken in this thesis) that shows that the chloroplast NDH proteins are closely related to other plant species (and not to their mitochondrial counterparts), was taken as sufficient evidence to use these antibodies in developmental studies in both silverbeet and white clover.

5.2.3 Accumulation of NDH-F and NDH-K in Plant Development

Though the regulation of chlororespiration is still unknown, many theories on the regulatory mechanism exist. These include up-regulation during periods of stress (Peltier and Schmidt, 1991; Sazanov *et al.*, 1998a), assisting photosynthetic metabolism (dePamphilis and Palmer, 1990), and increased activity in non-photosynthetic chloroplasts (Vera *et al.*, 1990; Catala *et al.*, 1997). This study involved determination of regulation of the NDH-F and NDH-K proteins of the NAD(P)H dehydrogenase complex in silverbeet and white clover during developmental processes where up-regulation or down-regulation of chlororespiratory activity is proposed to occur.

5.2.3.1 Diurnal Regulation

This section of work involved the examination of whether subunits of the NAD(P)H dehydrogenase complex involved in chlororespiration were regulated over a 24 hour period. It has been hypothesised that chlororespiration is most active in the fours hours following sunset due to the high levels of NADH present in the chloroplast from the degradation of starch produced by photosynthesis (Sazanov *et al.*, 1998a). It may also be that chlororespiration is most active during periods of low rates of photosynthesis, such as early morning, so poising the chain for the bombardment of electrons.

In this study we examined the levels of NDH-K protein in green leaves of silverbeet over a 24 hour light/dark period. Though equal concentrations of protein was attempted to be loaded onto the gels, coomassie staining of the proteins revealed that more protein in the midday and 5am samples was present when compared with the 6pm, 10pm and 9am samples. Difficulty exists in loading of equal concentrations of protein in these experiments due to the fact that the Bio-Rad detergent-compatible protein assay does not produce reliable, reproducible results with samples in the presence of Triton X. Therefore, protein concentrations were determined prior to extraction in Triton X, although it is acknowledged that this may introduce errors since this is not the final stage of protein extraction. Protein concentrations need to be determined using an alternative assay than the Bio-Rad DC assay. Therefore, coomassie blue staining of separated proteins was always performed with every western blot, to provide some notion of equivalence of protein staining.

If the hypothesis is correct, highest accumulation of NDH-K would have been expected at 10pm (2 hours after sunset), and again at 5am (just prior to dawn). Recognition of a protein of 31 kDa by the NDH-K antibody was seen in all samples with higher intensity bands in the 5am and midday samples, and lower intensity bands in the 6pm, 10pm and 9am samples. However, these varying levels of band intensity also appear to correlate with the levels of protein loaded, and so the conclusion drawn from this experiment is that there may be no appreciable change in levels of NDH-K in mature green silverbeet leaves over a 24 hour period. Though levels of NDH-K protein accumulation may not alter over the course of a day, activity of the NAD(P)H dehydrogenase may still be

regulated, just not at the level of protein synthesis/degradation. Further characterisation of a diurnal regulation of the NAD(P)H dehydrogenase requires analysis of the enzyme activity of the complex. Increasingly, research involved in determination of NAD(P)H dehydrogenase activity is being done, although as yet little on the diurnal regulation has been published.

5.2.3.2 Developmental Regulation

It is hypothesised that chlororespiration is most active in chloroplasts with limited photosynthetic capabilities, with levels of some NDH proteins shown to be highest in young, non-photosynthetic leaves and older, senescent leaves (Catala *et al.*, 1997; Guera *et al.*, 2000). Therefore, the accumulation of NDH-F and NDH-K proteins was examined at different stages of leaf development in white clover. White clover leaves (rather than silverbeet) were used for this part of the investigation because the plant produces leaves at varying stages of leaf development (young, mature, pre-senescent and senescent) on a single stolon thus making sampling easier.

In the first experiment, expression levels of NDH-F in developing white clover leaves, was examined using tissues from the apex through to node 4 along a stolon. Coomassie staining of the SDS-PAGE revealed unequal concentrations of protein loaded, with highest levels in nodes 3 and 4, moderate levels in the apex and node 1 and the least amount in node 2. Western analysis, though patchy, suggests approximately equal levels of accumulation of a protein of 72.4 kDa is recognised by the NDH-F antibody. While it is difficult to conclude from this result, it does suggest that in young through to mature tissue, levels of the NAD(P)H dehydrogenase complex remains relatively constant. This may suggest that once a leaf becomes photosynthetically competent, as all samples in this experiment are, chlororespiration slows or ceases. This seems to fit the general hypothesis of chlororespiratory activity in non-photosynthetic tissues (Catala *et al.*, 1997). The fact that some NDH-F protein is still present in the samples may suggest that while chlororespiratory activity is not necessarily high in these tissues, it may still have a role to play either in photosynthetic metabolism or to prevent over-reduction of PS II in times of environmental stress.

In the second experiment, white clover leaves ranging in stages of development from young through to senescent were used for the investigation of NDH-F and NDH-K accumulation. Samples were analysed using both NDH-F and NDH-K antibodies. Coomassie blue staining performed at the time of each western blot show highest protein concentrations in the young and mature samples, with less protein in the pre-senescent and senescent samples. The NDH-F antibody recognised a protein of ca. 69 kDa with higher accumulation in pre-senescent and senescent tissues when compared with the young and mature, photosynthetically active tissues (Figure 4.11). Levels of the putative NDH-F protein are slightly lower in the senescent leaf tissue when compared with the pre-senescent sample. This may be due to the fact that senescence involves the (eventual) degradation of proteins in the leaf, and so degradation of the NAD(P)H dehydrogenase complex is beginning by this stage. This NDH-F result supports the hypothesis that levels of NDH proteins are highest in senescing tissues (Vera *et al.*, 1990; Catala *et al.*, 1997). High levels of NDH-F expression implies a large number of NAD(P)H DH complex is present in the thylakoids. While it is not possible to make any conclusions about the activity of the enzyme, we can hypothesise that chlororespiration is more active in tissues with declining photosynthetic capacity, such as senescent leaves, when compared with tissues with a high level of photosynthetic activity.

In contrast, the NDH-K antibody recognition (Figure 4.12) suggests that levels of NDH-K protein is highest in young and mature tissues when compared with the pre-senescent and senescent samples, although a protein of 35 kDa was recognised. This observation contradicts reported results (Vera *et al.*, 1990; Elortza *et al.*, 1999) and also the result obtained in this thesis using the NDH-F antibody. The varying levels of NDH-K antibody recognition does not appear to be an artefact of unequal protein loading. Instead, the NDH-K subunit of the dehydrogenase may not be under a strict developmental regulation as regulation of the complex may lie only with a few of the subunits. The NDH-K antibody is thought to potentially cross-react with a light sensitive thylakoid protein, possibly involved in photosynthesis. These NDH-K results are in agreement of hybridisation with a protein involved in photosynthesis, as highest levels are seen in the mature leaves which will have high levels of photosynthetic

activity. However, this is not likely as our preliminary analysis of the specificity of the NDH-K antibody in cotyledons harvested after 0, 12 and 24 hours of light suggests that the antibody does not recognise a light specific protein.

It is noteworthy that the proteins recognised by the NDH-K antibodies were of different sizes (28.8 kDa, 31 kDa, 33.1 kDa). This suggests that either contaminating proteins were recognised by the antibody, or the method of calculating molecular weight is not wholly accurate. In this thesis, molecular weight was calculated by plotting the mobility of the marker proteins against the $\log_{10}$ of molecular mass. While this method is accurate, it does give best results with gradient gels. To more consistently identify the proteins identified by the NDH-K antibody, gradient electrophoresis should be used.

The overall conclusion from this section of research is for the developmental regulation of subunits of the chlororespiratory NAD(P)H dehydrogenase complex in both silverbeet and white clover. Though western analysis does not directly reflect activity of the complex, the results have shown that the dehydrogenase could be most active in tissue of limited photosynthetic capacity such as etioplasts and senescent chloroplasts.

5.2.4 Future Work

Much work is still required to determine and characterise regulation of chlororespiration. Optimising the protein extraction protocol is necessary as unequal concentrations of protein loaded complicates analysis. The next logical step in analysis is then to sequence the protein bands that hybridised with the antibodies. This will allow a more conclusive statement that the bands we saw are the proteins of interest. Also, measurements of NAD(P)H dehydrogenase activity in each experiment would be advantageous as this would give a clearer idea of the regulation of the complex. Simply identifying levels of protein accumulation does not give the full picture.

This section of research has relied heavily on the specificity of the antibodies obtained from overseas laboratories. Further analysis of the expression of NDH proteins would benefit from the raising of antibodies against NDH proteins of silverbeet or white clover

in-house. While the antibody preparations received were satisfactory, the patchiness of some of the NDH-F blots may have been due to the freeze drying of the antibodies. Further optimisation of the western blot procedure is also required. Longer incubation times of the primary antibody does produce clearer blots, though background levels and non-specific binding increases. Better primary antibody may also overcome this problem.

As the silverbeet chloroplast genome is largely unsequenced, it would be interesting to design primers to silverbeet *ndh* genes to probe for the presence of all the subunits known to date for the NAD(P)H dehydrogenase, and also compare silverbeet *ndh* genes with *ndh* genes from other plant species.

Chlororespiration does not just involve the NAD(P)H dehydrogenase enzyme. Recently a protein called IMMUTANS (IM) has been proposed to be the terminal oxidase of this pathway (Carol *et al.*, 1999; Wu *et al.*, 1999). Western analysis and activity studies of IM on the developmental samples would further reveal information as to the regulatory control of chlororespiration.

5.3 Conclusions

This Masters research has utilised a variety of biochemical and molecular biological techniques to investigate a couple of aspects of chlororespiration. Evidence for an inhibitory action of SHAM on photosynthetic electron transfer through PS II, and therefore not necessarily a putative terminal oxidase as once believed has been presented. However, further characterisation of the actual site of inhibition is still required. Preliminary work on the developmental regulation of the NAD(P)H dehydrogenase complex involved in chlororespiration has also been presented. Much refining of the protocols and further analysis is still required, however the data is in general agreement of reported results. While at present the overall picture of chlororespiration is still unclear, much research is being done to determine the presence

and activity of the two primary enzymes involved in the pathway, the NAD(P)H dehydrogenase and the putative terminal oxidase (IM?).

BIBLIOGRAPHY

Altschul, S.F., Madden, T.L., Schäffer, A.A., Zhang, J., Zhang, Z., Miller, W., Lipman, D.J. (1997), Gapped BLAST and PSI-BLAST: a new generation of protein database search programs. *Nucleic Acids Res.* **25:**3389-3402.

Arnon D.I. (1949) Copper enzymes in isolated chloroplasts. Polyphenoloxidase in *Beta vulgaris*. *Plant Physiol.* **24:** 1-15.

Asada K., Heber U., Schreiber U. (1992) Pool size of electrons that con be donated to P700+, as determined in intact leaves: donation the P700+ from stromal components via the intersystem chain. *Plant Cell Physiol.* **33:** 927-932.

Bartlett S.G., Grossman A.R., Chua N.H. (1982) *In vitro* synthesis and uptake of cytoplasmically-synthesized chloroplast proteins. *Methods in chloroplast molecular biology*. (Edelman M., Hallick R.B., Chua N.H. Eds). 1081-1091

Bennoun P. (1982) Evidence for a respiratory chain in the chloroplast. *Proc. Natl. Acad. Sci. USA.* **79:** 4352-4356.

Bennoun P. (1994) Chlororespiration revisited: mitochondrial-plastid interactions in *Chlamydomonas*. *Biochimica et Biophysica Acta.* **1186:** 59-66.

Berger S., Ellersiek U., Westhoff P., Steinmuller K. (1993) Studies in the expression of NDH-H, a subunit of the NAD(P)H-plastoquinone-oxidoreductase of higher-plant chloroplasts. *Planta.* **190:** 25-31.

Berman H.M., Westbrook J., Feng Z., Gilliland G., Bhat T.N., Weissig H., Shindyalov I.N., Bourne P.E. (2000) The Protein Data Bank. *Nucleic Acids Research*, **28:** 235-242.

Cournac L., Redding K., Ravenel J., Rumeau D., Josse E.-M., Kuntz M., Peltier G. (2000) Electron flow between photosystem II and oxygen in chloroplasts of photosystem I-deficient algae is mediated by a quinol oxidase involved in chlororespiration. *The Journal of Biological Chemistry.* **275:** 17256-17262.

Cuello J., Quiles M.J., Albacete M.E., Sabater B. (1995a) Properties of a large complex with NADH dehydrogenase activity from barley thylakoids. *Plant Cell Physiol.* **36:** 265-271.

Cuello J., Quiles M.J., Rosauro J., Sabater B. (1995b) Effects of growth regulators and light on chloroplasts NAD(P)H dehydrogenase activities of senescent barley leaves. *Plant Growth Regulation.* **17:** 225-232.

Damdinsuren S., Osaki M., Tadano T. (1995) Quenching of chlorophyll alpha fluorescence by oxygen in normal air in higher plant leaves. *Soil Science and Plant Nutrition.* **41:** 529-537.

Debus R.J., Feher G., Okamura M.Y. (1986) Iron-depleted reaction centers from *Rhodopseudomonas sphaeroides*. *Biochemistry.* **25:** 2276-2287.

dePamphilis C.W., Palmer J.D. (1990) Loss of photosynthetic and chlororespiratory genes from the plastid genome of a parasitic flowering plant. *Nature.* **348:** 337-339.

Diethelm R., Miller M.G., Shibles R., Stewart C.R. (1990) Effect of salicylhydroxamic acid on respiration, photosynthesis, and peroxidase activity in various plant tissues. *Plant Cell Physiol.* **31:** 179-185.

Doyle J.J., Doyle J.L. (1987) Isolation of DNA from fresh plant tissue. *Focus.* **12:** 13-15.

El Amrani A., Couee I., Carde J.-P., Gaudillere J.-P., Raymond P. (1994) Modifications of etioplasts in cotyledons during prolonged dark growth of sugar beet seedlings. *Plant Physiol.* **106:** 1555-1565.

Elotza F., Asturias J.A., Arizmendi J.M. (1999) Chloroplast NADH dehydrogenase from *Pisum sativum*: characterization of its activity and cloning of *ndhK* gene. *Plant Cell Physiol.* **40:** 149-154.

Endo T., Shikanai T., Sato F., Asada K. (1998) NAD(P)H dehydrogenase-dependent, antimycin A-sensitive electron donation to plastoquinone in tobacco chloroplasts. *Plant Cell Physiol.* **39:** 1226-1231.

Field T.S., Nedbal L., Ort D.R. (1998) Nonphotochemical reduction of the plastoquinone pool in sunflower leaves originates from chlororespiration. *Plant Physiol.* **116:** 1209-1218.

Friedrich T., Scheide D. (2000) The respiratory complex I of bacteria, archaea and eukarya and its module common with membrane-bound multisubunit hydrogenases. *FEBS.* **479:** 1-5.

Friedrich T., Steinmuller K., Weiss H. (1995) The proton-pumping respiratory complex I of bacteria and mitochondria and its homologue in chloroplasts. *FEBS Letters.* **367:** 107-111.

Garab G., Lajko F., Mustardy L., Marton L. (1989) Respiratory control over photosynthetic electron transport in chloroplasts of higher-plant cells: evidence for chlororespiration. *Planta.* **179:** 349-358.

Godde D. (1982) Evidence for a membrane bound NADH-plastoquinone-oxidoreductase in *Chlamydomonas reinhardii* CW-15. *Arch Microbiol.* **131:** 197-202.

Godde D., Trebst A. (1980) NADH as electron donor for the photosynthetic membrane of *Chlamydomonas reinhardtii*. *Arch. Microbiol.* **127:** 245-252.

Groom Q.J., Kramer D.M., Crofts A.R., Ort D.R. (1993) The non-photochemical reduction of plastoquinone in leaves. *Photosynthesis Research.* **36:** 205-215.

Guedeney G., Corneille S., Cuine S., Peltier G. (1996) Evidence for an association of *ndh* B, *ndh* J gene products and ferredoxin-NADP-reductase as components of a chloroplastic NAD(P)H dehydrogenase complex. *FEBS Letters.* **378:** 277-280.

Guera A., de Nova P.G., Sabater B. (2000) Identification of the Ndh (NAD(P)H-Plastoquinone-oxidoreductase) complex in etioplast membranes of barley: changes during photomorphogenesis of chloroplasts. *Plant Call Physiology.* **41:** 49-59.

Haberhausen G., Zetsche K. (1994) Functional loss of all *ndh* genes in an otherwise relatively unaltered plastid genome of the holoparasitic flowering plant *Cuscuta reflexa*. *Plant Molecular Biology.* **24:** 217-222.

Harnes B.D., Rickwood D. (1981) Gel electrophoresis of proteins: a practical approach. IRL Press Ltd. Oxford, England.

Horvath E.M., Peter S.O., Joet T., Rumeau D., Cournac L., Horvath G.V., Kavanagh T.A., Schafer C., Peltier G., Medgyesy P. (2000) Targeted inactivation of the plastid *ndhB* gene in tobacco results in an enhanced sensitivity of photosynthesis to moderate stomatal closure. *Plant Physiology.* **123:** 1337-1349.

Hunter D.A. (1998) Characterisation of ACC oxidase during leaf maturation and senescence in white clover (*Trifolium repens* L.). *PhD Thesis*. Massey University, Palmerston North, New Zealand.

Izawa S. (1980) Acceptors and donors for chloroplast electron transport. *Methods in Enzymol.* **69:** 413-434.

Josse E.-M., Simkin A.J., Gaffe J., Laboure A.-M., Kuntz M., Carol P. (2000) A plastid terminal oxidase associated with caroternoid desaturation during chromoplast differentiation. *Plant Physiology.* **123:** 1427-1436.

Kofer W., Koop H.U., Wanner G., Steinmuller K. (1998) Mutagenesis of the genes encoding subunits A, C, H, I, J and K of the plastid NAD(P)H-plastoquinone-oxidoreductase in tobacco by polyethylene glycol-mediated plastome transformation. *Molecular and General Genetics.* **258:** 166-173.

Koulougliotis D., Kostopoulos T., Petrouleas V., Diner B.A. (1993) Evidence for CN^- binding at the PS II non-heme Fe^{2+}. Effects on the EPR signal for $Q_A^-Fe^{2+}$ and on Q_A/Q_B electron transfer. *Biochimica et Biophysica Acta.* **1141:** 275-282.

Lajko F., Kadioglu A., Borbely G., Garab G. (1997) Competition between the photosynthetic and the (chloro)respiratory electron transport chains in cyanobacteria, green algae and higher plants. Effect of heat stress. *Photosynthetica.* **33:** 217-226.

Lowry O.H., Rosebourgh N.J., Lewis Farr A., Randall R.J. (1951) Protein measurement with the folin phenol reagent. *Journal of Biological Chemistry.* **193:** 265-275.

Maione T.E., Gibbs M. (1986) Association of the chloroplastic respiratory and photosynthetic electron transport chains of *Chlamydomonas reinhardii* with photoreduction and the oxyhydrogen reaction. *Plant Physiol.* **80:** 364-368.

Matsubayashi T., Wakasugi T., Shinozaki K., Yamaguchi-Shinozaki K., Zaita N., Hidaka T., Meng B.Y., Ohto C., Tanaka M., Kato A., Maruyama T., Sugiura M. (1987) Six chloroplast genes (*ndhA-F)* homologous to human mitochondrial genes encoding components of the respiratory chain NADH dehydrogenase are actively expressed: determination of the splice sites in *ndhA* and *ndhB* pre-mRNAs. *Mol. Gen. Genet.* **210:** 385-393.

Robinson H.H., Yocum C.F. (1980) Cyclic photophosphorylation reactions catalysed by ferredoxin, methyl viologen and anthraquinone sulfonate. Use of photochemical reactions to optimise redox poising. *Biochimica et Biophysica Acta.* **590:** 97-106.

Sazanov L.A., Burrows P.A., Nixon P.J. (1998a) The chloroplast Ndh complex mediates the dark reduction of the plastoquinone pool in response to heat stress in tobacco leaves. *FEBS Letters.* **429:** 115-118.

Sazanov L.A., Burrows P.A., Nixon P.J. (1998b) The plastid *ndh* genes code for an NADH-specific dehydrogenase: isolation of a complex I analogue from pea thylakoid membranes. *Proceedings of National Academy of Science USA.* **95:** 1319-1324.

Seidelguyenot W., Schwabe C., Buchel C. (1996) Kinetic and functional characterization of a membrane-bound NAD(P)H dehydrogenase located in the chloroplasts of *Pleurochloris meiringensis*. *Photosynthesis Research.* **49:** 183-193.

Shikanai T., Endo T., Hashimoto T., Yamada Y., Asado K., Yokota A. (1998) Directed disruption of the tobacco *ndhB* gene impairs cyclic electron flow around photosystem I. *Proceedings of the National Academy of Science USA.* **95:** 9705-9709.

Springer V., Hornackova M., Karlicek R., Kopecka B. (1987) Salicylhydroxamic acid and its iron (III) complexes. *Collection of Czechoslovak Chemical Communications.* **52:** 602-608.

Trebst A. (1980) Inhibitors in electron flow: Tools for the functional and structural localization of carriers and energy conservation sites. *Methods in Enzymology.* **69:** 675-715.

Vera A., Tomas R., Martin M., Sabater B. (1990) Apparent expression of small single copy cpDNA region in senescent chloroplasts. *Plant Science.* **72:** 63-67.

Wakasugi T., Tsudzuki J., Ito S., Keiko N., Tsudzuki T., Sugiura M. (1994) Loss of all *ndh* genes as determined by sequencing the entire chloroplast genome of the black pine *Pinus thunbergii*. *Proc. Natl. Acad. Sci. USA.* **91:** 9794-9798.

Willeford K.O., Gombos Z., Gibbs M. (1989) Evidence for chloroplastic succinate dehydrogenase participating in the chloroplastic respiratory and photosynthetic electron transport chains of *Chlamydomonas reinhardtii*. *Plant Physiol.* **90:** 1084-1087.

Wolfe K.H., Morden C.W., Palmer J.D. (1992) Function and evolution of a minimal plastid genome from a nonphotosynthetic parasitic plant. *Proc. Natl. Acad. Sci. USA.* **89:** 10648-10652.

Wu D., Wright D.A., Wetzel C., Voytas D.F., Rodermel S. (1999) The *IMMUTANS* variegation locus of Arabidopsis defines a mitochondrial alternative oxidase homolog that functions during early chloroplast biogenesis. *The Plant Cell.* **11:** 43-55.

Yamashita T., Butler W.L. (1968) Photoreduction and photophosphorylation with tris-washed chloroplasts. *Plant Physiol.* **43:** 1978-1986.

APPENDIX I

ABI PRISM

Version 3.3
ABI100
Version 3.2

Loaded 1ul onto the sequencer
F
Lane 60

DT {BD Set Any-Primer}
377XL 48CM Matrix
Points 1290 to 10066 Pk 1 Loc: 1290

Thu, 14 Sep 2000 9:36 AM
Wed, 13 Sep 2000 12:30 PM
Spacing: 11.56{11.56}

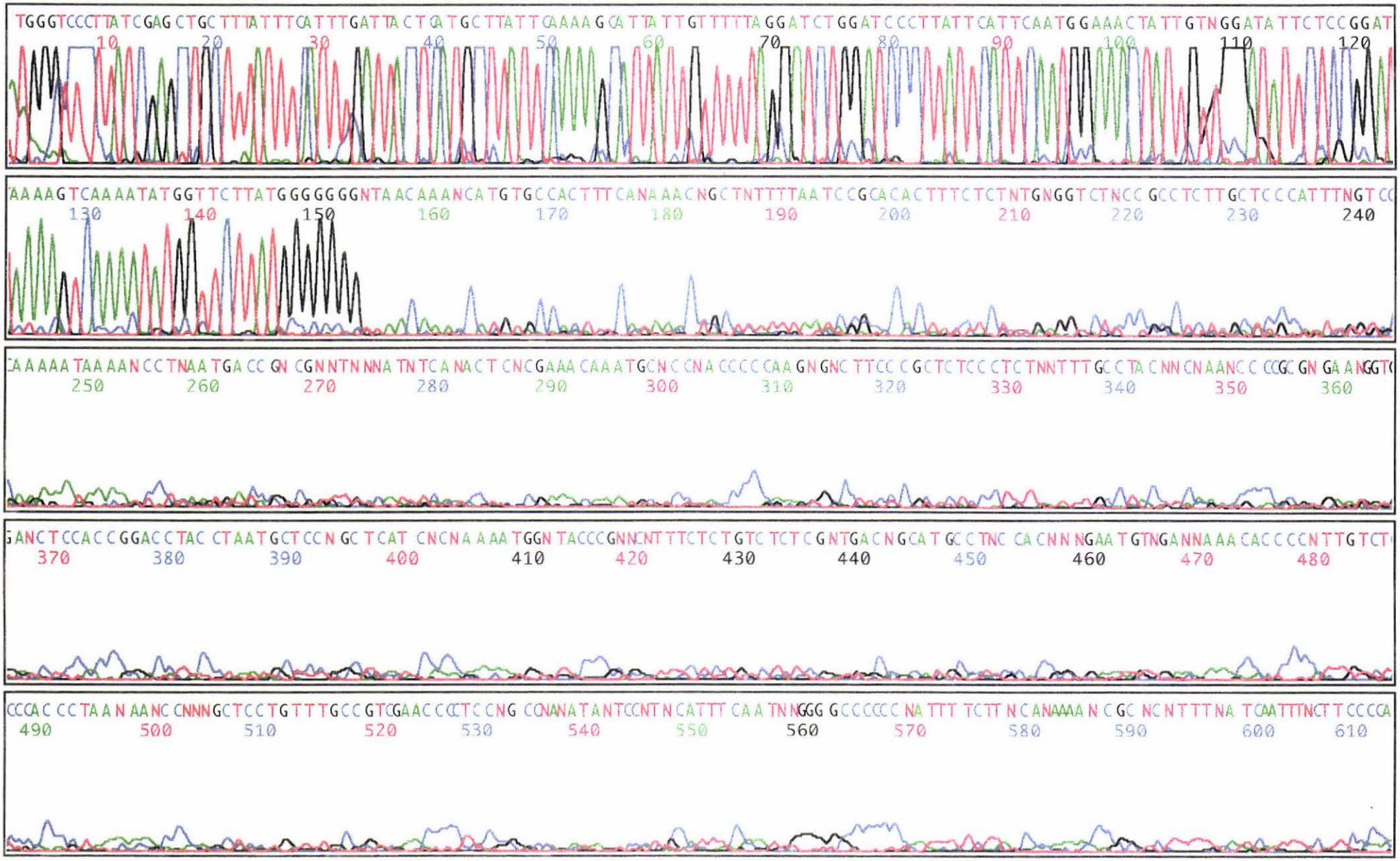

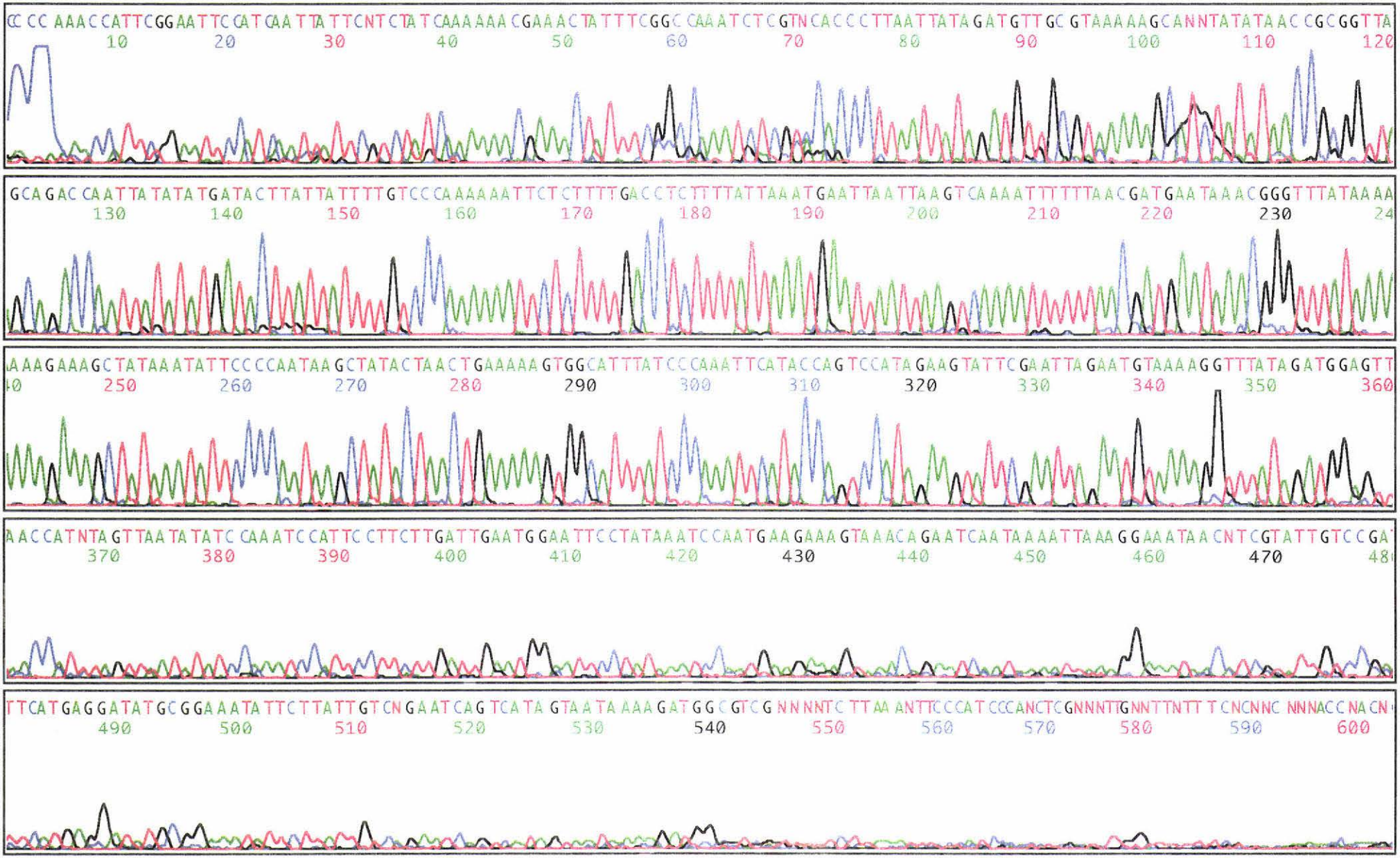
CC CC AAACCATTCGGAATTCCATCAATTATTCNTCTATCAAAAAACGAAACTATTTCGGCCAAATCTCGTNCACCCTTAATTATAGATGTTGCGTAAAAAGCANNTATATAACCGCGGTTA
10 20 30 40 50 60 70 80 90 100 110 120
GCAGACCAATTATATATGATACTTATTATTTTGTCCCAAAAAATTCTCTTTTGACCTCTTTTATTAAATGAATTAATTAAGTCAAAATTTTTTAACGATGAATAAACGGGTTTATAAAA
130 140 150 160 170 180 190 200 210 220 230 24
AAAGAAAGCTATAAATATTCCCCAATAAGCTATACTAACTGAAAAAGTGGCATTTATCCCAAATTCATACCAGTCCATAGAAGTATTCGAATTAGAATGTAAAAGGTTTATAGATGGAGTT
40 250 260 270 280 290 300 310 320 330 340 350 360
AACCATNTAGTTAATATATCCAAATCCATTCCTTCTTGATTGAATGGAATTCCTATAAATCCAATGAAGAAAAGTAAACAGAATCAATAAAATTAAAGGAAATAACNTCGTATTGTCCGA
370 380 390 400 410 420 430 440 450 460 470 48
TTCATGAGGATATGCGGAAATATTCTTATTGTCNGAATCAGTCATAGTAATAAAAGATGGCGTCGNNNNTCTTAAANTTCCCATCCCANCTCGNNNTTGNNTTNTTTCNCNNC NNNACCNACN
490 500 510 520 530 540 550 560 570 580 590 600